Bandwidth-Efficient Wireless Multimedia Communications

LAJOS HANZO, SENIOR MEMBER, IEEE

Commencing with the brief history of mobile communications and the portrayal of the basic concept of wireless multimedia communications, the implications of Shannon's theorems regarding joint source and channel coding for wireless communications are addressed. Following a brief introduction to speech, video, and graphical source coding as well as the cellular concept, a rudimentary overview of flexible, reconfigurable, mobile radio schemes is provided. We then summarize the fundamental concepts of modulation, introduce an adaptive modem scheme, and argue that third-generation transceivers might become adaptively reconfigurable under network control in order to meet backward compatibility requirements with existing systems and to achieve best compromise among a range of conflicting system requirements in terms of communications quality, bandwidth requirements, complexity and power consumption, robustness against channel errors, etc.

Keywords— Cellular communications, channel coding, graphical source coding, modern transceiver, modulation, multimedia system schematic, multimode speech system, speech source coding, video-phone systems, video source coding, wireless channels, wireless communications, wireless multimedia communicator.

NOMENCLATURE

ACI	Adjacent channel interference.
ACTS	Advanced communications technologies and services.
ADPCM	Adaptive differential pulse code modulation.
AGC	Automatic gain control.
AMPS	Advanced Mobile Phone System.
ATM	Asynchronous transfer mode.
AWGN	Additive white Gaussian noise.
BCH	Bose–Chaudhuri–Hocquenghem, a class of forward error-correcting codes.
BER	Bit error rate, the number of bits received incorrectly.
B-ISDN	Broad-band ISDN.
BPS	Bits per symbol.
BS	Base station.
CC	Chain coding.
CCI	Cochannel interference.
CDMA	Code division multiple access.
CELP	Code excited linear prediction.
CIF	Common intermediate format frames, containing 352 pixels vertically and 288 pixels horizontally.
CSI	Channel state information.
CT	Cordless telephone.
CT2	British cordless telephone system.
DAB	Digital audio broadcasting.
DAMPS	Digital AMPS.
DCA	Dynamic channel allocation.
DCC	Differential chain coding.
DCT	Discrete cosine transform, which transforms data into the frequency domain. Commonly used for video compression by removing high-frequency components in the video frames.
DECT	Digital European cordless telephone.
DFT	Discrete Fourier transform.
DoD	U.S. Department of Defense.
DRI	Decoder reliability information.
DRMA	Dynamic reservation multiple access.
DSP	Digital signal processing.
FDMA	Frequency division multiple access.
FEC	Forward error correction.
FFT	Fast Fourier transform.
FL-DCC	Fixed-length differential chain coding.
FM	Frequency modulation.
FPLMTS	Future public land mobile telecommunications system.
FS	Fixed station.
FV	Fixed-length vector.
G.722	7-kHz-bandwidth wide-band speech-coding standard.
G.728	ITU 16-kbits/s speech-coding standard.
G.729	ITU 8-kbits/s speech-coding standard.
GOS	Grade of service.

GSM   A pan-European digital mobile radio standard operating at 900 MHz.

H.263   A video-coding standard [193] published by the ITU in 1996.

HIPERLAN HIPERformance LAN.

HMM   Hidden Markov model.

I   In-phase component in modulation.

IS-54   The pan-American DAMPS TDMA mobile radio standard.

IS-95   The pan-American CDMA mobile radio standard.

ISDN   Integrated services digital network, digital replacement of the analog telephone network.

ISI   Intersymbol Interference International Telecommunications Union, formerly the CCITT, a standardization group.

ITU   International Telecommunications Union.

IZFPE   Interpolated zinc function pulse excitation.

LAN   Local-area network.

LCD   Liquid crystal display.

LOS   Line of sight.

LSB   Least significant bit.

MAC   Multiple access.

MAP   Maximum *a posteriori*.

MBE   Multiband excitation.

MC   Motion compensation.

MCER   Motion-compensated error residual.

MELP   Mixed excitation linear prediction.

MF-PRMA Multiframe packet reservation multiple access.

MLH-CR   Maximum likelihood correlation receiver.

MLSE   Maximum likelihood sequence estimation.

MPEG   Moving Picture Experts Group, also a video-coding standard designed by this group that is widely used.

MS   Mobile station.

MSB   Most significant bit.

MSC   Mobile switching center.

MV   Motion vector, a vector to estimate the motion in a frame.

NAMTS   Nippon mobile telephone system.

NMT   Nippon Mobile Telephone.

NTT   Nippon Telegraph and Telephone Company.

OFDM   Orthogonal frequency division multiplexing.

PCM   Pulse code modulation.

PCN   Personal communications network.

PCS   Personal communications system.

PD   Pen-down.

PDC   Personal digital cellular.

PHP   Personal handy phone.

PLMR   Public land mobile radio.

PRMA   Packet reservation multiple access.

PS   Portable station.

PSAM   Pilot symbol assisted modulation, a technique where known symbols (pilots) are transmitted regularly. The effect of channel fading on all symbols can then be estimated by interpolating between the pilots.

PSI   Pitch synchronous innovation.

PU   Pen-up.

PWI   Prototype waveform interpolation.

Q   Quadrature-phase component in modulation.

QAM   Quadrature amplitude modulation.

QCIF   Quarter-CIF frames, containing 176 pixels vertically and 144 pixels horizontally.

QT   Quad tree.

RACE   Research in advanced communications equipment.

RAMA   Resource auction multiple access.

RF   Radio frequency.

RPE   Regular pulse excitation.

RSC   Recursive systematic convolutional code.

SBC   Subband coding.

SDI   Soft decision information.

SIR   Signal-to-interference ratio.

SNR   Signal-to-noise ratio, noise energy compared to the signal energy.

SOVA   Soft output Viterbi algorithm.

SPAMA   Statistical packet assignment multiple access.

SSI   Source significance information.

SV   Starting vector.

T.150   ITU handwriting coding standard.

TACS   Total access communications system.

TCM   Trellis coded modulation.

TDMA   Time division multiple access.

TS   Transmission scheme.

TTIB   Transparent tone in band.

UMTS   Universal Mobile Telecommunications System.

VAD   Voice activity detection.

VC   Vector count.

VQ   Vector quantization.

VSELP   Vector sum excited linear prediction.

WATM   Wireless ATM.

WLAN   Wireless LAN.

I. THE WIRELESS COMMUNICATIONS SCENE

Since the end of the last century, when Marconi and Hertz demonstrated the feasibility of radio transmissions, mankind has endeavoured to fulfil the dream of wireless multimedia personal communications, enabling people to communicate with anyone, anywhere, at any time, using a range of multimedia services. The evolution of wireless systems and their subsystems has been well documented in a range of monographs by Jaykes [1], Lee [2], Parsons and Gardiner [3], Feher [4], and others. Glisic and Vucetic [5], as well as Prasad [6], concentrated on various aspects of CDMA in their monographs, while the compilation of excellent overviews edited by Glisic and Leppanen [7] treated both TDMA and CDMA along with a range of other associated aspects, such as smart antennas [53], [55], [56]

and trellis coding, as well as emerging topics, referred to as "time-space" processing [55], "per-survivor" processing [57], etc.

Meyer *et al.* [8] focused on various modern receiver techniques in their monograph. Steele [9] compiled a monograph that considers most physical-layer aspects of modern TDMA systems, including speech and channel coding, modulation, frequency hopping, and so on, amalgamating them in the last chapter in the context of the global system of mobile communications known as GSM. Further important references are, for example, those by Rappaport [10] and Garg and Wilkes [11], or the compilation edited by Gibbson [12]. These developments are also portrayed in magazine special issues [13]–[18] and excellent reviews by McDonald [19], Steele [20]–[22], Cox [30], Li and Qiu [32], Kucar [31], etc. This paper attempts to provide an update on some of the subsystems and trends in the broad field of wireless multimedia communications. Let us commence our discourse with a glimpse of history.

The first mobile radio systems were introduced by the military, police, and other emergency services, most of which were limited to voice-only communications. During the pre-very large scale integration (VLSI) era, the realizable signal-processing complexity was severely limited, and hence the handsets provided typically poor voice quality at a high cost. This was due to the phenomenon of multipath wave propagation, where the different multipath components arriving at the receiver's antenna suffer different attenuation and phase rotation, and hence they sometimes add constructively, sometimes destructively. This situation is further aggravated by the so-called delay spread, when the various propagation paths have rather different path lengths and consequently exhibit different delays, spilling intersymbol interference (ISI) into the adjacent signalling or symbol intervals. These phenomena can today often be combated by sophisticated signal-processing methods at the cost of added implementational complexity, which was not possible in the pre-VLSI era. Hence, until quite recently, the quality and variety of wireless services have been inferior to conventional tethered communications.

The first public cellular radio system, known as AMPS, was introduced in 1979 in the United States, shortly followed by the Nordic mobile telephone system in Scandinavia in 1981. The first British system was TACS, operated by Cellnet and Vodafone, while the Japanese introduced NAMTS. All of these so-called *first-generation* national systems were based on analog FM but used digital network control. However, they did not support international roaming.

In 1982, the Conference Europeene des Postes et Telecommunication (CEPT), the main governing body of the European postal, telephone, and telegraph organizations, created the Groupe Speciale Mobile (GSM) Committee and tasked it with standardizing a digital cellular pan-European public mobile communications system to operate in the 900-MHz band. This was followed by the launch of experimental programs of different types of digital cellular radio systems in a number of European countries. By the middle of 1986, nine proposals were received for the future pan-European system, and GSM organized a trial in Paris to identify the one having the best performance. The technical details of the candidate systems are described in [33]–[37], while a short summary of their salient features is given in [39]. A detailed description of the standardized GSM system's main features can be found in [40]. This scheme constitutes the first so-called *second-generation* PLMR system, which was designed for the worst case propagation scenario of high-elevation antennas' providing radio coverage for large rural cells. The corresponding channel conditions and techniques for mitigating their effects will be highlighted during our further discourse.

Following GSM, in 1989, the American second-generation scheme, known as the DAMPS system [41] had also been standardized, with the advantage of being able to accommodate three higher quality digital channels in a conventional 30-kHz analog AMPS channel slot. Its unique feature is that similar to the Japanese second-generation scheme referred to as the PDC system [42] it uses a 2-bits/symbol nonbinary modem, which implicitly assumes a more benign propagation environment than that of the GSM PLMR system. The improved wave propagation conditions are a consequence of employing so-called microcells, where, in contrast to a hostile PLMR system, the high antenna elevation is reduced to below the urban skyline. Hence, there is typically a strong LOS path between the BS and MS, reducing the fading depth and mitigating the effect of ISI induced by delay spread. These issues will be revisited in more depth at a later stage.

With respect to the improved propagation conditions, the multilevel IS-54 and PDC systems provide a seamless transition toward the so-called CT system concept contrived mainly for friendly indoors office and domestic propagation environments. Hence, CT products are designed to have a low transmitted power and small coverage area, where typically there is a dominant LOS propagation path between the FS and PS. The low transmitted power and small transmission range facilitate a low-complexity, low-cost, lightweight construction. The standardization and development of CT products was hallmarked by the British CT2 system, the DECT, and the Japanese PHP systems. A further important milestone was the standardization of the British DCS-1800 system, which is essentially an up-converted GSM system implemented at 1.8 GHz. The standardization of the so-called half-rate GSM system [330] supporting twice as many subscribers within the 200-kHz channel bandwidth, as the full-rate system was also an important development in the field. These second-generation systems and CT schemes were described in dedicated chapters of [12].

Currently, there exist a range of initiatives worldwide that attempt to define the *third-generation* PCN, which is referred to as a PCS in North America. The European Community's RACE program [12], [13] and the consecutive framework referred to as the ACTS program [44], [45] spearheaded these initiatives. In the RACE program, there were two dedicated projects, endeavoring to resolve the ongoing debate as regards the most appropriate multiple
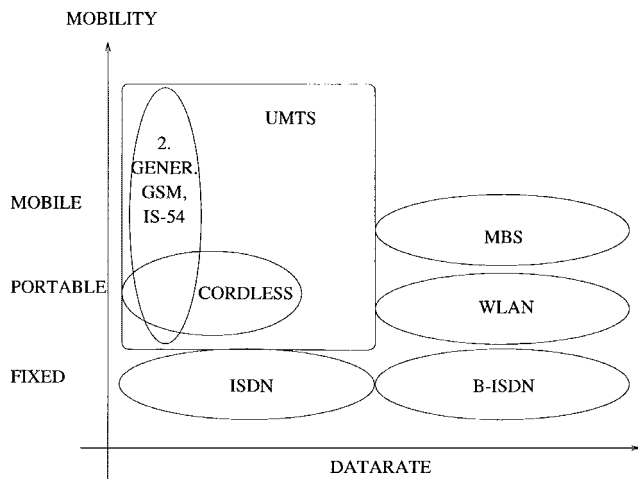
Fig. 1. Stylized mobility versus bit-rate plane classification of existing and future wireless systems.

access scheme, studying TDMA [9], [12], [13], [40], [41] and CDMA [9], [12], [13], [43].

European third-generation research is conducted under the umbrella of the so-called UMTS [13] initiative, and so far, the following proposals have been submitted to the European Telecommunication Standard Institute [54]: wide-band CDMA [46]–[48], adaptive TDMA [49], hybrid TDMA/CDMA [50], OFDM [51], [68], and opportunity-driven multiple access. We note that the Nokia testbed portrayed in [48] was designed with video transmission capabilities of up to 128 kbits/s in mind. Similarly, cognizance was given to the aspects of less-bandwidth-constrained—i.e., higher rate—video communications by the Japanese wide-band CDMA proposal [52] for the intelligent mobile terminal IMT 2000 emerging from NTT DoCoMo. These standardization activities are portrayed in more depth in [54].

In the ACTS workplan [44], there are a number of projects dealing with multimedia source and channel coding, modulation, and multiple access techniques for both cellular and wireless LAN's. These studies will design the architecture and produce demonstration models of the UMTS, which the Europeans intend to accomplish before the turn of the century. Somewhere along the line, UMTS is expected to merge with the CCIR study on the FPLMTS. These systems are characterized with the help of Fig. 1 in terms of their expected grade of mobility and bit rate. These fundamental features predetermine the range of potential applications.

Specifically, the fixed networks are evolving from the basic 2.048 Mbit/s ISDN toward higher rate B-ISDN. A higher grade of mobility, which we refer to here as portability, is a feature of cordless telephones, such as the DECT, CT2, and PHP systems, although their transmission rate is more limited. The DECT systems is the most flexible one among them, allowing the multiplexing of 23 single-user channels in one direction, which provides rates up to 23×32 kbits/s $= 736$ kbits/s for advanced services. WLAN's can support bit rates up to 155 Mbits/s in order

to extend existing ATM links to portable terminals, but they usually do not support full mobility functions, such as location update or handover from one BS to another. A rapidly evolving field that is also gaining considerable commercial interest is associated with the research and development of HIPERLAN's [66], [67] for "customer premises"-type communications. Contemporary second-generation PLMR systems, such as GSM and IS-54, cannot support high-bit-rate services, since they typically have to communicate over lower quality channels, but they exhibit the highest grade of mobility, including high-speed international roaming capabilities.

The third-generation UMTS is expected to have the highest grade of flexibility both in terms of its service bit-rate range and in terms of mobility. In its design, cognizance is given to the second-generation systems. Indeed, we may anticipate that some of the subsystems of GSM and DECT may find their way into UMTS, either as a primary subsystem or as a component to achieve backward compatibility with systems in the field. This approach may result in hand-held transceivers that are intelligent multimode terminals, able to communicate with existing networks, while having more advanced and adaptive features that we would expect to see in the next generation of wireless multimedia PCN's. Following the above brief overview of the wireless communications scene, let us now briefly speculate on the practical embodiment of the multimedia communicator of the near future.

II. OUTLINE

The rest of this paper concentrates mainly on bandwidth-efficient low-rate systems, although many of the proposed techniques are suitable for high-rate systems as well. Following some introductory conceptual notes as regards a possible manifestation of the future wireless multimedia communicator in Section III, we analyze the ramifications of Shannon's message for wireless systems in Section IV. This is followed by sections on speech, video, and graphical source coding before we focus our attention on transmission aspects. Section VIII-A highlights the basic cellular concept, while Section VIII-B introduces a few multiple access concepts, leading to the introduction of the concept of "software radios" or adaptive intelligent transceivers in Section IX. We then make a short excursion to the field of modulation schemes in Section XI and FEC coding before concluding with the portrayal of the expected system-performance figures characterizing such an intelligent multimode speech system in Section XIII and the characterization of a video-phone transceiver in Section XIV.

This paper addresses the so-called physical-layer functions of wireless systems in more depth but attempts also to devote some attention to higher layer aspects, such as multiple access, dynamic channel allocation, handover, etc. Given the wide scope of this paper, it is inevitable that some important trends and seminal contributions by highly acclaimed authors remain beyond its coverage, although
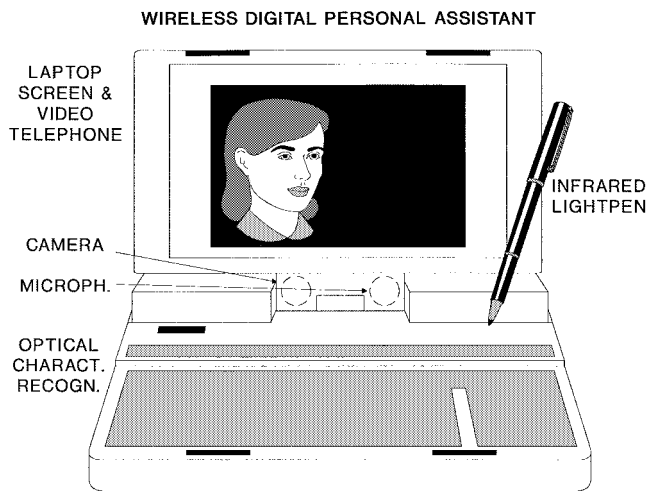
WIRELESS DIGITAL PERSONAL ASSISTANT

LAPTOP SCREEN & VIDEO TELEPHONE

INFRARED LIGHTPEN

CAMERA

MICROPH.

OPTICAL CHARACT. RECOGN.

Fig. 2. Wireless multimedia communicator.

with the number of references provided there is sufficient scope for the interested reader to probe further in certain deeper subject areas.

III. WIRELESS MULTIMEDIA COMMUNICATOR

A possible manifestation of the multimedia PS is portrayed in Fig. 2, which is equipped with a bird's-eye camera, microphone, and liquid crystal screen, serving as both a video-telephone screen and a computer screen. The conventional keyboard is likely to be replaced by a pressure-sensitive writing tablet, facilitating optical handwriting recognition [208]–[213], signature verification, etc.

The pivotal implementational point of such a multimedia PS is that of finding the best compromise among a number of contradicting design factors, such as low power consumption, high robustness against transmission errors among various channel conditions, high spectral efficiency, good audio/video quality, low-delay, high-capacity networking, and so forth. In this paper, we will address a few of these issues in the context of the proposed PS depicted in Fig. 2. The time-variant optimization criteria of a flexible multimedia system can only be met by an adaptive scheme, comprising the firmware of a suite of system components and invoking that combination of speech codecs, video codecs, embedded channel codecs, VAD's, and modems that fulfills the currently prevalent requirement [68].

These requirements lead to the concept of arbitrarily programmable, flexible, so-called software radios [16], which is virtually synonymous with the so-called tool-box concept invoked, for example, in the forthcoming MPEG-4 video codec proposed for wireless video communications [70]. This concept appears attractive also for UMTS-type transceivers. A few examples of such optimization criteria are maximizing the teletraffic carried or the robustness against channel errors, while in other cases, minimization of the bandwidth occupancy, the blocking probability, or the power consumption is of prime concern.

The corresponding network architecture is shown in Fig. 3. The multimedia PS's communicate with the so-

called BS's in their vicinity, which are interconnected either directly using optical fiber or in more complex systems via MSC's. The PS's can access through the BS a range of services, including business data bases, multimedia data bases, mainframe computers, etc. Let us now turn our attention to some of the information theoretical aspects of wireless communications in order to be able to understand the underlying system's technical ramifications.

IV. SHANNON'S MESSAGE AND ITS IMPLICATIONS FOR WIRELESS CHANNELS

In mobile multimedia communications, it is always of prime concern to maintain an optimum compromise in terms of the contradictory requirements of low bit rate, high robustness against channel errors, low delay, and low complexity. The minimum bit rate at which the condition of distortionless communications is possible is determined by the entropy of the multimedia source message. Note, however, that in practical terms, the minimum information transmission rate required for the lossless representation of the source signal, which is referred to as the source entropy, is only asymptotically achievable, as the encoding memory length or delay tends to infinity. Any further compression is associated with information loss or coding distortion. Note that the optimum source encoder generates a perfectly uncorrelated source-coded stream, where all the source redundancy has been removed. Therefore, the encoded symbols are independent, and each one has the same significance. Having the same significance implies that the corruption of any of the source-encoded symbols results in identical reconstructed signal distortion over imperfect channels.

Under these conditions, according to Shannon's fundamental work [72], [73], [75], the best protection against transmission errors is achieved, if source and channel coding are treated as separate entities. When using a block code of length N channel coded symbols in order to encode K source symbols with a coding rate of $R = K/N$, the symbol error rate can be rendered arbitrarily low if N tends to infinity and the coding rate to zero. This condition also implies an infinite coding delay. Based on the above considerations and on the assumption of AWGN channels, source and channel coding have historically been separately optimized.

Mobile radio channels are typically subjected to multipath propagation and hence constitute a more hostile transmission medium than AWGN channels, exhibiting path loss, log-normal slow fading, and Rayleigh fast fading [216], [217]. Furthermore, if the signaling rate used is higher than the channel's so-called coherence bandwidth [216], [217], additional impairments are inflicted by dispersion, which is associated with frequency-domain linear distortions. Under these circumstances the channel's error distribution versus time becomes bursty and an infinite-memory symbol interleaver is required in order to disperse the bursty errors and render the errors as independent, as possible, such as over AWGN channels. Clearly, for mobile
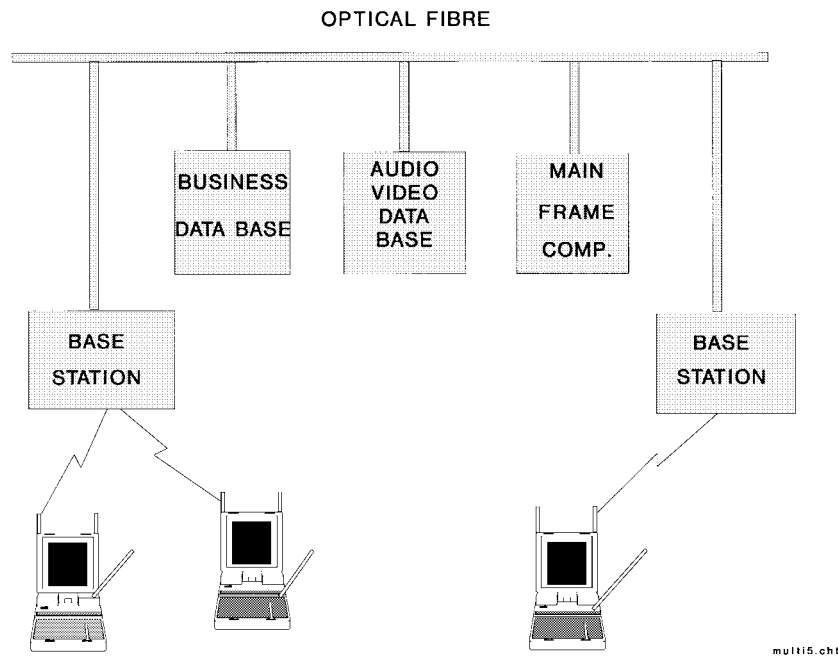
OPTICAL FIBRE

BUSINESS DATA BASE

AUDIO VIDEO DATA BASE

MAIN FRAME COMP.

BASE STATION

BASE STATION

multi5.cht

Fig. 3. Wireless multimedia network.

channels, many of the above-mentioned, asymptotically valid ramifications of Shannon's theorem have a limited applicability.

A range of practical limitations must be observed when designing wireless multimedia links. Although it is often possible to reduce the required bit rate of state-of-the-art multimedia source codecs while maintaining a certain reconstructed signal quality, in practical terms, this is only possible at a concomitant increase of the implementational complexity and encoding delay. A good example of these limitations is the half-rate GSM speech codec, which was required to approximately halve the encoding rate of the 13 kbits/s full-rate codec, while maintaining less than quadrupled complexity, similar robustness against channel errors, and less than doubled encoding delay. Naturally, the increased algorithmic complexity is typically associated with higher power consumption, while the reduced number of bits used to represent a certain speech segment intuitively implies that each bit will have an increased relative significance. Accordingly, their corruption may inflict increasingly objectionable speech degradations unless special attention is devoted to this problem. It is worth noting that despite its quadruple complexity, the half-rate GSM speech codec maintains a lower power consumption due to low-power 3-V technology than the first launched full-rate codec had.

In a somewhat simplistic approach, one could argue that due to the reduced source rate, we could accommodate an increased number of parity symbols using a more powerful, implementationally more complex, and lower rate channel codec while maintaining the same transmission bandwidth. However, the complexity, quality, and robustness tradeoff of such a scheme would not be very attractive.

A more intelligent approach will be required in order to design better wireless multimedia transceivers [73], [74] for

bursty mobile radio channels. The simplified schematic of such an intelligent transceiver is portrayed in Fig. 4. Perfect source encoders operating close to the information theoretical limits of Shannon's predictions can only be designed for stationary source signals, a condition not satisfied by most multimedia source signals. Further previously mentioned limitations are the encoding complexity and delay. As a consequence of these limitations, the source-coded stream will inherently contain residual redundancy, and the correlated source symbols will exhibit unequal error sensitivity, requiring unequal error protection. Following Hagenauer [73], [74], we will refer to the additional knowledge as regards the different importance or vulnerability of various source-coded bits as SSI, whereas we will refer to the confidence associated with the channel decoder's decisions as DRI.

These additional links between the source and channel codecs are also indicated in Fig. 4. Further potential performance gains are possible when exploiting the *a posteriori* information accruing from decoding a received message. This is possible, for example, when the difference between consecutive decoded symbols violates some threshold condition and thereby facilitates the detection of a channel decoding error. Then the channel decoder can attempt a second tentative decoding by passing the second most likely corrected message to the source decoder, which in turn subjects this again to the previously failed threshold test, etc. A variety of such techniques have successfully been used in robust source-matched source and channel coding [73], [74], [82], [83]. Another practical manifestation of the time-variant source statistics of speech signals is the fact that during silent speech spurts, some speech codecs do not surrender their reserved physical link; they reduce their output bit rate instead, which can reduce the interference inflicted to other users in CDMA systems,
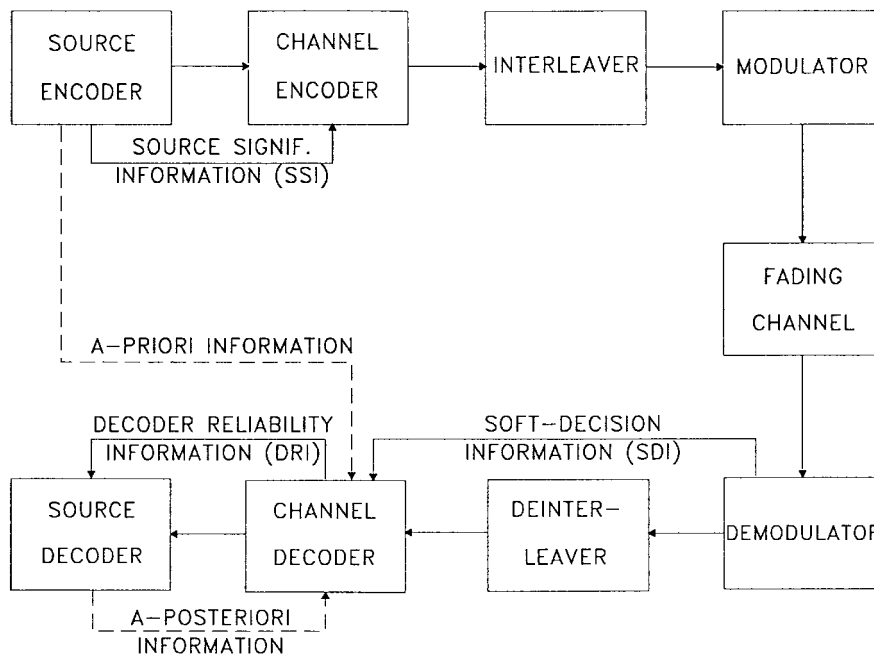
Fig. 4. Intelligent transceiver schematic.

such as the American IS-95 system [43]. Video codecs, such as the variable-rate MPEG-1 [80] and MPEG-2 [81] codecs, even more explicitly rely on the fluctuation of the source statistics. For example, when a new object is introduced in the scope of the camera, which cannot be predicted on the basis of already known previous video frames, then the bit rate is typically increased.

The role of the interleaver and deinterleaver [79] seen in Fig. 4 is to rearrange the channel coded bits before transmission. The mobile radio channel typically inflicts bursts of errors during deep channel fades, which often overload the channel decoder's error-correction capability in certain source-signal segments while other segments are not benefiting from the channel codec at all, since they may have been transmitted between fades and hence are error free even without channel coding. This problem can be circumvented by dispersing the bursts of errors more randomly between fades so that the channel codec is faced always with an "average-quality" channel rather than the bimodal faded/nonfaded condition, although only at the cost of increased system delay, which may become an impediment in interactive multimedia communications. In other words, channel codecs are most efficient if the channel errors are near uniformly dispersed over consecutive received segments.

In its simplest manifestation, an interleaver is a memory matrix that is filled with channel coded symbols on a row-by-row basis, which are then passed on to the modulator on a column-by-column basis. If the transmitted sequence is corrupted by a burst of errors, the deinterleaver maps the received symbols back to their original positions, thereby dispersing the bursty channel errors. An infinite-memory channel interleaver is required in order to perfectly randomize the bursty errors and therefore to transform the Rayleigh-fading channel's error statistics into that of an

AWGN channel, for which Shannon's information theoretical predictions apply. Since in interactive multimedia communications the tolerable delay is strictly limited, the interleaver's memory length and efficiency are also limited. For further details on the effects of various interleavers on the error-correction codec's efficiency, the interested reader is referred to [79].

A specific deficiency of the above-mentioned rectangular interleavers is that in case of a constant vehicular speed, the Rayleigh-fading mobile channel typically produces periodic fades [216], [217] and error bursts at travelled distances of $\lambda/2$, where λ is the carrier's wavelength, which may be mapped by the rectangular interleaver into another set of periodic bursts of errors. Again, a range of more random rearrangement or interleaving algorithms exhibiting a higher performance than rectangular interleavers has been proposed for mobile channels in [79], where also a variety of practical channel coding schemes have been portrayed. Section V gives a brief overview of the recent activities in speech source coding, Section VI provides a rudimentary introduction to video source coding, while Section VII highlights the principles of graphical source coding. For a full review of speech source coding schemes for mobile systems, the interested reader is referred to [84]–[91]. Joint source and channel coding was the subject of [92], whereas modulation and transmission arrangements for wireless channels have been studied in [4], [6], [9], [68], and [69].

Returning to Fig. 4, SDI is passed by the demodulator to the FEC decoder, indicating that the demodulator refrained from making a hard decision concerning the received bit. Instead, it passes the estimated reliability of the received information to the FEC decoder, thereby improving its efficiency. The CSI, which is in simple terms representative of the current fade depth, can be used to weight the SDI in the detection process. This weighted reliability information

is then often used by the channel decoder in order to invoke MLSE based on the Viterbi algorithm [79], [311] in order to improve the system's performance with respect to conventional hard-decision decoding. Following the above rudimentary review of Shannon's information theory, the rest of this paper is devoted to practical issues of wireless multimedia communications. Let us initially consider briefly the recent advances in speech source coding.

V. SPEECH SOURCE CODING

A. A Historical Perspective on Speech Codecs

Following the 64 kbits/s PCM and 32 kbits/s ADPCM G.721 recommendations standardized by the ITU, in 1986, the 13 kbits/s RPE [105], [106] codec was selected for the pan-European mobile system known as GSM. More recently, VSELP [107], [108] codecs operating at 8 and 6.7 kbits/s were favored in the American IS-54 and Japanese PDC wireless networks. These developments were followed by the 4.8 kbits/s DoD codec [112]. The state of the art was documented in a range of excellent monographs by O'Shaughnessy [87], Furui [88], Anderson and Seshadri [92], Kondoz [89], and Kleijn and Paliwal [90], and in a tutorial review by Gersho [78]. More recently, the 5.6 kbits/s half-rate GSM quadruple-mode VSELP speech codec standard developed by Gerson *et al.* [109] was approved, while in Japan, the 3.45 kbits/s half-rate PDC speech codec invented by Ohya *et al.* [113] using the PSI CELP principle was standardized. Other currently investigated schemes are the PWI proposed by Kleijn [114], MBE suggested by Griffin *et al.* [115], and IZFPE codecs advocated by Hiotakakos and Xydeas [116]. In the low-delay but more error sensitive backward adaptive class, the 16 kbits/s ITU G.728 codec [117] developed by Chen *et al.* from the AT&T speech team hallmarks a significant step. This was followed by the equally significant development of the more robust, forward-adaptive, 15–ms-delay G.729 algebraic (A)CELP arrangement proposed by the University of Sherbrooke team [122], [123], AT&T, and NTT [118]. Last, the standardization of the 2.4 kbits/s DoD codec led to intensive research in this very low rate range, and the MELP codec by Texas Instruments was identified [119] in 1996 as the best overall candidate scheme.

Before concluding our discourse on speech codecs, let us briefly highlight the problems associated with 7-kHz-bandwidth commentatory quality speech coding.

B. Wide-Band Speech Codecs

For the sake of completeness, we note briefly that 7-kHz-bandwidth speech codecs offer more transparent speech quality than their narrow-band counterparts at typically higher bit rate and algorithmic complexity.

One of the problems associated with full-band coding of wide-band speech is the codec's inability to treat the less predictable high-frequency, low-energy speech band, which was tackled by the ITU G.722 codec using split-band or subband coding. Although the upper subband is important for maintaining an improved intelligibility and naturalness, it only contains a small fraction of the speech energy, which is on the order of 1%, and therefore its bit-rate contribution has to be limited appropriately. The ITU G.722 codec [131] uses two equal-width subbands, whose signals are encoded employing ADPCM techniques. It has the ability of transmitting speech at 64, 56, or 48 kbits/s, while allocating 0, 8, or 16 kbits/s capacity for data transmission.

Quackenbush [132] suggested a transform-coded approach in order to allow for a higher flexibility in terms of allocating the bits available, which was proposed originally by Johnston [133] for 30-kHz-sampled high-fidelity audio signals, and reduced the bit rate required according to the lower sampling rate of 16 kHz. Ordentlich and Shoham proposed a low-delay CELP-based 32 kbits/s wide-band codec [134], which achieved a similar speech quality to the G.722 64 kbits/s codec at a concomitant higher complexity. The backward-adaptive linear predictive coding (LPC) filter used had an order of 32, which was significantly lower than the filter order of 50 used in the G.728 codec [117]. The G.728 filter order of 50 was able to cater for long-term periodicities of up to 6.25 ms, corresponding to pitch frequencies down to 160 Hz at a sampling rate of 8 kHz without a long-term predictor (LTP), allowing better reconstruction for female speakers. The filter order of 32 at a sampling frequency of 16 kHz cannot cater for long-term periodicities. Nonetheless, the authors opted for using no LTP. In contrast to the G.728 codebook of 128 entries, here 1024 entries were used to model the five-sample excitations.

In a contribution by Black *et al.* [135], the backward-adaptive principle was retained for the sake of low delay, but it was combined with a split-band approach. The low-band was encoded by a backward-adaptive CELP codec using a tenth-order LPC filter updated over 148-kHz-sampled samples or 1.75 ms. The authors argued that it was necessary to incorporate a forward-adaptive LTP in order to counteract the potentially damaging error feedback effect of the backward-adaptive LPC analysis. The upper band typically contains a less structured, noise-like signal, which has a slowly varying dynamic range. Black *et al.* here proposed to use a sixth order forward-adaptive predictor updated over a 56-sample interval, which is quadrupled in comparison to the low band. Backward-adaptive prediction would be unsuitable for this less accurately quantized band, which would precipitate the effect of quantization errors in future segments.

The prestigious speech-coding group at Sherbrooke University [136]–[138] proposed a range of ACELP-based codecs, since Laflamme *et al.* argued that ACELP codecs are amenable to wide-band coding, when employing vast codebooks in conjunction with a reduced-complexity focused codebook search strategy using a number of encapsulated search loops. This technique facilitates searching only a fraction of a large codebook, while achieving a similar performance to that of a full search. Suffice it to say here that this technique was proposed by the authors also for the

ITU G.729 8-kbits/s low-delay codec using a 15-bit ACELP codebook and five encapsulated loops [121], [122].

Here, we conclude our discussion of speech source codecs and briefly classify a range of video codecs suitable for wireless videophony and other wireless visual communications services before focusing our attention on wireless transmission aspects.

VI. Video Source Coding

A. Motivation and Background

Motivated by the proliferation of wireless multimedia services [139], [140], a plethora of video codec schemes have been proposed for various applications [141]–[156], but perhaps the most significant advances in the field are hallmarked by the MPEG-4 initiative [70]. The design of video-phone schemes centers around the best compromise among a number of inherently contradictory specifications, such as video quality, bit rate, implementational complexity, robustness against channel errors, coding delay, bit-rate fluctuation, and the associated buffer-length requirement. Many of these aspects have been treated in a number of established monographs by Netravali and Haskell [143], Jain [191], and Jayant and Noll [85], as well as Gersho and Gray [149]. A plethora of video codecs have been proposed in the excellent special issues edited by Tzou *et al.* [157], Hubing [158], and Girod *et al.* [159] for a range of bit rates and applications, but the individual contributions by a number of renowned authors are too numerous to review. Khansari *et al.* [166] as well as Pelz [180] reported promising results on adopting the H.261 codec for wireless applications by invoking powerful signal-processing and error-control techniques in order to remedy the inherent source-coding problems due to stretching its application domain to hostile wireless environments. Färber *et al.* [167]–[170] also contributed substantially toward advancing the state of the art in the context of the H.263 codec as well as in motion compensation [168], [169], as did Eryurtlu, Sadka, and Kondoz [174]–[175]. Further important contributions in the field were due to Chen *et al.* [181], Illgner and Lappe [182], Zhang [183], Ibaraki *et al.* [184], Watanabe *et al.* [185], the MPEG-4 consortium's endeavors [71], and the efforts of the Mobile Audio-Video Terminal Consortium. VQ-based schemes were advocated by Ramamurthy and Gersho [149], as well as by Torres and Huguet [150]. A major feature topic of the European Community's Fourth Framework Program [44], [45] on ACTS is video communications over a range of wireless and fixed links.

In this section, initially we focused our attention on the design and performance evaluation of wireless video telephone systems suitable for the robust transmission of QCIF sequences over conventional mobile radio links, such as the pan-European GSM system [40], the American IS-54 [41] and IS-95 [43] systems, and the Japanese PDC system [42]. In contrast to existing standard codecs, such as the ITU H.261 scheme and the MPEG-1 [80], MPEG-2 [81], and MPEG4 [70] arrangements, our proposed video codec's
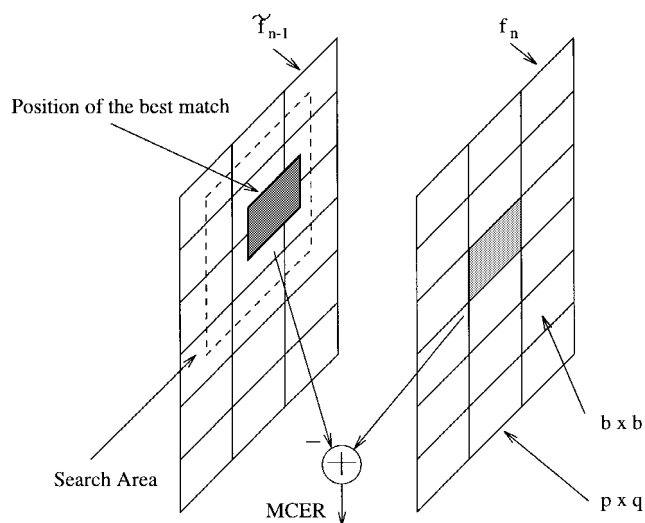

Fig. 5. Simplified schematic of motion compensation [186].

fixed but arbitrarily programmable bit rate facilitates its employment also in future intelligent systems, which are likely to vary their bit rate in response to various propagation and teletraffic conditions. We will conclude the section with a brief overview of the ITU H.263 standard video codec, which is a flexible scheme suitable for a range of multimedia visual applications at various bit rates and video resolutions.

B. Motion Compensation

The ultimate goal of low-rate image coding is to remove redundancy in both spatial and temporal domains and thereby reduce the required transmission bit rate. The temporal correlation between successive image frames is typically removed using block-based motion compensation, where each block to be encoded is assumed to be a motion-translated version of the previous locally decoded frame.

The vector of motion translation or MV is typically found with the help of correlation techniques, as seen in Fig. 5. Specifically, a legitimate motion-translation region or search scope is stipulated within the previous locally decoded frame, the block to be encoded is slid over this region according to a certain algorithm, and the location of highest correlation is deemed to be the destination of the motion translation. Motion compensation (MC) is then carried out by subtracting the appropriately motion-translated previous decoded block from the one to be encoded in order to generate the MCER. Clearly, the image is decomposed in motion translation and MCER, and both components have to be encoded and transmitted to the decoder for image reconstruction. The motion compensation removes some of the temporal redundancy, and the variance of the MCER becomes much lower than that of the original image, which ensures bit-rate economy.

The MCER frame can then be represented using a range of techniques [190], including SBC [144], [145], wavelet coding [146], DCT [80], [81], [188], [191], VQ [149]–[151], or QT coding [147], [148], [155], [189]. Some
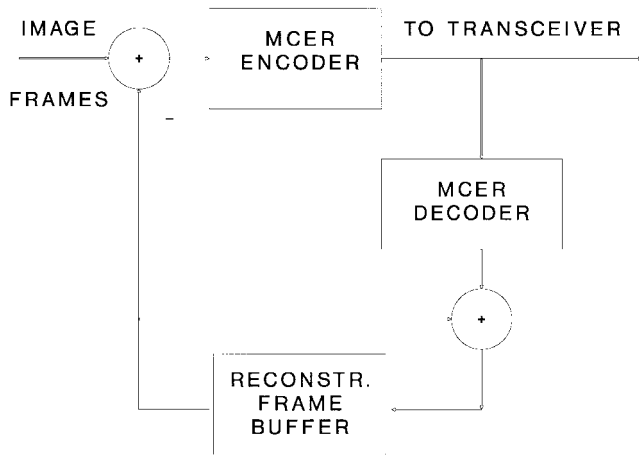
Fig. 6. Simple video codec schematic.

of these techniques will be highlighted in the forthcoming subsections.

When a low codec complexity and low bit rate are required, the motion-compensation technique described above can be replaced by simple frame differencing. In frame differencing, the whole of the previous locally decoded image frame is subtracted from the one to be encoded without the need for the above correlation-based motion prediction, which may become very computationally intensive for high-resolution, high-quality video portraying high-dynamic scenes. Such a simple video codec schematic based on simple frame differencing is shown in Fig. 6. Although the MCER residual variance remains somewhat higher for frame differencing than in case of full motion compensation, there is no pattern-matching search, which reduces the complexity, and no MV's have to be encoded, which may reduce the overall bit rate. Observe in Fig. 6 that after frame differencing, the encoded MCER is conveyed to the transceiver and also locally decoded. This is necessary to be able to generate the locally reconstructed video signal, which is invoked by the encoder in subsequent MC steps. The encoder uses the locally reconstructed rather than the original input video frames, since these are not available at the decoder, which would result in misalignment between the encoder and decoder. This local reconstruction operation is carried out by the adder in the figure, superimposing the decoded MCER on the previous locally decoded video frame. The operations are similar if full MC is used. Practical codecs such as, for example, the ITU H.263 scheme, often combine the inter- and intraframe coding techniques on a block-by-block basis, where MC is employed only if it is deemed advantageous in MCER reduction terms.

In the case of highly correlated consecutive video frames, the MCER typically exhibits "line-drawing" characteristics, where large sections of the frame difference signal are "flat," characterized by low pixel magnitude values, while the motion contours, where the frame differencing has failed to predict the current pixels on the basis of the previous locally decoded frame, are represented by larger values, as seen in at the center of Fig. 9. Consequently,

efficient MCER residual coding algorithms must be able to represent such textured MCER patterns adequately, a topic to be addressed in the forthcoming subsections. Let us initially consider a bandwidth-efficient cost-gain quantized DCT-based codec [188].

C. DCT-Based Video Codec

Our DCT-based video codec's outline is depicted in Fig. 7. The DCT [191] has been popular in video-compression standards [80], [81] since it exhibits a so-called energy compaction property, implying that upon transforming a correlated or predictable signal to the spatial frequency domain, most of its energy will be compacted to a few high-energy, low-frequency coefficients. This is a consequence of the Wiener–Khnitsin theorem, stating that the power spectral density (PSD) and the autocorrelation function (ACF) are Fourier transform pairs. Hence, the flat ACF of a predictable, slowly varying signal implies a compact low-pass-type PSD, which is amenable to compression since in the spatial frequency domain, a lower number of coefficients has to be transmitted than in the temporal domain. It is important to note that the MC often removes most of the redundancy from the correlated temporal-domain video frame, and hence the DCT of the MCER may even result in an expanded spatial frequency-domain representation, which can be counteracted, for example, by adaptive bit-allocation schemes. Strobach [147] proposed QT coding in order to encode the MCER and mitigate this problem. Alternative frequency-domain solutions include SBC [144], [145] or wavelet coding [146], which facilitate a flexible control over the allocation of bits in the spatial frequency domain. The MPEG standard codecs [80], [81] and the H.261 and H.263 codecs scan and entropy code the DCT coefficients and also allow direct encoding of the more correlated video signal on a block-by-block basis. VQ [149]–[151] can be carried out in both the frequency and time domains, but a persistent deficiency is their difficulty to handle sharp edges adequately.

Returning to the DCT principle, our proposed DCT-based codec was designed to achieve a time-invariant compression ratio associated with a fixed but programmable encoded video rate of 5–13 kbits/s.[1] The codec's operation is initialized in the intraframe mode, but once it switches to the interframe mode, any further mode switches are optional and only required if a drastic scene change occurs.

In the intraframe mode, the encoder transmits the coarsely quantized block averages for the current frame, which provides a low-resolution initial frame required for the operation of the interframe codec both at the commencement and during later stages of communications in order to prevent encoder/decoder misalignment. For 176× 144-pixel ITU standard QCIF images in a specific scenario [188], we limited the number of video-encoding bits per frame to 1136, corresponding to a bit rate of 11.36 kbits/s at 10 frames/s.

---

[1] The Miss America sequence encoded at various bit rates can be viewed at http://www-mobile.ecs.soton.ac.uk.
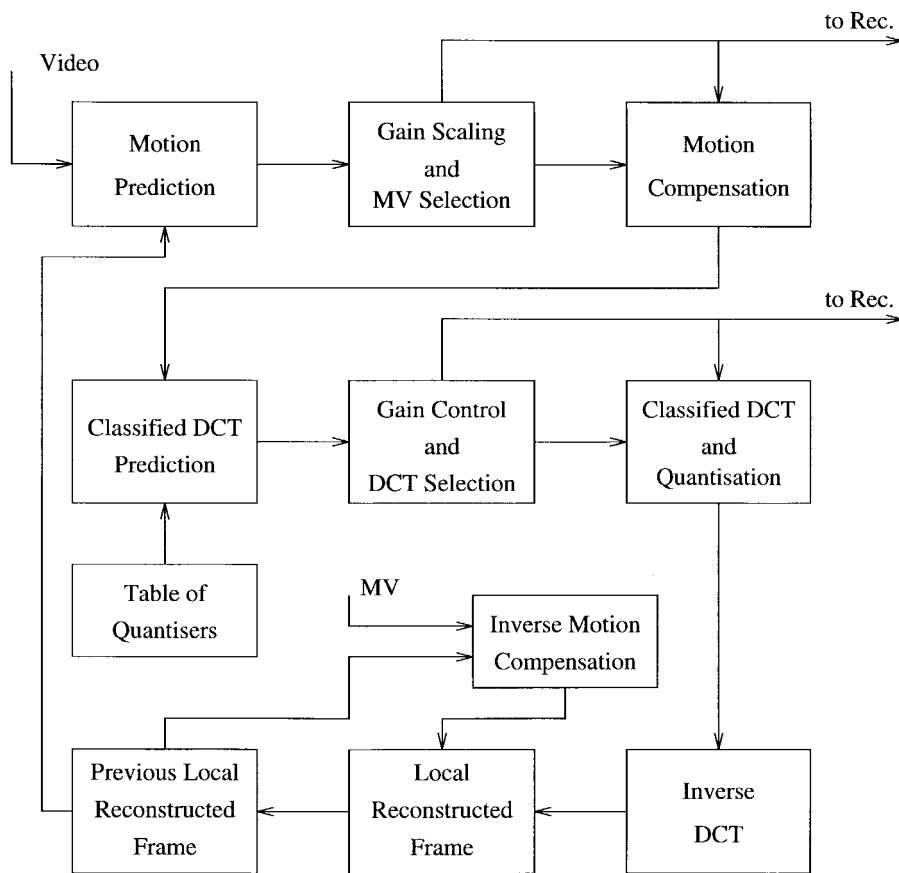
Fig. 7. DCT-codec schematic [188].

In the motion compensation, 8×8 blocks are used. At the commencement of the encoding procedure, the MC scheme determines an MV for each of the 8×8 blocks using full search. The MC search window is fixed to 4×4 pels around the center of each block, and hence a total of 4 bits are required for the encoding of 16 possible positions for each MV. Before the actual motion compensation takes place, the codec tentatively determines the potential benefit of the compensation in terms of motion-compensated error energy reduction. Then the codec selects as "motion active" those blocks whose gain exceeds a certain threshold. This method of classifying the blocks as motion active and motion passive results in an active/passive table, which consists of a 1-bit flag for each block, marking it as passive or active.

Pursuing a similar approach, gain control is also applied to the DCT-based compression. Every block is DCT transformed and quantized. To take account of the nonstationary nature of the MCER and its time-variant frequency-domain distribution, four different sets of DCT quantizers were designed. The quantization distortion associated with each quantizer is computed in order to be able to choose the best one. Ten bits are allocated for each quantizer, each of which is a trained Max–Lloyd quantizer catering for a specific frequency-domain energy distribution class. All DCT blocks whose coding gain exceeds a certain threshold are marked as DCT-active, resulting in a similar active/passive table as for the motion vectors. For this second table, we apply the same run-length compression technique as above. Again, if the number of bits required for the encoding of the DCT-active blocks exceeds half of the maximum allowable number, blocks around the fringes of the image, rather than those in the central eye and lip sections, are considered DCT-passive. If, however, the active DCT coefficient and activity table do not fill up the fixed-length transmission burst, the thresholds for active DCT blocks are lowered and all tables are recomputed.

The bit-allocation scheme was designed to deliver 1136 bits per frame, which is summarized in Table 1. The encoded bitstream begins with a 22-bit frame alignment word (FAW). This is necessary to assist the video decoder's operation in order to resume synchronous operation after loss of frame synchronization over hostile fading channels. The partial intraframe update refreshes only 22 out of 396 blocks every frame. Therefore, every 18 frames, or 1.8 seconds, the update refreshes the same blocks. This periodicity is signalled to the decoder by transmitting the inverted FAW. An MV is stored using 13 bits, where 9 bits are required to identify one of the 396 block indexes using the enumerative method and 4 bits for encoding the 16 possible combinations of the X and Y displacements. The 8×8 DCT-compressed blocks use a total of 21 bits, again 9 for the block index, 10 for the DCT coefficient quantizers, and 2 bits to indicate which of the four quantizers has been applied. The total number of bits becomes $30 \cdot (13 + 21) + 22 \cdot 4 + 22 + 6 = 1136$, where six dummy bits were

Table 1 Bit-Allocation Table Per QCIF Video Frame for the Fixed-Rate DCT Codec [188]

FAW	PFU	MV Index	MV	DCT Index	DCT	Padding	Total
22	22×4	30×9	30×4	30×9	30×12	6	1136
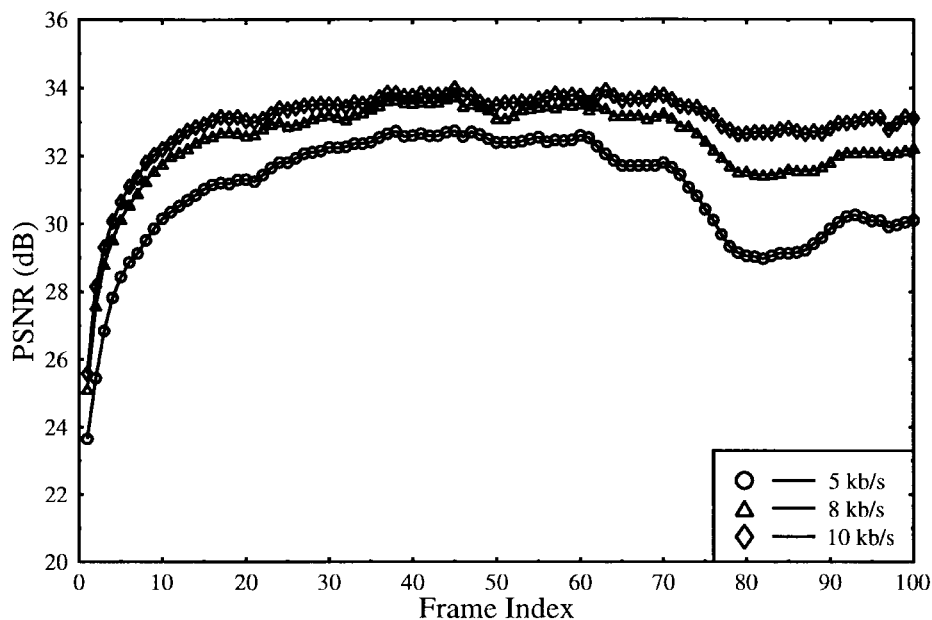
Fig. 8. PSNR versus frame index performance at various bit rates for the "Miss America" sequence [188].

added in order to obtain a total of 1136 bits suitable in terms of bit packing requirements for the specific forward error-correction block codec used.

The encoded parameters are transmitted to the decoder and also locally decoded in order to be used in future motion predictions. The video codec's peak (P)SNR versus frame index performance is shown in Fig. 8, where the PSNR is defined as the conventional SNR except that instead of the actual video signal power, a video pixel value of 255 is assumed, yielding a pixel power of 255^2 for all pixel positions across the video frame. Since 255 is the highest possible value for an 8-bit pixel representation, the PSNR is typically higher than the conventional SNR. The codec proposed was subjected to bit-sensitivity analysis, and a QAM-based [68] source-sensitivity matched transceiver was designed in order to transmit the video stream over wireless channels. The interested reader is referred to [188] for further details. Having described the principles of DCT-based video coding, let us now consider QT coding of the MCER [189].

D. QT Structured Coding

The proposed QT codec shares the structure of the previous DCT-based scheme portrayed in Fig. 7 but employs QT coding of the MCER. QT's represent a subclass of the so-called region growing techniques, where the image, in our case the MCER generated by the MC scheme, is described with the help of variable-size sectors characterized by similar features, in this case, similar gray levels. Explicitly,

the MCER is described in terms of two sets of parameters: the structure of similar regions and their gray levels. Note that the information characteristic of the QT structure is potentially much more sensitive to bit errors than the gray-level coding bits.

Before QT decomposition takes place, the frame difference signal is divided in 16 × 16-pixel blocks perfectly tiling the original difference frame. Creating the QT regions is a recursive operation. Considering each individual pixel, two or more neighbors are merged together if a certain merging criterion is satisfied. This criterion may be, for instance, a similar gray level. This merging procedure is repeated until no more regions satisfy the merging criterion; hence, no more merging is possible. Similarly, the QT regions can be obtained in a top-down approach, dividing the MCER in a number of sections, if the sections do not satisfy the similarity criterion and continue until the pixel level is reached and no further splits are possible.

The QT approach is one possible implementation of the region growing techniques. This process can be observed in Fig. 9. For a rectangular region, an algorithmically attractive implementation is: when commencing at the pixel level, four quadrants of a square are merged together if the matching criterion is met. The gray levels of the quadrants of a square are represented by $m1 \cdots m4$, and their mean is computed according to $m = (m_1 + m_2 + m_3 + m_4)/4$. If the absolute difference of all four pixels and the mean gray level is less than the system parameter σ, then these pixels satisfy the merging criterion. Explicitly, a simple merging

Fig. 9. QT segmentation example with and without overlaid MCER and original video frame [189].

criterion can be formulated as follows:

$$(|m - m_1| < \sigma) \cap (|m - m_2| < \sigma) \cap (|m - m_3| < \sigma)$$
$$\cap (|m - m_4| < \sigma) = \text{True} \quad (1)$$

where $\cap$ represents the logical AND operation.

It is expected that if the system parameter σ is reduced, the matching criterion becomes more stringent and hence less merging takes place, which is likely to increase the required encoding rate at a concomitantly improvement of the MCER's representation quality. In contrast, an increased σ value is expected to allow more merging to take place and hence reduce the bit rate, as we will show in our results section.

If the merging criterion is satisfied, the mean gray level m becomes the gray level of the merged quadrant in the next generation, and so on. At this stage, it is important to note that the quality-control threshold σ does not need to be known to the QT decoder. Therefore, the image representation quality can be rendered position dependent within the frame being processed, which allows weighting to be applied to important image sections such as the eyes and lips without increasing the complexity of the decoder or the transmission rate.

Pursuing the top-down QT decomposition approach, the frame difference signal constitutes a so-called node in the QT. After splitting, this node gives rise to four further nodes, which are classified on the basis of the "similarity criterion." Specifically, if all the pixels at this level of the QT differ from the mean m by less than the threshold σ, then they are considered to be a "leaf node" in the QT. Hence, they do not have to be subjected to further "similarity tests"; they can be represented simply by the mean value m.

If, however, the pixels constituting the current node to be classified differ by more than the threshold σ, the pixels forming the node cannot be adequately represented by their mean m, and thus they must be further split until the threshold condition is met. This repetitive splitting process is continued until there are no more nodes to split, since all the leaf nodes satisfy the threshold criterion, as shown in Fig. 9. Consequently, the QT structure describes the contours of similar gray levels in the frame difference signal.

To be able to reproduce the encoded image, not only the gray levels of the leaf nodes but also the QT structure must be efficiently encoded and communicated to the decoder. Fortunately, the QT structure can be efficiently described with the help of a variable-length code. At the commencement of image communications, a low-resolution version of the first image frame is encoded and transmitted to the decoder in order to assist in its operation. Then the MCER signal is computed, which is subjected QT coding, before transmission to the decoder. Again, the schematic of the QT codec obeys the structure of Fig. 6. The QT-coded MCER is locally decoded and added to the previous locally decoded frame and stored in the frame buffer for the duration of one frame in order to generate the next block estimates for the MC operation. A range of techniques related to the optimum QT splitting and bit-allocation techniques were suggested in [189], where also details of the source-matched video transceiver can be found. Adequate video quality was achieved for the Miss America sequence for a bit rate of 11.36 kbits/s when using scanned QCIF images of 10 frames/s.

Without aiming for an in-depth treatment, we briefly allude to the concept of vector quantized video codecs, where the MCER of an 8×8 pixel block is represented by the best matching entry of the two-dimensional codebook shown in Fig. 10. This principle also allowed us to contrive an 11.36-kbits/s QCIF codec for wireless video telephony, the details of which were presented in [187], where the full transceiver performance over fading channels is also characterized. The above-mentioned range of fixed-rate video codecs is compared in terms of error resilience and video quality in [190]. In [187]–[189], a range of flexible reconfigurable multilevel transceivers were designed for the transmission of the VQ-, DCT-, and QT-coded video streams by allocating an addition physical speech channel for video telephony. For reasons of space economy, however, these results were not included here. Similar video PSNR versus channel SNR results are provided here using the ITU H.263 video codec and a reconfigurable transceiver in order to characterize the expected video performance in Figs. 27 and 28.[2]

In closing, we note again that the literature of video compression is very rich [139]–[156], and recent developments led to the definition of the MPEG-1, MPEG-2, H.261, and H.263 standards. Although these codecs rely on vulnerable

---

[2] The exposition of this section can be augmented by studying the corresponding real-time video quality at http://www-mobile.ecs.soton.ac.uk.
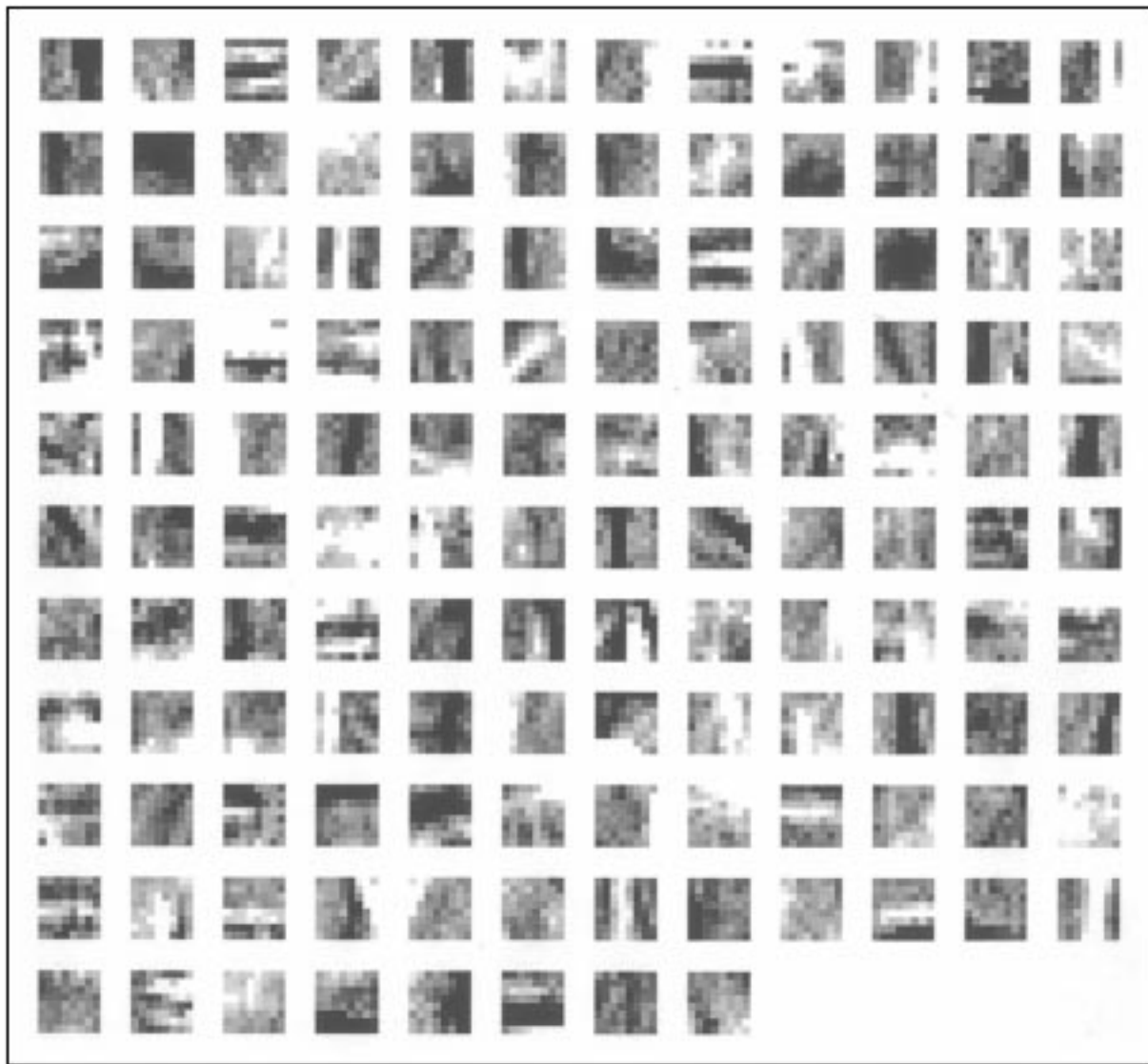
Fig. 10. Enhanced sample codebook with 128 8 × 8 vectors [190].

variable-length coding techniques, work is also under way toward contriving more robust coding algorithms, such as those to be incorporated in the forthcoming MPEG-4 scheme [71], [70]. In the next subsection, we briefly highlight the features of the standard H.263 scheme, which is an error-sensitive, variable-rate scheme but achieves a very high compression ratio. Hence, to date, it is the best existing standardized video codec. We will also propose appropriate transmission techniques to support its operation in a wireless video-phone scheme.

E. The H.263 ITU Codec

The H.263 codec was detailed in [193] and [194], while a number of transmission schemes designed for accommodating its rather error-sensitive bit stream were proposed in [167], [170], [179]. As an illustrative example, in Table 2, we summarize the various video resolutions supported by the H.261 and H.263 ITU codecs in order to demonstrate their flexibility [192]. Their uncompressed bit rates at frame scanning rates of both 10 and 30 frames/s for both gray

and color video are also listed. The mature H.261 standard defined two different picture resolutions, namely, QCIF and CIF, while the H.263 codec has the ability to support five different resolutions. All H.263 decoders must be able to operate in sun (S)QCIF and QCIF modes and optionally support CIF, 4 × CIF, and 16× CIF formats.

The H.261 and H.263 codecs share the simplified schematic of Fig. 11, which operates under the instructions of the coding control block, selecting the required inter/intraframe mode, the quantization and bit-allocation scheme, etc. DCT is invoked to compress either the original or the MCER blocks, and the encoded video signal is also locally decoded and stored in the frame memory in order to be used in future MC steps. All encoded information is multiplexed for transmission by the video multiplex coder. The codec's PSNR versus encoded bit-rate performance is portrayed in Fig. 12 for Miss America simulations at 10 and 30 frames/s using SQCIF, QCIF, and CIF sequences [192]. Observe in the figure that the codec guarantees near linear rate scalability over a wide operating range, which is

Table 2 Various Video Formats and Their Uncompressed Bit Rate. Upon Using Compression 10–100 Times Lower, Average Bit Rates Are Realistic

Video Format	Luminance dimensions	No. of Pels per frame	Uncompressed bitrate (Mbit/s)			
			10 frame/s		30 frame/s	
			Grey	Colour	Grey	Colour
SQCIF	128 x 96	12 288	0.983	1.47	2.95	4.42
QCIF	176 x 144	25 344	2.03	3.04	6.09	9.12
CIF	352 x 288	101 376	8.1	12.2	24.3	36.5
4CIF	704 x 576	405 504	32.4	48.7	97.3	146.0
16CIF	1408 x 1152	1 622 016	129.8	194.6	389.3	583.9
CCIR 601	720 x 480	345 600	27.65	41.472	82.944	124.416
HDTV 1440	1440 x 960	1 382 400	110.592	165.888	331.776	497.664
HDTV	1920 x 1080	2 073 600	165.9	248.832	497.664	746.496

SQCIF: Sub-Quarter Common Intermediate Format
QCIF: Quarter Common Intermediate Format
CIF: Common Intermediate Format
HDTV: High Definition Television
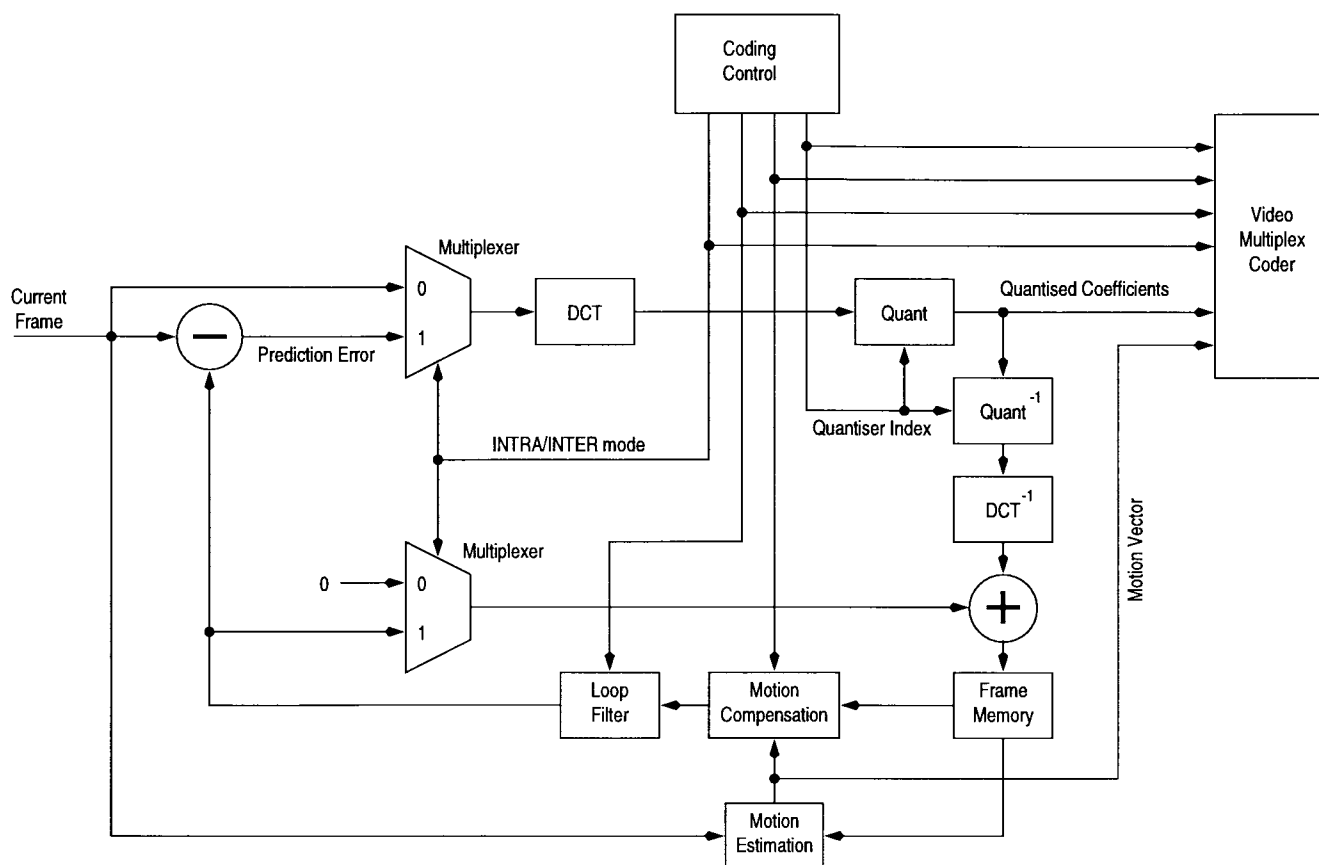
Fig. 11. Simplified H.261/H.263 schematic [192].

partly explained by the extensive employment of entropy coding schemes. The performance of a complete adaptive video-phone system will be portrayed after considering the associated wireless transmission aspects.

Here, we curtail our discussion on video codecs and provide some notes on another aspect of multimedia communications, namely, graphical correspondence.

VII. GRAPHICAL SOURCE CODING

A. Background

Telewriting is a multimedia telecommunications service enabling the bandwidth-efficient transmission of handwritten text and line graphics through fixed and wireless communication networks [196]–[201]. Differential chain coding has been successfully used for graphical communications over e-mail networks [196] or teletext systems [199], where bit-rate economy is achieved by exploiting the correlation between successive vectors. References [197] and [202] address some of the associated communications aspects. A plethora of further excellent papers were contributed to the literature of chain coding by Prasad and his colleagues from Delft University [203]–[205].

B. Fixed-Length Differential Chain Coding [206]

In CC, a square-shaped coding ring is slid along the graphical trace from the current pixel, which is the origin
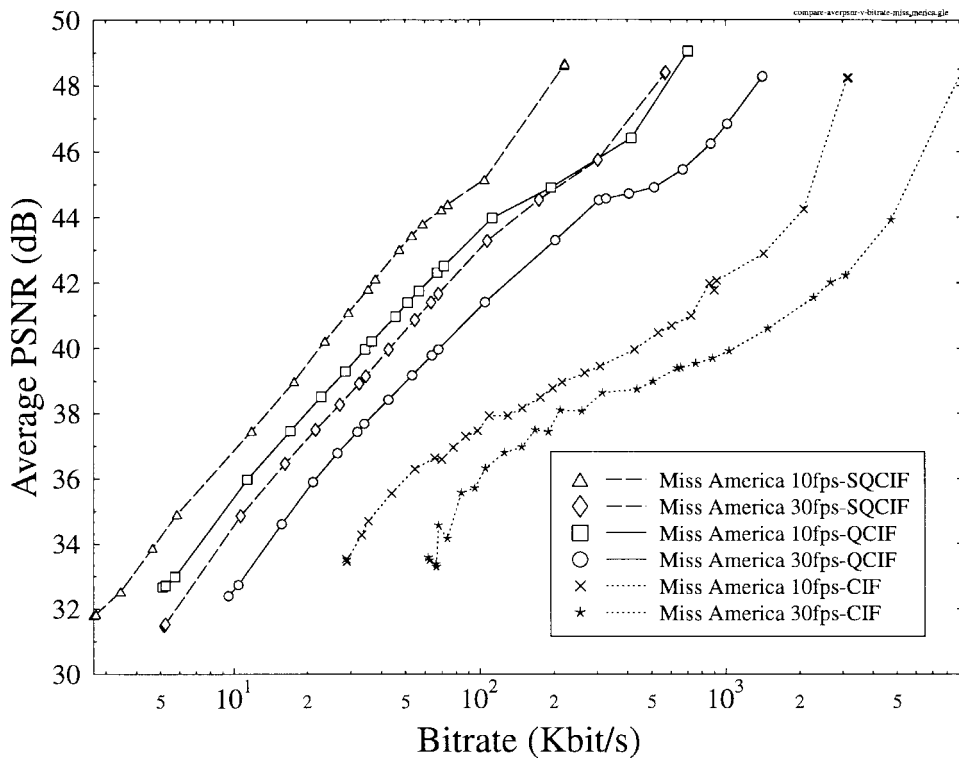
Fig. 12. Image quality (PSNR) versus coded bit rate for H.263 Miss America simulations at 10 and 30 frames/s using SQCIF, QCIF, and CIF sequences [192].

of the legitimate motion vectors, in steps represented by the vectors portrayed in Fig. 13. The bold dots in the figure represent the next legitimate pixels during the graphical trace's evolution. In principle, the graphical trace can evolve to any of the surrounding eight pixels, and hence a 3-bit code word is required for lossless coding. DCC [203] exploits that the most likely direction of stylus movement is a straight extension, corresponding to vector zero, and with a gradually reducing probability of sharp turns, corresponding vectors having higher indexes. Explicitly, we have found that while vector zero typically has a probability of around 0.5 for a range of graphical source signals, including English and Chinese handwriting, a map, and a technical drawing, the relative frequency of vectors ± 1 is around 0.2, while vectors ± 2, ± 3 have probabilities around 0.05. This suggests that the coding efficiency can be improved using the principle of entropy coding by allocating shorter code words to more likely transitions and longer ones to less likely transitions.

In [206], we embarked on exploring the potential of a graphical coding scheme dispensing with variable-length coding, which we refer to as FL-DCC. FL-DCC was contrived in order to comply with the time-variant-resolution and/or bit-rate constraints of intelligent adaptive multimode terminals, which can be reconfigured under network control to satisfy the momentarily prevailing teletraffic, robustness, quality, etc. system requirements. To maintain lossless graphics quality under lightly loaded traffic conditions, the FL-DCC codec can operate at a rate of $b = 3$ bits/vector, although it has a higher bit rate than DCC. However, since in voice and video coding typically perceptually unimpaired
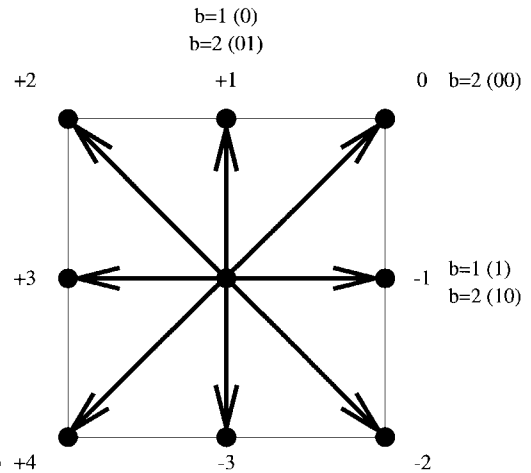

Fig. 13. Coding ring.

lossy quantization is used, we embarked on exploring the potential of the reconfigurable FL-DCC codec under $b < 3$ low-rate, lossy conditions.

Based on our findings as regards the relative frequencies of the various differential vectors, we decided to evaluate the performance of the FL-DCC codec using the $b = 1$ and $b = 2$ bit/vector lossy schemes. As demonstrated by Fig. 13, in the $b = 2$-bit mode, the transitions to pixels -2, -3, $+2$, $+3$ are illegitimate, while vectors 0, $+1$, -1, and $+4$ are legitimate. To minimize the effects of transmission errors, the Gray codes seen in Fig. 13 were assigned. It will be demonstrated that due to the low probability of occurrence of the illegitimate vectors, the
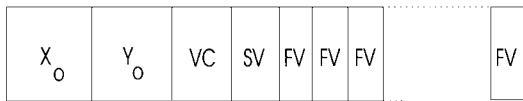
Fig. 14. FL-DCC coding syntax [206].

associated subjective coding impairment is minor. Under degrading channel conditions or higher teletraffic load, the FL-DCC coding rate has to be reduced to $b = 1$ in order to be able to invoke a less bandwidth-efficient but more robust modulation scheme or to generate less packets contending for transmission. In this case, only vectors $+1$ and -1 of Fig. 13 are legitimate. The subjective effects of the associated zigzag trace will be removed by the decoder, which can detect these characteristic patterns and replace them by a fitted straight line.

In general terms, the size of the coding ring is given by $2n\tau$, where $n = 1, 2, 3 \cdots$ is referred to as the order of the ring and τ is a scaling parameter characteristic of the pixel separation distance. Hence, the ring shown in Fig. 13 is first order. The number of nodes in the ring is $M = 8n$.

The data syntax of the FL-DCC scheme is displayed in Fig. 14. The beginning of a trace can be marked by a typically 8-bit-long PD code, while the end of a trace can be marked by a PU code. To ensure that these codes are not emulated by the remaining data, if this would be incurred, bit stuffing must be invoked. We found that in complexity and robustness terms using a VC constituted a more attractive alternative for our system. The starting coordinates X_0, Y_0 of a trace are directly encoded using, for example, ten and nine bits in case of a video graphics array resolution of 640×480 pixels.

The first vector displacement along the trace is encoded by the best fitting vector defined by the coding ring as the SV. The coding ring is then translated along this starting vector to determine the next vector. A differential approach is used for the encoding of all the following vectors along the trace in that the differences in direction between the present vector and its predecessor are calculated, and these vector differences are mapped into a set of 2^b fixed-length b-bit code words, which we refer to as FV's.

We designed a wireless 4-QAM-based [68] transceiver for the transmission of FL-DCC encoded graphical source signals and evaluated the system's robustness over Rayleigh-fading channels with second-order switched diversity, using automatic repeat requests limited to a maximum of three transmission attempts (TX3) [207]. Here, we refrain from providing PSNR versus channel SNR curves; for these, the interested user is referred to [207]. However, the corresponding subjective graphical quality and the associated PSNR values are summarized in Fig. 15 for the channel SNR range of 5–12 dB, respectively. Due to its low channel capacity requirement, the FL-DCC coded signal is readily accommodated by the voice signal during passive speech spurts when using a VAD [40]. Last, it is noteworthy that the ITU standardized two different CC schemes in the T.150 recommendation for use over conventional low-BER fixed telephone lines.

For wireless channels, however, the proposed FL-DCC scheme is preferable due to its higher robustness and programmable-rate operation.

We note that an associated multimedia signal manipulation relying on writing tablets is the field of handwriting recognition for both on-line and off-line applications [208]–[213]. Many of the techniques used are based on HMM's, which are widely employed in the field of speech recognition. Previous research has shown that HMM's are applicable to both off-line [212] and on-line [208], [210], [213] handwriting recognition problems. The advantage of such statistical methods is that they can handle variability in the writing process of an individual but are also capable of identifying and capturing the individual features of the handwritten characters by taking into account dynamic, pressure-dependent features. In many applications, the handwritten data are described by the directional writing angle as a function of the distance along the writing trajectory.

Following the above brief excursion to graphical source compression and signal processing, here we turn our attention to wireless communications aspects, commencing with a review of the frequency reuse concept of cellular systems.

VIII. Cellular Communications Basics

A. The Cellular Concept

A common feature of the previously mentioned mobile radio systems is that communications take place between a stationary BS and a number of roaming MS's or PS's [1]–[9]. The BS's and the MS's transmitter is expected to provide a sufficiently high received signal level for the far-end receivers in order to maintain the required communications integrity. This is usually ensured by power control. The geographical area in which this condition is satisfied is termed a traffic cell, which typically has an irregular shape, depending on the prevailing propagation environment determined by terrain and architectural features as well as the local paraphernalia. In theoretical studies, often a simple hexagonal cell structure is favored for its simplicity, where the BS's are located at the centers of the cells.

In an ideal situation, the total bandwidth available to a specific mobile radio system could be allocated within each cell, assuming that there is no energy spilt in the adjacent cell's coverage area. However, since wave propagation cannot be shielded at the cell boundary, PS's near the cell edge would experience approximately the same signal energy within their channel bandwidth from at least two BS's. This phenomenon is called *cochannel interference*. A remedy to this problem is to divide the total bandwidth B_{total} in frequency slots of $B_{\text{cell}} = B_{\text{total}}/N$ and assign a mutually exclusive reduced bandwidth of B_{cell} to each traffic cell within a *cluster* of N cells, as demonstrated in Fig. 16 for $N = 7$. The seven-cell clusters are then tesselated in order to provide contiguous radio coverage. Observe from the figure that the phenomenon of cochannel

Fig. 15. Subjective effects of transmission errors for the $b = 1$ 16-QAM, Rayleigh/diversity, TX3 scheme for PSNR values of (left to right, top to bottom) 49.47, 42.57, 37.42, 32.01, 27.58, and 21.74 dB [207].

interference between the black cochannel cells having an identical frequency set is not eliminated, but due the increased cochannel BS distance or *frequency reuse distance,* the interference is significantly reduced. Note also that in analytical and simulation-based interference studies, the "second tier" of interfering cells, which are hatched, is typically neglected.

A consequence of the above cellular concept, however, is that the total number of MS's that can be supported simultaneously over a unit area is now reduced by a factor of N. This is because assuming a simple FDMA scheme, where each MS is assigned an RF carrier and a user bandwidth of B_{user}, now only $M = B_{\mathrm{cell}}/B_{\mathrm{user}}$ number of MS's can be serviced, rather than $N \cdot M = B_{\mathrm{total}}/B_{\mathrm{user}}$. This problem can be circumvented by making the clusters as small as the original cells, which is achieved by reducing the transmitted power. In fact, further reduction of the cell size has the advantage of serving more and more users while requiring a reduced transmitted signal power and hence lightweight batteries. A further favorable effect is that the smaller the traffic cell, the more benign the propagation environment due to the presence of a dominant

LOS propagation path and the mitigated effects of the multipath propagation. These arguments lead to the concept of *micro- and picocells* [20]–[22], which are often confined to the size of a railway station or airport terminal and an office, respectively. Cluster sizes smaller than $N = 7$ are often used in practice in order to enhance the system's spectral efficiency, but such schemes require modulation arrangements that are resilient against the increased cochannel interference. These different cells will have to coexist in practical systems, where, for example, an "oversailing" macrocell can provide an emergency handover capability for the microcells when the MS roams in a propagation blind spot but cannot hand over to another microcell, since in the target microcell no traffic channels are available.

The various cell scenarios are exemplified by Fig. 17, where the conventional macrocell BS is allocated to a high tower, illuminating a large area but providing a rather hostile propagation cell, since often there is no LOS path between the BS and PS. Hence the communications are more prone to fading than in the stylized microcell illuminated by the antenna at the top of the lower buildings. The smaller microcells typically use lower transmit power
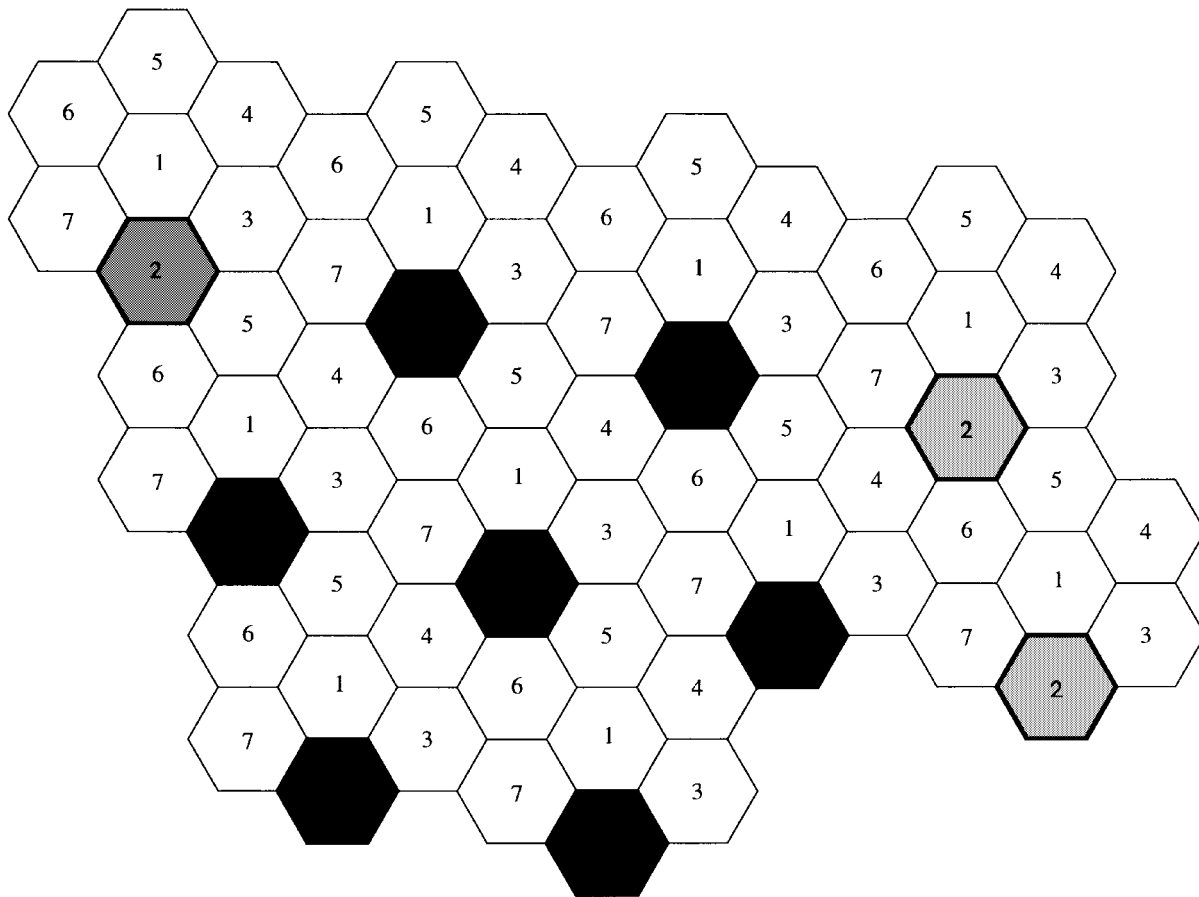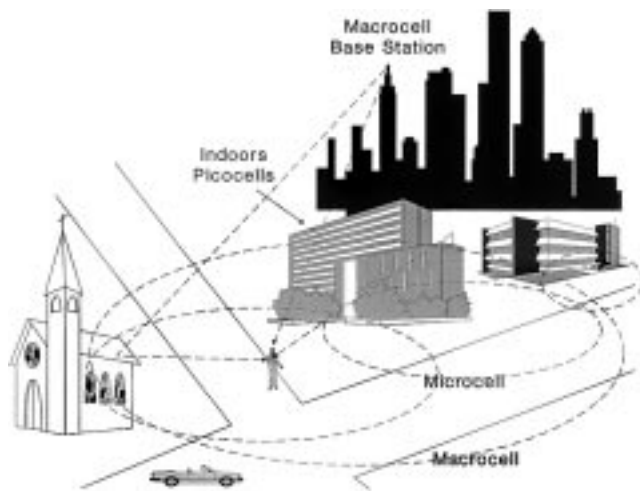
Fig. 16. Hexagonal cells and seven-cell clusters.

Fig. 17. Various traffic cells.

Fig. 18. Handover control parameters.

and channel most of the energy in the street canyon, which mitigates the signal's variability and hence has more benign fading. Furthermore, microcells also reduce the signal's dispersion due to path-loss differences. Last, indoors, picocells provide typically even better channels and tend to mitigate cochannel interferences due to partitions and ceilings.

The previously mentioned handover process is crucial as regards the perceived GOS, and a wide range of different complexity techniques have been proposed—for example,

by Tekinay *et al.* in [23] and [24]—for the various existing and future systems, some of which are summarized in Fig. 18. Explicitly, the BS and PS keep compiling the statistics of a range of communications quality parameters shown in the figure and weight them according to the prevalent optimization criterion before a handover or mode of operation reconfiguration command is issued. Although the PS plays an active role in monitoring the various parameters, these are typically reported to the BS, which carries out the required decisions.

A further important issue associated with the cellular concept and cellular planning is DCA, where a variety of algorithms can be invoked to support the system's operation [25]–[29] in order to mitigate the effects of CCI and to maximize the number of traffic channels supported. These techniques are typically invoked in cordless telephone systems, such as DECT and CT2 [12]. The basic concept of DCA is fairly plausible, since the MS scans the physical channels in order to identify the specific channel exhibiting the lowest signal level before camping on the one that was deemed to inflict the lowest level of cochannel interference. Chuang *et al.* [25]–[27] documented the performance of a variety of DCA algorithms, arguing that these techniques under certain conditions can converge to a local minimum of the total interference averaged over the network. In closing, we note that there exists a different dynamic channel-allocation philosophy, which was proposed by Bernhardt [28], [29], advocating the employment of the worst possible channel that satisfies a minimum SIR condition. This is equivalent to invoking the worst "just tolerable" physical channel for communications, which intuitively allows a more compact frequency reuse pattern to be employed but naturally requires a robust modulation scheme. The overall benefit is an expected higher number of accommodated users.

The family of DCA algorithms is closely related to a range of multiple access schemes; hence, we consider multiple access next.

B. Multiple Access

The physical channel, which the MS and BS use for their communications, can be manifested by a given frequency slot, assigned to the MS for the entire duration of a call. This was the case in most first-generation FDMA mobile radio systems. In the second-generation systems, such as the pan-European GSM [330], the American IS-54 [41], and the Japanese PDC system [42], TDMA was proposed, assigning the whole bandwidth of a TDMA carrier to an MS for a fraction of the time, i.e., for the duration of a time slot. The American IS-95 CDMA system [43] uses all the system bandwidth all the time for all users, communicating with orthogonal *signature* codes. However, these systems employ *contentionless bandwidth allocation,* where the physical channel is not exploited to its full capacity due to being assigned to users also during their passive speech spurts, when they are listening or thinking, etc.

By contrast, *statistical multiplexing* schemes surrender the physical channel during passive speech spurts, when the channel is not actively used by the MS. This often leads to substantially increased user numbers' being supported by the system. A range of MAC protocols have been advocated in the literature [218]–[228], most of which were featured in a recent excellent overview by Li and Qiu in [32].

PRMA is a statistical multiplexing method for conveying speech signals via TDMA systems, which was proposed by Goodman [218] and Wei [220]. A range of various PRMA-assisted CT systems were proposed in [229]–[233]. The operation of PRMA is based on the VAD's being able reliably to detect inactive speech segments [330]. Inactive users' TDMA time slots are allocated to other users, who become active. The users, who are just becoming active, have to contend for the available time slots with a certain permission probability P_p, which is an important PRMA parameter to be augmented at a later stage.

Previously colliding users contend for the next available time slot with a less-than-unity permission probability P_p in order to prevent them from consistently colliding in their further attempts to attain reservation. If more than one user is contending for a free slot, neither of them will be granted it. If, however, only one user requires the time slot, he can reserve it for future use until he becomes inactive. Under heavily loaded network conditions, when many users are contending for a reservation, a speech packet might have to contend for a number of consecutive slots. When the contention delay exceeds a latency of about 30 ms, the contending speech packet of typically 20-ms duration must be dropped. The probability of packet dropping must be kept below 1%, a value inflicting minimal degradation in terms of perceived speech quality.

Suffice it to say here that in order to find the optimum permission probability P_p, the number of users supported at less than 1% packet dropping must be determined for various P_d values, and the curve's maximum has to be identified. The rule of thumb is that when a system can support twice the number of slots in comparison to another, the corresponding P_p value must be halved in order to maintain the desirable contention rate for each slot. When P_p is high, too vigorous contentions are encouraged, resulting in unacceptably high collision rates. By contrast, too low a P_p value does not exploit the system's full teletraffic capacity due to a modest statistical multiplexing gain.

The performance potential of PRMA was analyzed using the *equilibrium point analysis* technique by Nanda *et al.* [221]. The underlying assumption of the equilibrium point analysis is that the PRMA system can be characterized by a Markov model, and the number of users entering a given Markov state is identical to the number of users leaving it. The above PRMA technique was refined by Dunlop *et al.* [222], where the authors have restricted contentions to *contention minislots,* thereby mitigating the effects of packet collisions. This scheme was termed PRMA++. PRMA was also suggested by Eastwood *et al.* [232] for multiplexing multimedia users' transmission packets for transmission to the BS.

A technique referred to as dynamic TDMA was advocated for integrated voice and data communication also by Dunlop *et al.* [223], where "request minislots" are employed for channel acquisition, and the "information slots" are assigned in a second phase. Another efficient MAC protocol was suggested by Amitay and Nanda, which the authors referred to as RAMA [224], where only one user is granted access to the system at any instant, hence preventing collisions. DRMA was introduced by Li and Qiu [219], while Brecht *et al.* suggested the employment of SPAMA [228] for supporting variable-rate multimedia
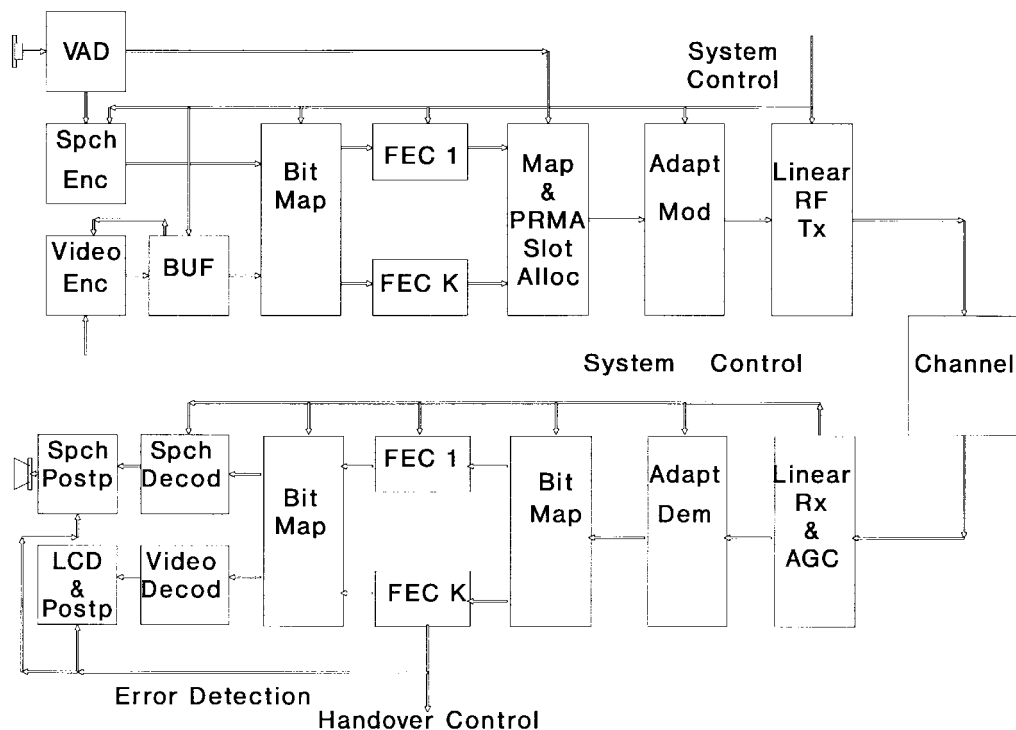
Fig. 19. Multimedia UMTS communicator schematic.

traffic. The statistical nature of the proposed centralized slot assignment scheme facilitated an accurate matching of bit-rate requirements for different multimedia services with a minimal amount of signaling, while maintaining a throughput of up to 93% at the cost of a low MAC delay.

A further alternative to support similar multirate multimedia users was also proposed by Brecht *et al.*, which was termed MF-PRMA [226], [329]. Here, we emphasize that most of the above statistical multiplexer schemes function also as multimedia packet multiplexers, supporting the delivery of multirate, multimedia traffic on a demand basis, giving cognizance to the different stability constraints of speech video and data sources. Speech and interactive video are delay sensitive, while data and distributive video are not. However, data and run-length-coded variable-rate video are extremely error sensitive, hence requiring higher integrity than speech and fixed-rate nonrun-length-coded video. Some of these aspects were also addressed in [226]–[228] and [232].

The first-generation PLMR systems were designed for low traffic density, and the typical cell radius was often on the order of tens of miles. Even the second-generation GSM system [40] was contrived to be able to cope with the hostile large-cell environment of rural cells of 35 km radius. Hence, it incorporated sophisticated and power-hungry signal processing in order to be able to combat a wide range of channel impairments associated with the hostile large-cell PLMR environment. The less robust DAMPS [41] and the second-generation Japanese digital mobile radio systems [42] reflect the more recent trend of moving toward small cells, exhibiting benign propagation characteristics, a tendency also adopted by the CT systems CT2 and DECT

[12]. These propagation aspects are well understood in the wireless communications community, but the above cell-size-dependent propagation factors can be augmented by referring to the relevant literature [1]–[3], [216], [217]. Hence, here we refrain from detailing deeper aspects of the wireless propagation environment.

Having covered some of the wireless communications basics, we are now equipped to consider the flexible system architecture of a mobile multimedia communicator of the next generation.

IX. FLEXIBLE MULTIMEDIA SYSTEM SCHEMATIC

The schematic of a flexible, toolbox-based multimedia PS is portrayed in Fig. 19 [152]. The pivotal implementational point of such a multimedia PS is that of finding the best compromise among a number of contradicting design factors, such as power consumption, robustness against transmission errors, spectral efficiency, audio/video quality, and so forth [229]. Here, we will address a few of these issues, mainly concentrating on the modulation and systems aspects of the proposed PS depicted in Fig. 19. The time-variant optimization criteria of a flexible multimedia system can only be met by an adaptive scheme, comprising the firmware of a suite of system components and loading that combination of speech codecs, video codecs, embedded channel codecs, VAD's, and modems that fulfills the prevalent one [68]. A few examples are maximizing the teletraffic carried or the robustness against channel errors, while in other cases, minimization of the bandwidth occupancy, the blocking probability, or the power consumption is of prime concern.

Focusing our attention on the speech and video links displayed in Fig. 19, the VAD [40] is deployed to control the PRMA slot allocator [68], [229]. A further task of the PRMA slot allocator is to multiplex digital source data from facsimile and other data terminals with the speech as well as graphics and other video signals to be transmitted.

Again, PRMA is a relative of slotted ALOHA contrived for conveying speech signals on a flexible demand basis via TDMA systems. PRMA was documented in a series of excellent papers by Goodman *et al.* [218]–[221], while various PRMA-assisted transceiver schemes were proposed in [229]–[233].

The VAD [40], [231], [330] queues the active speech spurts to contend for an uplink TDMA time slot for transmission to the BS. Inactive users' TDMA time slots are offered by the BS to other users, who become active and are allowed to contend for the unused time slots with a less-than-unity permission probability. This measure prevents previously colliding users from consistently colliding in their further attempts to attain a time-slot reservation. If several users contend for an available slot, neither of them will be granted it, while if only one user requires the time slot, he can reserve it for future communications. When many users are contending for a reservation, the collision probability is increased, and hence a speech packet might have to contend for a number of consecutive slots until its maximum contention delay of typically 32 ms expires. In this case, the speech packet must be dropped, but the packet-dropping probability must be kept below 1%, a value inflicting minimal degradation in perceivable speech quality in contemporary speech codecs.

Control traffic and system information is carried by packet headers added to the composite signal by the *bit mapper* before K-class source sensitivity-matched FEC takes place. Observe that the *video encoder* supplies its bits to an adaptive buffer having a feedback loop. If the PRMA video packet delay becomes too high or the buffer fullness exceeds a certain threshold, the video encoder is instructed to lower its bit rate, implying a concomitant dropping of the image quality.

The bit mapper assigns the MSB's to the input of the strongest FEC codec, FEC K, while the LSB's are protected by the weakest one, FEC 1. K-class FEC coding is used after mapping the speech and video bits to their appropriate bit-protection classes, which ensures source sensitivity-matched transmission. *Adaptive modulation* is deployed [68], [229], with the number of modulation levels, the FEC coding power, and the speech/video source-coding algorithm adjusted by the *system control* according to the dominant propagation conditions, bandwidth, and power efficiency requirements, channel blocking probability, or PRMA packet dropping probability. If the communications quality or the prevalent system optimization criterion cannot be improved by adaptive transceiver reconfiguration, the serving BS will hand the PS over to another BS providing a better grade of service.

One of the most important and reliable parameters used to control these algorithms is the *error detection* flag of the FEC decoder of the MSB class of speech and video bits, namely, FEC K. This flag can also be invoked to control the speech and video postprocessing algorithms. The adaptive modulator transmits the user bursts from the PS to the BS using the specific PRMA slot allocated by the BS for the PS's speech, data, or video information via the linear RF transmitter. Although the linear RF transmitter has a low power efficiency, its power consumption is less critical due to the lower transmitted power requirement of the multimedia PCN than that of the DSP hardware.

The receiver structure essentially follows that of the transmitter. After linear class-A amplification and AGC, the system-control information characterizing the type of modulation and the number of modulation levels must be extracted from the received signal before demodulation can take place. This information also controls the various internal bit-mapping algorithms and invokes the appropriate speech and video decoding as well as FEC decoding procedures. After adaptive demodulation at the BS, the source bits are mapped back to their original bit-protection classes and are FEC decoded. As mentioned, the error-detection flag of the strongest FEC decoder, FEC K, is used to control handovers or speech and video postprocessing. The FEC decoded speech and video bits are finally source decoded, and the recovered speech arrives at the earpiece, while the video information is displayed on a flat LCD.

The system-control algorithms of the reconfigurable mobile multimedia communicator will dynamically evolve over the years. PS's of widely varying complexity will coexist, with newer ones providing backward compatibility with existing ones while offering more intelligent new services and more convenient features. After this rudimentary system-level introduction, let us now focus our attention on a range of modern transceiver techniques.

X. MODERN TRANSCEIVER TECHNIQUES

In recent years, a powerful architecture referred to as software radio [16] was advocated by many researchers, essentially employing a flexible baseband signal-processing "toolbox" of speech, video, and channel codecs, modulation and "user signature" functions, plus a sufficiently wide-band, linear RF stage, which is interfaced to the baseband section using a high-speed digital-to-analog (D–A) converter. The software radio system architecture is capable of supporting intelligent multimode and multistandard operation, although many of the research issues are in their infancy at the time of writing. Smart antennas and cochannel interference reduction adaptive beam-forming methods inherited from radar and sonar researchers were characterized, for example, by Litva and Lo [53] and Baier *et al.* [56], and were also advocated by Kohno [55] in the context of intelligent, *space-time processing* receivers.

Furthermore, the sophisticated "per-survivor processing" detection algorithms proposed by Polydoros and Chugg [57] and the receiver techniques portrayed in the monograph by Meyer *et al.* [8] are expected to improve the performance of the next generation of receivers. Verdu [58] contrived

the optimum multiuser detector for CDMA transceivers, although its complexity is exponentially proportional to the number of users detected by the scheme, which may become excessive. These multiuser detection techniques exploit the *a priori* information concerning the user signature or spreading sequences and the channel estimates derived in order to remove the CDMA-specific multiuser interference and hence to approach the "single-user" Shannonian performance. The more practical suboptimum multiuser receivers are often classified as interference cancellation (IC) or suppression and joint detection arrangements [5].

Despite accurate power control, some user signals arrive at the receiver at a higher power, and hence IC attempts initially to detect the highest power user's signal from the superposition of all users' signals. Upon error-free detection, the strongest user's signal can be remodulated and deducted from the received multiuser signal, a procedure that can be invoked for the next strongest users in turn until all users are detected. The philosophy of multiuser detection is slightly different, since it is based on recognizing that the multiuser interference (MUI) is essentially similar to ISI, and hence the classic equalization techniques [68] developed for conventional ISI cancellation in dispersive channels can be readily modified for this application. Explicitly, the MUI of CDMA, which is generated by a number of users, can be interpreted as conventional ISI inflicted by a multipath channel having the same number of paths as the number of interfering CDMA users. Joint detection research was spearheaded in recent years by Jung and Blanz [59], Klein *et al.* [60], and a number of other researchers at the University of Kaiserslautern in Germany, but the impressive individual contributions in this field are too numerous to mention [61]–[65]. Let us now consider the issues affecting the choice of the appropriate modulation scheme.

XI. Modulation Issues

A. Choice of Modulation

In some of the European mobile systems, such as the pan-European GSM system [40], [214], [330] or the DECT scheme, constant envelope, partial response, Gaussian minimum shift keying (GMSK) [9], [69] is employed. Its main advantage is that it ignores any fading-induced amplitude fluctuation present in the received signal and hence facilitates the utilization of power-efficient nonlinear class-C amplification. In third-generation personal communication systems, however, benign pico- and microcells will be employed, where low transmitted power and low signal dispersion are characteristic. Hence, the employment of more bandwidth-efficient multilevel modulation schemes becomes realistic. In fact, the American and Japanese second-generation digital systems, namely, IS-54 and PDC, have already opted for 2-bits/symbol multilevel modulation [68].

The basic schematic of a modem is shown in Fig. 20. If an analog source signal must be transmitted, the signal is first low-pass filtered and analog-to-digital converted. The generated digital bit stream is then mapped to complex modulation symbols, such as those seen in Fig. 21, which are suitable for transmission over the bandlimited channel. In Fig. 21, there are 16 such complex points, represented by two distinct amplitude and eight different phase values, which can be described by 4 bits. This mapping operation is carried out by the MAP block of Fig. 20, assigning the appropriate I and Q components to four incoming bits. To ensure that I and Q components do not change abruptly, which would require an infinite bandwidth, the square-root N block carries out the Nyquist-filtering operation in the baseband, before the signal is up-converted to the intermediate frequency band by the help of two carrier waves, which are in 90° phase shift, i.e., they are orthogonal. This orthogonality allows us to transmit the independent I and Q components within the same bandwidth without their interfering with each other. Such *multilevel constellations* are more prone to channel impairments than binary schemes due to their comparatively low distance between constellation. Hence, they are employed typically over benign channels, where the guaranteed higher Shannonian channel capacity can be exploited this way to provide higher bit rates.

Multilevel modulation schemes have been considered in depth in [68], where Chapters 17 and 18 show that the bandwidth efficiency and minimum required SNR and SIR of a modulation scheme in a given frequency reuse structure is dependent on the BER targeted. The required BER, in turn, is dependent on the robustness of the source codecs used. Furthermore, in indoor scenarios, the partitioning walls and floors mitigate the cochannel interference, and this facilitates the employment of 16-level QAM.

The "maximum minimum distance" square-shaped QAM constellation [68], [234] is optimum for transmissions over AWGN channels, simply because the minimum distance among the modulation constellation points is as high as possible. In other words, this constellation has the highest possible average distance among its constellation points under the constraint of a given average power, yielding the highest "noise protection distances" when contaminated by AWGN. Until quite recently, QAM developments were focused on the benign AWGN telephone line and on point-to-point radio applications [235], which led to the definition of the CCITT telephone circuit modem standards V.29–V.33 based on various QAM constellations ranging from uncoded 16-QAM to trellis coded (TC) 128-QAM. In recent years, QAM research for hostile fading mobile channels has been motivated by the ever increasing bandwidth-efficiency demand for mobile telephony [236]–[247], although it requires power-inefficient class A or AB linear amplification [248]–[251]. However, the power consumption of the low-efficiency class-A amplifier [250], [251] is less critical than that of the digital speech, image, and channel codecs. Out-of-band emissions due to class AB amplifier nonlinearities' generating adjacent channel interferences can be reduced by some 15–20 dB using the adaptive predistorter proposed by Stapleton *et al.* [252]–[254].
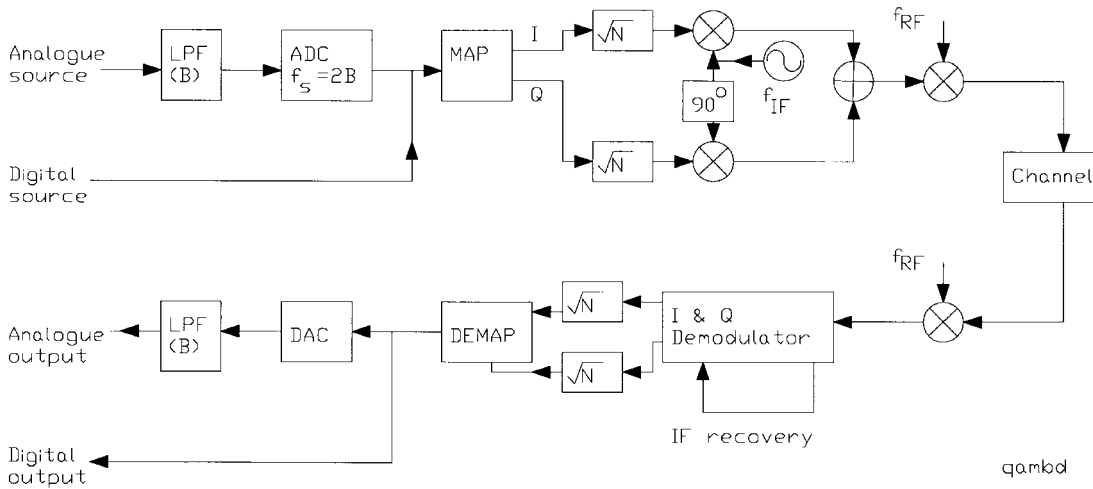
Fig. 20. Basic modem schematic [68].

When using the square-shaped 16-QAM constellation, it is essential to be able to separate the information modulated onto the I and Q carriers with the help of coherent demodulation, invoking the TTIB principle invented by McGeehan and Bateman [256]–[258] or invoking PSAM [255]. Although these methods can eliminate the residual BER, they are significantly more complex to implement than their noncoherently detected differentially coded counterparts. Based on the above arguments and constrained by the high bandwidth-efficiency requirement, in this paper, we have opted for noncoherently detected 16-QAM.

B. Noncoherent Star 16-QAM

The pivotal point of differentially coded noncoherent QAM demodulation is that of finding a rotationally symmetric QAM constellation, where all constellation points are rotated by the same amount. Such a rotationally symmetric "star constellation" was proposed in [245] and is shown in Fig. 21. A disadvantage of the proposed star 16-QAM (16-StQAM) constellation is its lower average energy. While square 16-QAM had an average phasor energy of $10d^2$, the 16-StQAM halves this value to $5d^2$, where $2d$ is the phasor spacing of the I and Q components. This implies a 3-dB disadvantage over Gaussian channels, but via Rayleigh-fading channels, this SNR penalty becomes less.

Our differential encoder obeys the following rules. The first bit $b1$ of a four-bit symbol is differentially encoded onto the phasor magnitude, yielding a ring-swap for an input logical one and maintaining the current magnitude, i.e., ring for $b1 = 0$. Bits $(b2, b3, b4)$ are then differentially Gray-coded onto the phasors of the particular ring pinpointed by $b1$. Accordingly, $(b2, b3, b4) = (0, 0, 0)$ implies no phase change, $(0, 0, 1)$ a change of $45°$, $(0, 1, 1)$ a change of $90°$, etc.

The corresponding noncoherent differential 16-StQAM demodulation is equally straightforward, having decision boundaries at a concentric ring of radius 2 and at phase rotations of $(22.5° + n.45°)$, $n = 0 \cdots 7$. Assuming received phasors of P_t and P_{t+1} at consecutive sampling instants of t and $t + 1$, respectively, bit $b1$ is inferred by evaluating
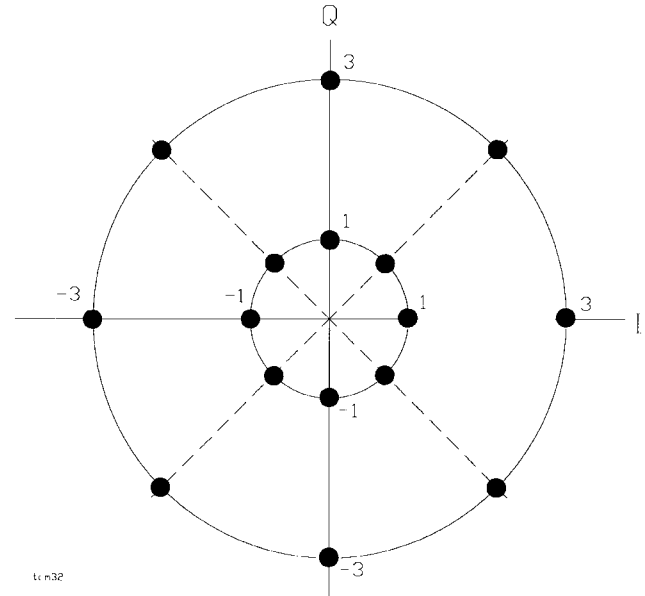

Fig. 21. Star QAM constellation.

the condition

$$\left| \frac{P_{t+1}}{P_t} \right| \geq 2. \tag{2}$$

If this condition is met, $b1 = 1$ is assigned; otherwise $b1 = 0$ is demodulated. Bits $(b2, b3, b4)$ are then recovered by computing the phase difference

$$\Delta\Theta = (\Theta_{t+1} - \Theta_t) \quad (\text{mod } 2\pi) \tag{3}$$

and comparing it against the decision boundaries $(22.5° + n.45°)$, $n = 0 \cdots 7$. Having decided which rotation interval the received phase difference $\Delta\Theta$ belongs to, Gray decoding delivers the bits $(b2, b3, b4)$.

From our previous discourse, it is plausible that the less dramatic the fading envelope and phase trajectory fluctuation between adjacent signalling instants, the better this differential scheme works. This implies that lower vehicular speeds are preferred by this arrangement if the

signalling rate is fixed. Therefore, the modem's performance improves for low pedestrian speeds when compared to typical vehicular scenarios. Alternatively, for a fixed vehicular speed, higher signalling rates are favorable since the relative amplitude and phase changes introduced by the fading channel between adjacent information symbols are less drastic. For a full treatise on QAM, the interested reader is referred to [68]. Let us now highlight the current research aspects of adaptive modems, which can adjust the number of bits per transmitted symbol in order to adapt to time-variant channel conditions.

C. Burst-by-Burst Adaptive Modems

Burst-by-burst adaptive multilevel modulation was first suggested by Steele and Webb in [68], [259], [260] for slowly fading wireless pedestrian channels, inspiring intensive further research in recent years [262]–[271], in particular by Kamio *et al.* at Osaka University and the Ministry of Post in Japan [261]–[264], as well as by Goldsmith and Chua [265] at the California Institute of Technology or by Pearce *et al.* [266] in the United Kingdom. The proposed schemes provide a means of realizing some of the time-variant channel capacity potential of the fading wireless channel [2], [274], invoking a more robust TS on a burst-by-burst basis, when the channel is of low quality and vice versa, while maintaining a certain target BER performance. The most appropriate TS is dependent upon the time-variant instantaneous SNR and SIR. The TS can be chosen according to the following regime [267]:

$$
\text{TS} = \begin{cases} \text{No Transmission (Notx)} & \text{if } l_1 > s^2/N \\ \text{BPSK} & \text{if } l_1 \leq s^2/N < l_2 \\ \text{QPSK} & \text{if } l_2 \leq s^2/N < l_3 \\ \text{Square 16 Point QAM} & \text{if } l_3 \leq s^2/N < l_4 \\ \text{Square 64 Point QAM} & \text{if } s^2/N \geq l_4 \end{cases}
$$
$$(4)$$

where s is the instantaneous signal level, N is the average noise power, and l_1, l_2, l_3, and l_4, are the BER-dependent optimized switching levels. Time-division duplex (TDD) was proposed in order to exploit the reciprocity of the channel under high SIR conditions, which allowed us to estimate the prevalent SNR on a burst-by-burst basis [268]. The reciprocity of the up- and downlink channel conditions in the TDD frame is best approximated if the corresponding TDD slots are adjacent.

In [267], the analytical upper-bound performance of such a scheme was characterized over slow Rayleigh-fading channels, while in [270], an unequal protection phasor constellation for signalling the current TS was proposed. The problem of appropriate power assignment was discussed, for example, in [263] and [265].

In [269], a combined BER- and BPS-based optimization cost function was defined and minimized in order to find the required TS switching levels for maintaining average target BER's of 1×10^{-2} and 1×10^{-4}, irrespective of the instantaneous channel SNR. These BER values can then be further mitigated by FEC coding, and in the case of the lower BER scheme, can be rendered virtually error free. The

Table 3 Switching Levels for Speech and Computer Data Systems Through a Rayleigh Channel, Shown in Instantaneous Channel SNR (dB) to Achieve Mean BER's of 1×10^{-2} and 1×10^{-4}, Respectively [267]

Switching levels(dB)	l_1	l_2	l_3	l_4
Mean-Speech (1%)	3.31	6.48	11.61	17.64
Mean-BER Data (0.01%)	7.98	10.42	16.76	26.33

former scheme was referred to as the speech TS, while the latter was referred to as the adaptive data TS. The optimized TS switching levels l_1, l_2, l_3, and l_4 are summarized in Table 3 [267]. The average BPS performance B of this adaptive modem was derived for a Rayleigh-fading channel in [267], which can be written as

$$
B = 1 \cdot \int_{l_1}^{l_2} F(s, S) \, ds + 2 \cdot \int_{l_2}^{l_3} F(s, S) \, ds
$$
$$
+ 4 \cdot \int_{l_3}^{l_4} F(s, S) \, ds + 6 \cdot \int_{l_4}^{\infty} F(s, S) \, ds \quad (5)
$$

where $F(s, S)$ is the probability density function of the Rayleigh channel, S is the average power, and the integrals characterize the received signal level domains, where the 1, 2, 4, and 6 bits/symbol TS's of (4) are used. In [271] and [272], the latency performance of these schemes was quantified, and frequency hopping as well as statistical multiplexing were proposed to mitigate its latency and buffer requirements.

D. Equalization Techniques

The performance of wide-band wireless channel equalizers was studied by a large cohort of researchers, such as Narayanan and Cimini [275] and Wu and Aghvami [276], as well as by Gu and Le-Ngoc [277]. To achieve fast equalizer coefficient convergence, these contributions typically invoked the Kalman algorithm [68] and its diverse incarnations, such as the square-root Kalman scheme, although Clark and Harun [278] argued that there were only marginal performance differences between the Kalman algorithm and the least mean squared [68] algorithm in typical practical situations. MLSE-type receivers typically outperform decision feedback equalizers at the cost of higher complexity. A range of hybrid compromise schemes were proposed, for example, by Wu and Aghvami [276], as well as by Gu and Le-Ngoc [277].

Let us now turn our attention to a transmission scheme that is particularly suitable for high-rate transmission over frequency-selective fading channels, although it refrains from employing the above equalization techniques.

E. Orthogonal Frequency-Division Modulation

In this section, we briefly introduce frequency-division multiplexing (FDM), also referred to as orthogonal multiplexing, as a means of dealing with the problems of frequency-selective fading encountered when transmitting over a high-rate wide-band radio channel. The fundamental principle of orthogonal multiplexing originates from Chang
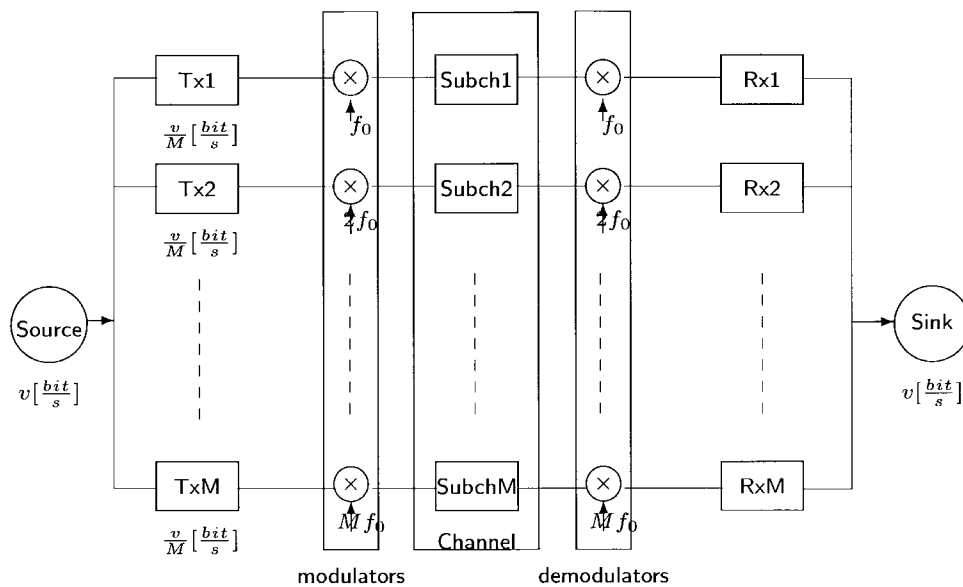
Fig. 22. Simplified block diagram of the orthogonal parallel modem.

[279], and over the years, a number of researchers have investigated this technique [280]–[291]. Despite its conceptual elegance, until recently, its employment has been mostly limited to military applications due to implementational difficulties. However, it has recently been adopted as the new European DAB standard. It is also a strong candidate for digital terrestrial television broadcast and for a range of other high-rate applications, such as 155-Mb/s WATM LAN's. These wide-ranging applications underline its significance as an alternative technique to conventional channel equalization in order to combat signal dispersion [292]–[296].

In the FDM scheme of Fig. 22, the serial data stream of a traffic channel is passed through a serial-to-parallel convertor, which splits the data into a number of parallel subchannels. The data in each subchannel are applied to a modulator, such that for M channels, there are M modulators whose carrier frequencies are $f_0, f_1, \cdots, f_M$. The difference between adjacent channels is Δf, and the overall bandwidth W of the N modulated carriers is $M\Delta f$.

These M modulated carriers are then combined to give an FDM signal. We may view the serial-to-parallel convertor as applying every Mth symbol to a modulator. This has the effect of interleaving the symbols into each modulator. Hence, symbols $S_0, S_M, S_{2M}, \cdots$ are applied to the modulator whose carrier frequency is f_1. At the receiver, the received FDM signal is demultiplexed into M frequency bands, and the M modulated signals are demodulated. The baseband signals are then recombined using a parallel-to-serial converter.

The main advantage of the above FDM concept is that because the symbol period has been increased, the channel delay spread is a significantly shorter fraction of a symbol period than in the serial system, potentially rendering the system less sensitive to ISI than the conventional serial system. In other words, in the low-rate subchannels, the signal is no longer subject to frequency-selective fading; hence, no channel equalization is necessary.

A disadvantage of the FDM approach shown in Fig. 22 is the increased complexity over the conventional system caused by employing M modulators and filters at the transmitter and M demodulators and filters at the receiver. It can be shown that this complexity can be reduced by the use of the DFT, typically implemented as an FFT [68]. The subchannel modems can use almost any modulation scheme, and 4- or 16-level QAM is an attractive choice in many situations.

The FFT-based QAM/FDM modem's schematic is portrayed in Fig. 23. The bits provided by the source are serial/parallel converted in order to form the n-level Gray coded symbols, M of which are collected in TX buffer 1, while the contents of TX buffer 2 are being transformed by the inverse FFT in order to form the time-domain modulated signal. The D–A-converted, low-pass-filtered modulated signal is then transmitted via the channel, and its received samples are collected in RX buffer 1, while the contents of RX buffer 2 are being transformed to derive the demodulated signal. The twin buffers are alternately filled with data to allow for the finite FFT demodulation time. Before the data is Gray coded and passed to the data sink, it can be equalized by a low-complexity method if there is some dispersion within the narrow subbands. For a deeper tutorial exposure, the interested reader is referred to [68, ch. 15].

Before concluding this section, we describe a typical channel characteristic of WLAN's transmitting at a rate of 155 Mb/s, where the above OFDM scheme can be advantageously employed. The 155-Mb/s rate is used in ATM systems. We assumed an indoor airport terminal or warehouse environment of dimensions 100×100 m and a seven-path channel corresponding to the four walls, ceiling, and floor, plus the LOS path. The LOS path and the two reflections from the floor and ceiling were combined into
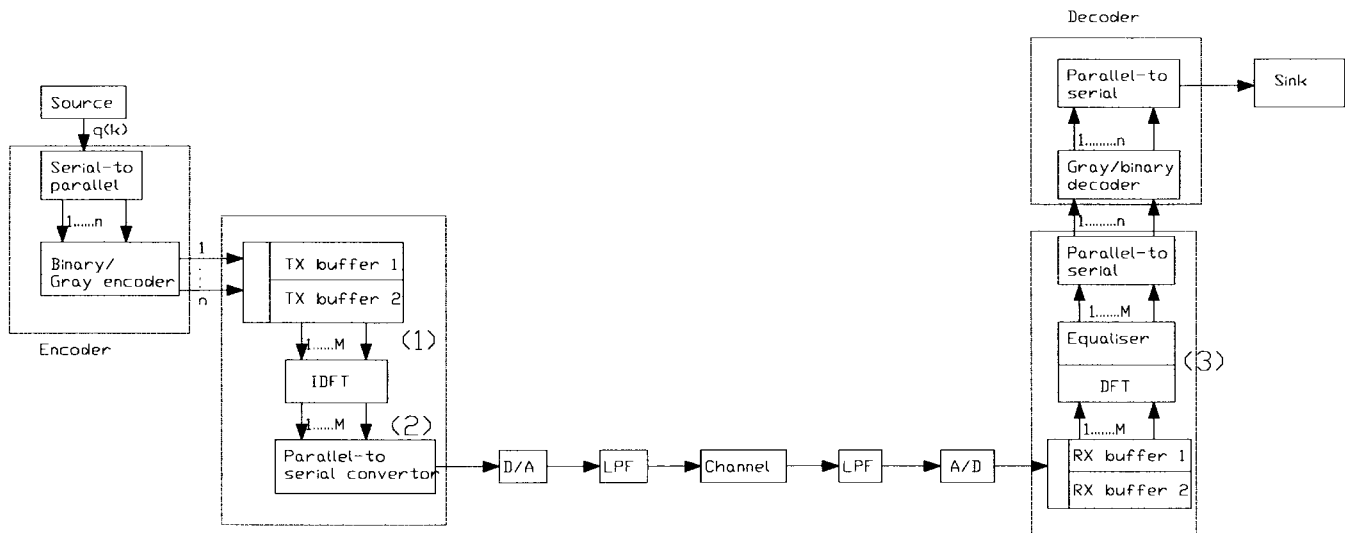
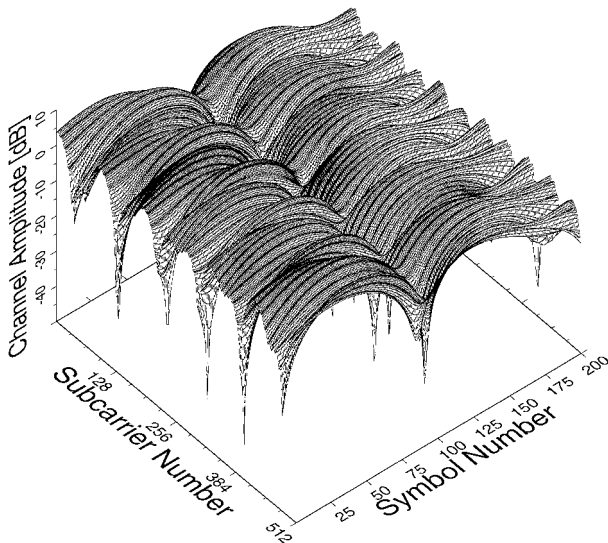**Fig. 23.** FFT-based OFDM modem schematic [68].

Fig. 24. Frequency response in the bandwidth of $M \times f_0$ for the 512-channel OFDM system at 155 Mb/s [344].

one single path in the impulse response. The worst case impulse response associated with the highest path length and delay spread is experienced in the farthest corners of the hall, which was determined using inverse second-power law attenuation and the speed of light for the computation of the path delays. The corresponding frequency response was plotted in Fig. 24 for a 512-channel system, as a function of both OFDM frame index and subchannel index. Observe the very hostile frequency-selective fading in the figure, which is efficiently combated by the OFDM modem, since for the narrow subchannels, the channel can be considered more or less flat fading. Again, the residual fading can be equalized using a simple pilot-assisted equalizer. In closing, we note that a variety of OFDM-related aspects were investigated in [179]–[301].

After this discussion on modulation techniques, let us briefly consider ways of reducing the BER using FEC techniques.

XII. CHANNEL CODING

The highest coding gain over AWGN channels is achieved using TCM [305] rather than consecutive FEC coding and modulation. Recently, similarly attractive TCM schemes have been proposed for fading mobile channels [306], [307]. To provide TCM schemes having unequal source-sensitivity matched error protection similarly to our approach in [145], [246], [247], Wei [309] suggested a range of nonuniformly spaced phasor constellations. Another method proposed by Wei [309] was to deploy a number of independent TCM schemes having different grades of protection and multiplex the sequences for transmission.

Both convolutional and block codes have been successfully used to combat the bursty channel errors [79]. Cox *et al.* [302] proposed rate-compatible punctured convolutional codecs [303] in order to provide bit-sensitivity-matched FEC protection for a subband speech codec using a $R = 1/2$ rate "mother code," where some of the encoded output bits can be obliterated or punctured from the bitstream. This then allows the designer to create a variety of different-rate bit-protection classes while using the same decoder and protecting the more error-sensitive bits by a stronger, low-rate code and the more robust source-coded bits by a higher-rate, less powerful FEC code.

A. Turbo Coding

In recent years, significant advances have been made toward the Shannonian performance predictions with the introduction of the *turbo codes* [310] and using iterative decoding techniques, which will be briefly highlighted below. Turbo coding was proposed by Berrou *et al.* [310], where the information sequence is encoded twice, using RSC encoders. As seen in Fig. 25, the second encoding takes place after a pseudorandom interleaving of the original information sequence in order to render the two encoded data sequences approximately statistically independent of each other.
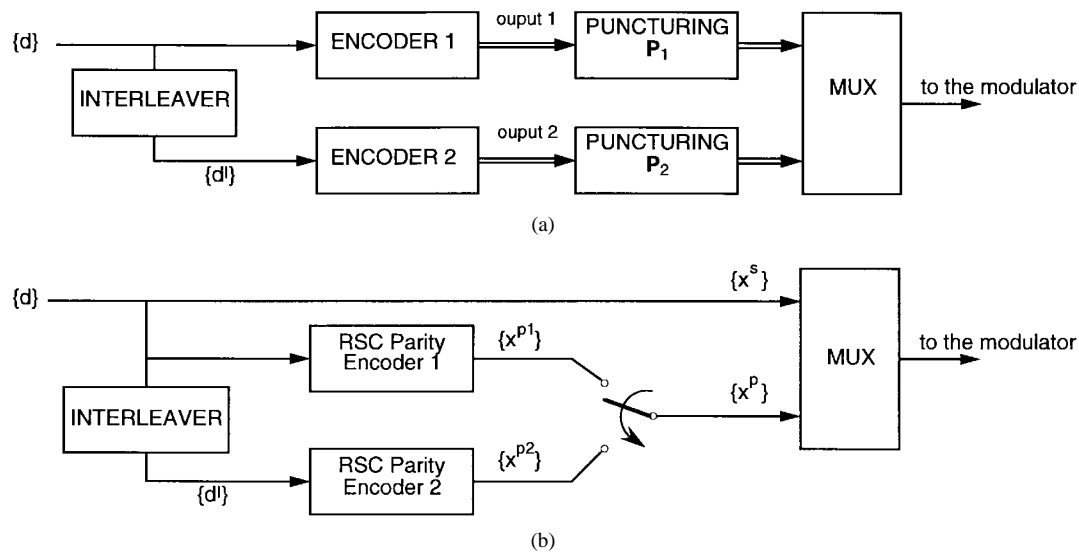
Fig. 25. (a) General and (b) originally proposed rate $1/2$ RSC turbo-code encoder structures [327].

In most turbo-coding schemes, a pair of half-rate RSC encoders are used, where each RSC encoder generates a systematically encoded output stream, which is equivalent to the original information sequence, as well as a stream of parity information. The two parity sequences are then punctured before being transmitted along with the original information sequence to the decoder. This puncturing of the parity information allows a wide range of coding rates to be realized, and often, half the parity information from each encoder is sent. Along with the original data sequence, this results in an overall coding rate of 1/2.

As portrayed in Fig. 26, at the receiver, two RSC decoders are used. Special decoding algorithms must be invoked that accept so-called soft inputs and give soft outputs for the decoded sequence rather than binary bits. These soft inputs and outputs provide not only an indication of whether a particular bit was a zero or a one but also a likelihood ratio, which quantifies the probability that the bit has been correctly decoded. The turbo decoder operates iteratively. In the first iteration the first RSC decoder provides a soft output, giving an estimation of the original data sequence based on the soft channel inputs alone. It also provides an *extrinsic* output. The extrinsic output for a given bit is based not on the channel input for that bit but on the information carried by surrounding bits and the constraints imposed by the code being used. This extrinsic output from the first decoder is used by the second RSC decoder as *a priori information,* and this information together with the channel inputs is used by the second RSC decoder to give its soft output and extrinsic information. In the second iteration, the extrinsic information from the second decoder in the first iteration is used as the *a priori* information for the first decoder, and using this *a priori* information, the decoder has an increased probability of decoding more bits correctly than it did in the first iteration. This cycle continues. Specifically, at each iteration, both RSC decoders produce a soft output and extrinsic information, which are based on the channel inputs and *a*

priori information obtained from the extrinsic information provided by the previous decoder. After each iteration, the BER in the decoded sequence drops, but the improvements obtained with each iteration fall as the number of iterations increases so that for complexity reasons, usually only 8 or 16 iterations are used.

If a bit appears in a rather corrupted section of the first encoded sequence, due to the independent parity information inherent in the second encoded sequence, the second decoder may be able to assist the first one to decode the original information correctly. The independent information delivered by the first decoder is likely to improve the performance of the second decoder, the output of which can now be again invoked by the first decoder. This iterative decoding process can be continued, alternating between decoding in the trellis of the first decoder and that of the second one in order to achieve near-Shannonian performance.

Hagenauer and Hoeher proposed to use the soft-output Viterbi [311] algorithm for the decoding of turbo codes in [312], while Hagenauer *et al.* [313] investigated also the feasibility of employing block codes as constituent codes, although most research is carried out in the context of convolutional codes. Robertson *et al.* [315] and Jung [317] investigated various turbo decoders, while Jung *et al.* [318] and Barbulescu *et al.* [319] studied various interleaving aspects of turbo coding. A range of other associated turbo-coding issues were considered in [320]–[323], while Breiling *et al.* recently proposed an optimum noniterative turbo decoder [324]–[326], [328], finding the maximum likelihood decoded information in a single, noniterative decision step.

Following our rudimentary description of some of the components of wireless multimedia systems, in the next section we consider the performance of a multimode transceiver, accommodating the firmware of a range of system components and hence ensuring a high grade of flexibility in terms of complexity, speech quality, robustness against channels errors, user capacity, etc.
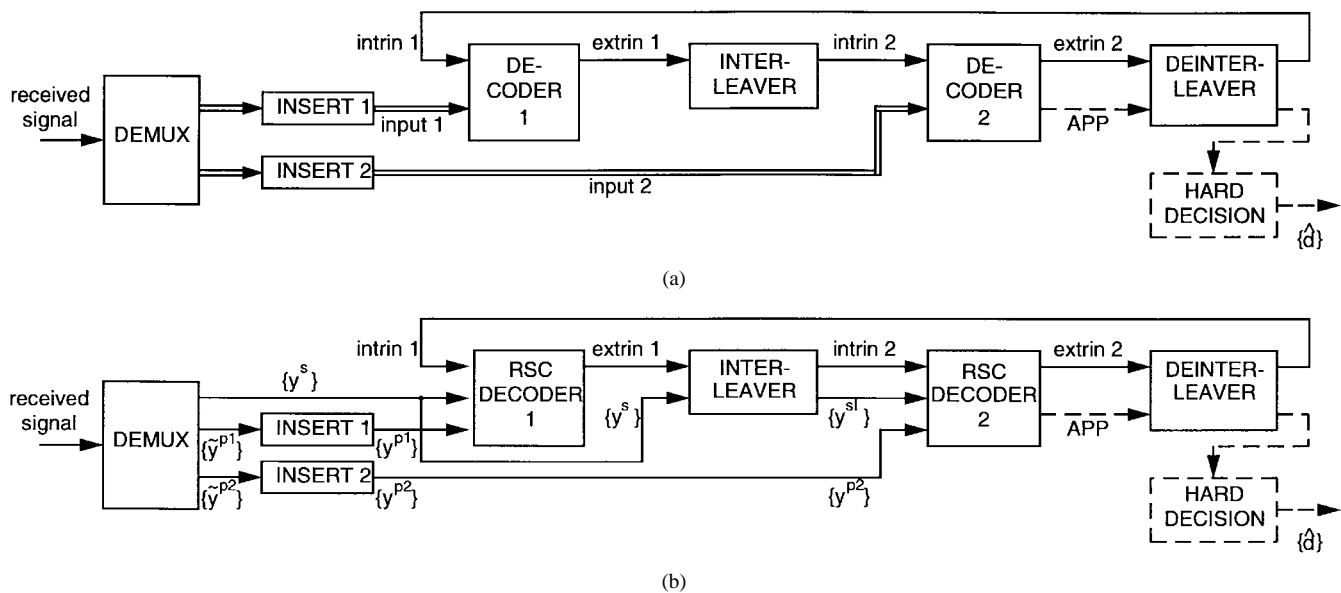
Fig. 26. (a) General and (b) RSC turbo-code decoder structures [327].

Table 4 System Parameters [229]

1 System	2 Modulator	3 Detector	4 FEC	5 Speech Codec	6 Complexity Order	7 Baud Rate (KBd)	8 TDMA User Bandw. (kHz)	9 No. of TDMA Users/Carrier	10 No. of PRMA Users/Carrier	11 No. of PRMA Users/slot	12 PRMA User Bandw. (kHz)	13 Min SNR (db) AWGN	14 Min SNR (dB) Rayleigh
A	GMSK	Viterbi Freq. Discr.	No	ADPCM	2	32	23.7	11	18	1.64	14.5	7	∞
B	GMSK		No	ADPCM	1	32	23.7	11	18	1.64	14.5	21	31
C	$\pi/4$-DQPSK	MLH-CR	No	ADPCM	4	16	19.8	22	42	1.91	10.4	10	28
D	$\pi/4$-DQPSK	Differential	No	ADPCM	3	16	19.8	22	42	1.91	10.4	10	28
E	16-StQAM	MLH-CR	No	ADPCM	6	8	13.3	44	87	1.98	6.7	20	∞
F	16-StQAM	Differential	No	ADPCM	5	8	13.3	44	87	1.98	6.7	21	31
G	GMSK	Viterbi Freq. Discr.	BCH	RPE-.LTP	8	24.8	18.4	12	22	1.83	10.1	1	15
H	GMSK		BCH	RPE-LTP	7	24.8	18.4	12	22	1.83	10.1	8	18
I	$\pi/4$-DQPSK	MLH-CR	BCH	RPE-.LTP	10	12.4	15.3	24	46	1.92	8	5	20
J	$\pi/4$-DQPSK	Differential	BCH	RPE-LTP	9	12.4	15.3	24	46	1.92	8	6	18
K	16-StQAM	MLH-CR	BCH	RPE-.LTP	12	6.2	10.3	48	96	2.18	4.7	13	25
L	16-StQAM	Differential	BCH	RPE-LTP	11	6.2	10.3	48	96	2.18	4.7	16	24

XIII. MULTIMODE SPEECH SYSTEM PERFORMANCE

A. Fixed Signalling-Rate Scenario [68], [229]

In the comparative study [229], we presented simulation results giving BER, bandwidth occupancy, and an estimate of complexity for 4-bit/symbol 16-Star QAM modems in order to characterize the potential of a UMTS-like system, 2-bit/symbol $\frac{\pi}{4}$-shifted differential quadrature phase shift keying ($\frac{\pi}{4}$-DQPSK) modems, since they are used in the IS-54 and PDC systems as well as binary GMSK modems. We used PRMA since it provided substantial improvements over TDMA in terms of the number of users supported.

Specifically, in our simulations, we used the GMSK, $\frac{\pi}{4}$-DQPSK and 16-Star QAM modems combined with both the unprotected low-complexity 32-kbits/s ADPCM codec (as in DECT and CT2) and the 13-kbits/s RPE-LTP GSM codec with its twin-class FEC. Each modem had the option of either a low- or a high-complexity demodulator. The high-complexity demodulator for the GMSK modem was an MLSE based on the Viterbi algorithm [311], while the low-

complexity demodulator was a frequency discriminator. For the two multilevel modems, either low-complexity noncoherent differential detection or an MLH-CR was invoked. Synchronous transmissions and perfect channel estimation were used in evaluating the relative performances of the systems listed in Table 4. Our results represent performance upper bounds, allowing relative performance comparisons under identical circumstances.

The system performances applied to microcellular conditions. The carrier frequency was 2 GHz, the data rate 400 kBd, and the mobile speed 15 m/s. At 400 kBd in microcells, the fading is flat and usually Rician. The best and worst Rician channels are the Gaussian- and Rayleigh-fading channels, respectively, and we performed our simulations for these channels to obtain upper and lower bound performances. Our conditions of 2 GHz, 400 kBd, and 15 m/s are arbitrary. They correspond to a fading pattern that can be obtained for a variety of different conditions, for example, at 900 MHz, 271 kBd, and 23 m/s. We compared the performances of the systems

defined in Table 4 when operating according to our standard conditions.

Returning to Table 4, the first column shows the system classification letter, the second the modulation used, the third the demodulation scheme employed, the fourth the FEC scheme, and the fifth the speech codec employed. The sixth column gives the estimated relative order of the complexity of the schemes, where the most complex one having a complexity parameter of 12 is the 16-Star QAM, MLH-CR, BCH, RPE-LTP arrangement. All the BCH-coded RPE-LTP schemes have complexity parameters larger than six, while the unprotected ADPCM systems are characterized by values of one to six, depending on the complexity of the modem used. The speech baud rate and the TDMA user bandwidth are given next.

An arbitrary signalling rate of 400 kBd was chosen for all our experiments, irrespective of the number of modulation levels, to provide a fair comparison for all the systems under identical propagation conditions. Again, these propagation conditions can be readily converted to arbitrary baud rates upon scaling the vehicular speed appropriately. The 400-kBd systems have a total bandwidth of $400/1.35 = 296$ kHz, $2 \cdot 400/1.62 = 494$ kHz, and $4 \cdot 400/2.4 = 667$ kHz, respectively. When computing the user bandwidth requirements, we took account of the different bandwidth constraints of GMSK, $(\pi/4)$-DQPSK, and 16-QAM, assuming an identical baud rate.

To establish the speech performance of systems A–L, we evaluated the segmental (SEG)SNR versus channel SNR and cepstral distance (CD) [68] versus channel SNR characteristics of these schemes. These experiments yielded 24 curves for AWGN and 24 curves for Rayleigh-fading channels, constituting the best and worst case channels, respectively. Then, for the 12 different systems and two different channels, we derived the minimum required channel SNR value for near unimpaired speech quality in terms of both CD and SEGSNR. These values are listed in columns 13 and 14 of Table 4. A range of interesting system design issues can be inferred from the table, but due to lack of space here, we refrain from a deeper discussion and refer the interested reader to [229] for more detail.

We note that the bandwidth-efficiency gains tabulated are reduced in SIR-limited scenarios due to the less dense frequency reuse of multilevel modems. Nevertheless, multilevel modulation schemes result in higher PRMA gains than their lower level counterparts. Following the above fixed-baud-rate scenario, let us now consider a fixed-bandwidth situation in the next section.

B. Fixed-Bandwidth Scenario [339]

1) Background and Motivation: In another study [339], PRMA-assisted adaptive modulation using 1, 2, and 4-bit/symbol transmissions was proposed as an alternative to DCA in order to maximize the number of users supported in a traffic cell. The cell was divided into three concentric rings: in the central high-SNR region, 16-StQAM was used; in the first ring, DQPSK was invoked; and in the outer ring DPSK was used. In our diversity-assisted modems, a channel SNR of about 7, 10, and 20 dB, respectively, was required in order to maintain a BER of about 1%, which can then be rendered error free by the binary BCH error-correction codes used. A 4.7-kbits/s, 30-ms frame-length ACELP speech codec [91] was employed, protected by a quad-class source-sensitivity-matched BCH coding scheme [79], yielding a total bit rate of 8.4 kbits/s. A GSM-like VAD controls the PRMA-assisted adaptive system. The achievable capacity improvement due to PRMA will be discussed at a later stage.

DCA [341] and PRMA [68] are techniques that potentially allow large increases in capacity over a fixed channel allocation (FCA) TDMA system. Although both DCA and PRMA can offer a significant improvement in system capacity, their capacity advantages typically cannot be jointly exploited, since the rapid variation of slot occupancy resulting from the employment of PRMA limits the validity of interference measurements, which are essential for the reliable operation of the DCA algorithm. One alternative to tackle this problem is to have mixed fixed and dynamic frequency reuse patterns, but this has the disadvantage of reducing the number of slots per carrier for the PRMA scheme, thus decreasing its efficiency.

In this study, we proposed diversity-assisted adaptive modulation as an alternative to DCA. The cells must be frequency planned as in an FCA system using a binary modulation scheme. When adaptive modulation is deployed, the throughput is increased by permitting high-level modulation schemes to be used by the mobiles roaming near to the center of the cell, which therefore will require a lower number of PRMA slots to deliver a fixed number of channel-encoded speech bits to the BS. In contrast, MS's near the fringes of the cell will have to use binary modulation in order to cope with the prevailing lower SNR and hence will occupy more PRMA slots for the same number of speech bits. Specifically, our adaptive system uses three modulation schemes—namely, binary DPSK, i.e., one bit per symbol at the cell boundary; DQPSK, i.e., two bits per symbol at medium distances from the BS; and 16-StQAM [68], which carries four bits per symbol close to the center of the cell.

2) PRMA-Assisted Adaptive Modulation: PRMA schemes have been documented, for example, in [68]. However, in the proposed PRMA-assisted adaptive modulation scheme, MS's can reserve more than one slot in order to deliver up to four bursts per speech frame, when DPSK is invoked toward the cell edges. When a free slot appears in the frame, each mobile that requires a new reservation contends for it based on a permission probability P_p. If the slot is granted to a 16-StQAM user, that slot is reserved in the normal way. If the slot is granted to a DQPSK user, then the next available free slot is also reserved for that user. Last, if the slot is granted to a DPSK user, then the next three free slots must also be reserved for this particular user. In this way, users that require more than one slot are not disadvantaged by being forced to contend for each slot individually. If, however, there are less than three slots available, DQPSK or 16-StQAM users still may be able to exploit the remaining slots.

Table 5 Parameters of the GSM-Like and DECT-Like
Adaptive Modulation PRMA Systems

Parameter	GSM	DECT	Unit
Channel Bandwidth	200	1728	kHz
Symbol Rate	133	1152	kBd
Bursts per Frame	48	416	

Again, we found that the difference in SNR required for the different diversity-assisted modulation schemes in order to maintain similar BER's was approximately 3 dB between DPSK and DQPSK and 12 dB between DPSK and StQAM when transmitting over Rayleigh-fading channels in our GSM- and DECT-type systems.

Thus, using an inverse fourth-power path-loss law, DPSK was invoked between radii $0.84R$ and the cell boundary R, which is one-quarter of the cell area. StQAM was used between the cell center and $0.5R$, which is a further quarter of the cell area; and DQPSK was used in the remaining area, which constitutes half of the total cell area. Accordingly, considering the number of slots needed by the various modulation schemes invoked and assuming a uniform traffic density, we can calculate the expected number of required slots per call as

$$E(n) = \frac{1}{4} \cdot 4 + \frac{1}{2} \cdot 2 + \frac{1}{4} \cdot 1 = 2.25 \text{ slots}.$$

Since a binary user would require four slots, this implies a capacity improvement of a factor of $4/2.25 \approx 1.78$.

3) Adaptive GSM-Like Schemes: The basic systems features are summarized in Table 5, where all modulation schemes assumed an excess bandwidth of 50%, resulting in a symbol rate that is two-thirds of the total bandwidth. If we consider the case of the 16-StQAM modem, which uses four bits per symbol, the 316 channel-coded bits to be transmitted may be encoded as 794-bit symbols. An additional pair of symbols was used to encode the modulation type, which was repeated three times in order to facilitate majority logic decisions. A further pair of dummy symbols was allocated for "power ramping" [68], yielding a total of 83 symbols—including all overheads—per 30-ms speech frame. This corresponds to a single-user signalling rate of $83/30$ ms ≈ 2.77 kBd, allowing us to create INT$\{133.33$ kBd$/2.77$ kBd$\} \approx 48$ time slots, where the INT$\{$ $\}$ function represents the integer part of the bracketed expression. When the DQPSK mode of operation is selected in areas of somewhat lower signal strength, we have to use two traffic bursts in order to convey the 316 bits of information, and when the binary DBPSK mode is selected, four bursts are required. Accordingly, we select the appropriate modulation type within the traffic cell considered as a function of the received signal strength.

Explicitly, the 8.4-kbits/s channel-coded rate, after accommodating the packet header carrying the required control information, allowed us to create 48 or 416 slots per 30-ms frame in the GSM-like and DECT-like systems, respectively, as shown in the table. Specifically, when using the 133.33-kBd GSM-like adaptive PRMA schemes, we can create 48 slots per 30-ms speech frame, which is equivalent to 12 slots for a binary-only BPSK system, since four slots are required for the transmission of a 30-ms speech packet. When the quaternary system is used, 24 pairs of slots can be created. Note that when fixed channel allocation is used, the adaptive scheme and the binary-only scheme can use the same cluster size. A quaternary-only system requires a 3-dB greater SIR than the binary scheme. According to Lee [342]

$$\frac{D}{R} = \sqrt{3K} \tag{6}$$

where D is the distance to the closest interferer, R is the cell radius, and K is the cluster size. The prevailing SIR can be expressed as

$$\text{SIR} \approx \left(\frac{D}{R}\right)^{\gamma} \tag{7}$$

where γ is the path-loss exponent and hence

$$K = \frac{1}{3}(\text{SIR})^{\frac{2}{\gamma}}. \tag{8}$$

In this paper, we have used a path-loss exponent of $\gamma = 4$. Therefore, increasing the SIR by 3 dB requires that the cluster size be increased by a factor of $\sqrt{2}$. The packet dropping versus number of users' performance of all the different schemes were evaluated for their respective optimum P_p values, which were different for the different schemes supporting different numbers of time slots.
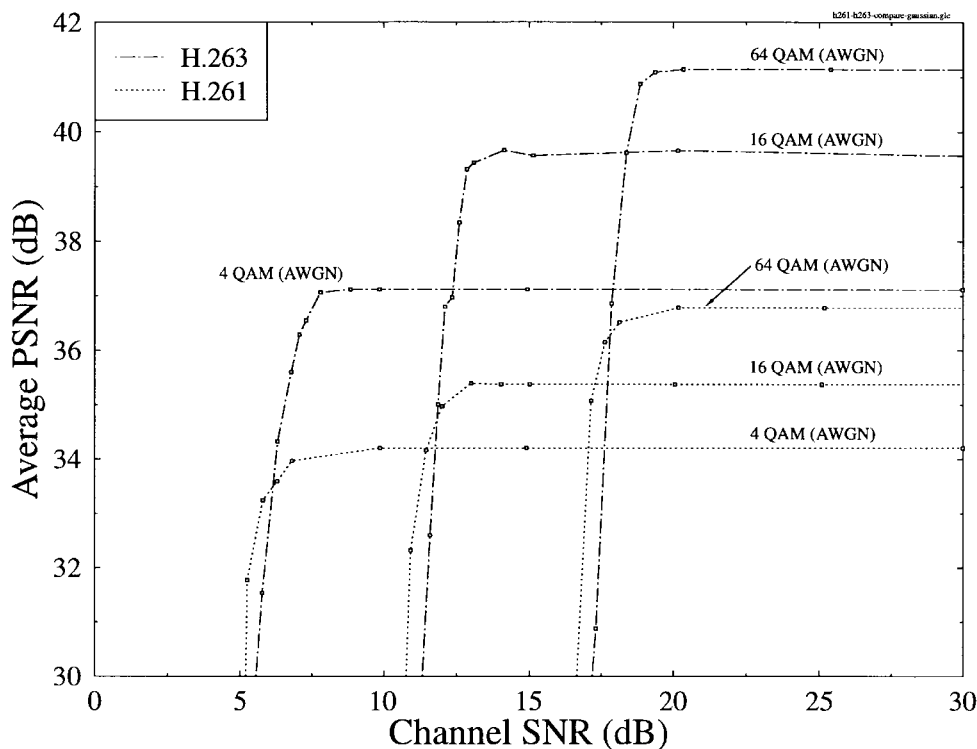
We found that a maximum of 19 simultaneous calls can be supported at a packet-dropping probability of 1% when using the binary scheme with a PRMA permission probability of 0.5. For the sake of comparison, this system can support only 12 TDMA users, each requiring four slots per frame. By contrast, the quaternary scheme can support 44 simultaneous calls when using the optimum permission probability of 0.4, assigning two slots per frame for each of them. The corresponding TDMA scheme could only support 24 such users. Last, our 48-slot adaptive scheme can accommodate 36 simultaneous calls while using the optimum permission probability of 0.5. The capacity improvements attainable by the proposed GSM-like scheme are presented in Table 6.

4) Adaptive DECT-Like Schemes: In our DECT-like schemes, we have INT$\{1152$ kBd$/2.77$ kBd$\} = 416$ slots per frame for the adaptive PRMA system. This is equivalent to 104 slots for a binary-only system and 208 slots for a quaternary-only system. Again, a quaternary-only system requires a 3-dB greater SIR than the binary scheme, and so the cluster size should be increased by a factor of $\sqrt{2}$.

We found that the binary scheme can support up to 220 simultaneous calls at a packet-dropping probability of 1%. When opting for the 208-slot quaternary scheme, the packet dropping versus number of users performance curve reveals that this system can accommodate 470 simultaneous calls with a permission probability of 0.1. Last, the packet-dropping performance of the 416-slot adaptive scheme suggests that the number of supported simultaneous conversations is about 400 when opting for a permission

Table 6 Improvements in Capacity Possible with Adaptive Modulation PRMA with 48 Slots [339]

System	Slots	Permission Probability	Simultaneous Calls	Normalised by cluster size K	Improvement over binary with PRMA	Improvement over binary without PRMA
DBPSK	12	0.5	19	19	-	58%
DQPSK	24	0.4	44	31.1	64%	159%
Adaptive	48	0.5	36	36	89%	200%

Fig. 27. Performance comparison of the proposed adaptive H.261 and H.263 transceivers over AWGN channels [176].

probability of 0.1. The achievable capacity improvements for our DECT-like system are displayed in Table 7.

In conclusion, adaptive modulation with PRMA gives the expected three- to fourfold capacity increase over the binary scheme without PRMA. Generally, the greater the number of slots, the greater the advantage of PRMA over non-PRMA systems, since the statistical multiplexing gain approaches the reciprocal of the speech activity ratio. Furthermore, PRMA-assisted adaptive modulation achieves an additional 80% capacity increase over PRMA-assisted binary modulation [340]. The speech performance of our adaptive system evaluated in terms of SEGSNR and CD is unimpaired by channel effects for SNR values in excess of about 8, 10, and 20 dB when using diversity-assisted DPSK, DQPSK, and 16-StQAM, respectively, although in dispersive environments, a reduced performance is expected.

Let us now consider the expected performance of a similar intelligent multimode video system.

XIV. VIDEO-PHONE SYSTEMS

Below, we follow the approach of Cherriman *et al.* [176], and as an example, let us consider transmitting

QCIF images, where the video codecs were programmed to generate 3560, 2352, and 1176 bits per frame. At a scanning rate of 10 frames/s, these coding modes resulted in video bit rates of 35.6, 23.52, and 11.76 kbits/s, respectively.

In our earlier work, we have shown that in QAM schemes, the bits assigned to the transmitted nonbinary modulation symbols exhibit different BER's, defining a number of different integrity classes [68]. The number of integrity classes depends on the number of modulation levels. In 4-QAM, there is only one such integrity class; in 16-QAM, there are two; and in 64-QAM, there are three classes, often also referred to as subchannels. By using FEC codes of different strength on each QAM subchannel, it is possible to equalize the probability of errors on the subchannels. This means that all subchannel FEC codes should break down at approximately the same channel SNR. This is desirable if all bits to be transmitted are equally important. Since our data streams are variable-length coded, one error can cause a loss of synchronization. Therefore, in this case, most bits are equally important, and so equalization of QAM subchannels BER is desirable. The FEC codes used in our system are summarized in Table 8,
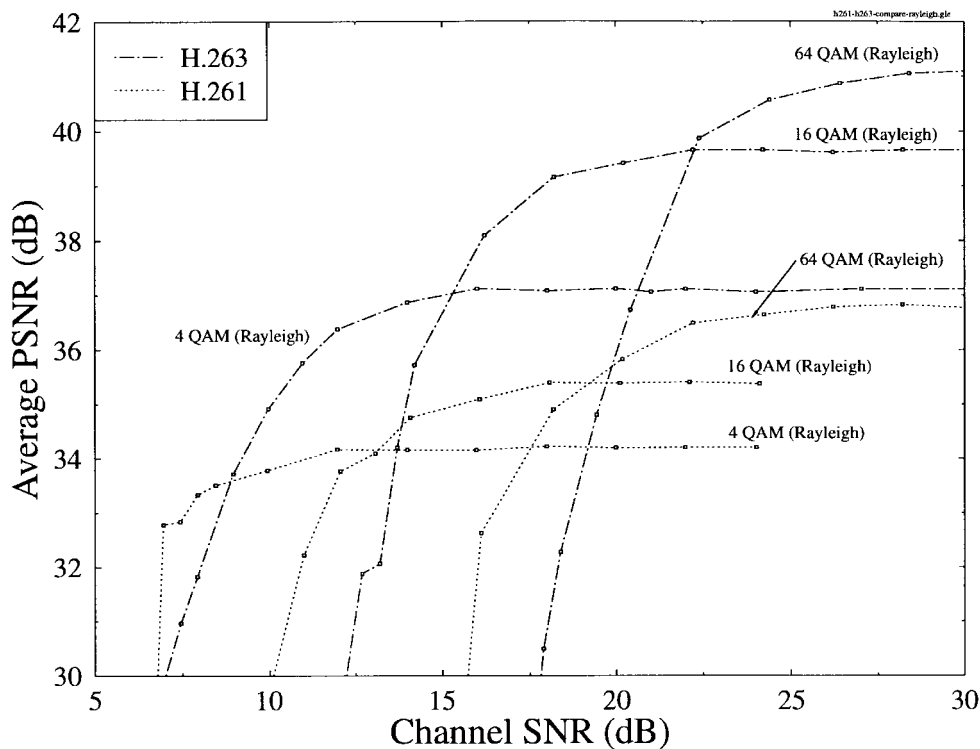
Fig. 28. Performance comparison of the proposed adaptive H.261 and H.263 transceivers over Rayleigh channels [176].

Table 7 Achievable Capacity Improvements for the Adaptive Modulation PRMA with 416 slots [339]

System	Slots	Permission Probability	Simultaneous Calls	Normalised by cluster size K	Improvement over binary with PRMA	Improvement over binary without PRMA
DBPSK	104	0.1	220	200	–	112%
DQPSK	208	0.1	470	332	51%	219%
Adaptive	416	0.1	400	400	82%	285%

where a BCH(n, k, t) code represents a binary BCH code encoding k bits to n bits and capable of correcting t errors per code word [79]. After including a control header, pilot, and ramp symbols [68], as suggested in [176], the FEC-coded single-user signalling rates became 11.84 kBd in all three modem operating modes. In case of a Nyquist excess bandwidth of 50%, this implies a single-user bandwidth requirement of 17.74 kHz. For example, in the 200-kHz bandwidth of the pan-European GSM system, eight voice-only users are supported, which corresponds to a 25-kHz user bandwidth. Consequently, our video-phone stream can replace a speech stream, making wireless videophony realistic if the cost of an additional time slot is acceptable to the users.

The video system performance was evaluated under the propagation conditions of a vehicular speed of 30 mph, signalling rate of 11.84 kBd, and propagation frequency of 1.9 GHz. The corresponding single-user bandwidth requirement is about 16 kHz when using a modulation excess bandwidth of 35% or a Nyquist rolloff factor of 0.35. In the various operating modes investigated, the PSNR versus channel SNR curves of Figs. 27 and 28 were obtained for

Table 8 FEC codes used for 4-, 16-, and 64-QAM [176]

Modulation scheme	FEC codes used
4 QAM	BCH(255,147,14)
16 QAM	Class 1: BCH(255,179,10)
	Class 2: BCH(255,115,21)
64 QAM	Class 1: BCH(255,199,7)
	Class 2: BCH(255,155,13)
	Class 3: BCH(255,91,25)

AWGN and Rayleigh channels, respectively. Since both the H.261 and H.263 source codecs have had similar robustness against channel errors, and their transceivers were identical, the associated "corner SNR" values, where unimpaired communications broke down, were virtually identical for both systems over both AWGN and Rayleigh channels. As expected, however, the H263 codec again exhibited always higher video quality at the same bit rate or system bandwidth.

Our current endeavors are focused on exploring the quality versus bit-rate performance of both systems for various image resolutions in order to be able to provide the required video quality, bit rate, frame rate, image size,

and resolution on a demand basis in intelligent adaptive multimode transceivers.

XV. SUMMARY AND CONCLUSIONS

This overview attempted to highlight some of the basic issues in bandwidth-efficient tetherless multimedia communications. Due to its wide scope, it was impossible to offer a full exposure of any of the topics, although we endeavored to provide references for the motivated reader to probe further in most topics of interest. In the source-coding area, substantial advances have been made over the past few years. A range of high-quality, error-resilient speech codecs have been developed, and with the advent of the 8-kbits/s G.729 ITU speech codec, this field reached a remarkable state of maturity. This is the first ITU codec, which was designed with the high prevalent BER of wireless systems in mind. Currently, research is under way toward the definition of the 4-kbits/s ITU standard speech codec. To provide narrow-band wireless multimedia services, we have proposed a variety of fixed-rate video codecs, which can generate a bitstream that can be accommodated by allocating an additional physical channel for video transmissions. We also suggested an H.263-based fixed-rate multimode transceiver for video telephony. Furthermore, handwriting or graphical information can also be robustly encoded using FL-DCC and multiplexed, for example, using the previously described PRMA or SPAMA schemes with speech and video signals. Multiplexing variable-rate multimedia sources was detailed, for example, in [227], [228], and [232]. When the increased complexity of turbo codecs becomes acceptable due to the advances in low-voltage VLSI, the performance of wireless personal communicators can approach the Shannonian performance limits more closely. Indeed, over AWGN channels, a BER of 10^{-5} was reported by Pietrobon [345] using a one-third-rate hardware turbo codec operating at 356 kbits/s and employing an interleaver size of 65 536 bits at an E_b/N_0 value of 0.32 dB, where E_b and N_0 are the bit energy and the noise power spectral density, respectively. In closing, we note that the intelligent wireless multimode, multimedia concept advocated in this paper is likely to provide substantial benefits for potential users, and its implementation is realistic at the current state of the art.

ACKNOWLEDGMENT

REFERENCES

[1] W. C. Jakes, *Microwave Mobile Communications*. New York: Wiley, 1974.
[2] W. Y. C. Lee, *Mobile Cellular Communications*. New York: McGraw-Hill, 1989.
[3] J. D. Parsons and J. G. Gardiner, *Mobile Communication Systems*. London: Blackie, 1989.
[4] K. Feher, *Wireless Digital Communications: Modulation and Spread Spectrum Applications*. Englewood Cliffs, NJ: Prentice-Hall, 1995.
[5] S. Glisic and B. Vucetic, *Spread Spectrum CDMA Systems for Wireless Communications*. Norwood, MA: Artech House, 1997.
[6] R. Prasad, *CDMA for Wireless Personal Communications*. Norwood, MA: Artech House, 1996.
[7] S. G. Glisic and P. A. Leppanen, Eds., *Wireless Communications—TDMA Versus CDMA*. Norwell, MA: Kluwer, 1997.
[8] H. Meyer, M. Moeneclaey, and S. Fechtel, *Digital Communications Receivers*. New York: Wiley, 1997.
[9] R. Steele, Ed., *Mobile Radio Communications*. New York: IEEE Press/Pentech, 1992.
[10] T. S. Rappaport, *Wireless Communications Principles and Practice*. Englewood Cliffs, NJ: Prentice-Hall, 1996.
[11] V. K. Garg and J. E. Wilkes, *Wireless and Personal Communications Systems*. Englewood Cliffs, NJ: Prentice-Hall, 1996.
[12] J. D. Gibbson, *The Mobile Communications Handbook*. New York: IEEE Press/CRC Press, 1996.
[13] "Special issue on the European path toward UMTS," *IEEE Personal Commun. Mag.*, vol. 2, no. 1, Feb. 1995.
[14] "Feature topic: Wireless personal communications," *IEEE Personal Commun. Mag.*, vol. 2, no. 2, Apr. 1995.
[15] "Feature topic: Universal telecommunications at the beginning of the 21st century," *IEEE Commun. Mag.*, vol. 33, no. 11, Nov. 1995.
[16] "Feature topic: Software radios," *IEEE Commun. Mag.*, vol. 33, no. 5, May 1995.
[17] "Feature topic: Wireless personal communications," *IEEE Commun. Mag.*, vol. 33, no. 1, Jan. 1995.
[18] "Feature topic: European research in mobile communications," *IEEE Commun. Mag.*, vol. 34, no. 2, Feb. 1996, pp. 60–106.
[19] V. H. MacDonald, "The cellular concept," *Bell Syst. Tech. J.*, vol. 58, no. 1, pp. 15–41, Jan. 1979.
[20] R. Steele, "Toward a high capacity digital cellular mobile radio system," *Proc. Inst. Elect. Eng.*, pt. F, no. 5, pp. 405–415, Aug. 1985.
[21] R. Steele and V. K. Prabhu, "Mobile radio cellular structures for high user density and large data rates," *Proc. Inst. Elect. Eng.*, pt. F, no. 5, pp. 396–404, Aug. 1985.
[22] R. Steele, "The cellular environment of lightweight hand-held portables," *IEEE Commun. Mag.*, pp. 20–29, July 1989.
[23] S. Tekinay and B. Jabbari, "A measurement-based prioritization scheme for handovers in mobile cellular networks," *IEEE J. Select. Areas Commun.*, vol. 10, no. 8, pp. 1343–1350, 1992.
[24] G. P. Pollini, "Trends in handover design," *IEEE Commun. Mag.*, pp. 82–90, Mar. 1996.
[25] J. C.-I. Chuang, "Performance issues and algorithms for dynamic channel assignment," *IEEE J. Select. Areas Commun.*, vol. 11, no. 6, pp. 955–963, Aug. 1993.
[26] J. C.-I. Chuang and N. Sollenberger, "Performance of autonomous dynamic channel assignment and power control for TDMA/FDMA wireless access," *IEEE J. Select. Areas Commun.*, vol. 12, pp. 1314–1323, Oct. 1994.
[27] M. M.-L. Cheng and J. C-I. Chuang, "Performance evaluation of distributed measurement-based dynamic channel assignment in local wireless communications," *IEEE J. Select. Areas Commun.*, vol. 14, pp. 698–710, May 1996.
[28] R. C. Bernhardt, "Timeslot management in digital portable radio systems," *IEEE Trans. Veh. Technol.*, pp. 261–272, Feb. 1991.
[29] ——, "Timeslot re-assignment in a frequency reuse TDMA portable radio system," *IEEE Trans. Veh. Technol.*, pp. 296–304, Aug. 1992.

[30] D. C. Cox, "Wireless personal communications: A perspective," in *The Mobile Communications Handbook*, J. D. Gibbson, Ed. New York: IEEE Press/CRC Press, 1996, pp. 209–241.

[31] A. D. Kucar, "Mobile radio: An overview," in *The Mobile Communications Handbook*, J. D. Gibbson, Ed. New York: IEEE Press/CRC Press, 1996, pp. 242–262.

[32] V. O. K. Li and X. Qiu, "Personal communications systems," *Proc. IEEE*, vol. 83, pp. 1210–1243, Sept. 1995.

[33] *Proc. Nordic Seminar on Digital Land Mobile Radio Communication (DMR)*, Espoo, Finland, Feb. 1985.

[34] *Proc. Second Nordic Seminar on Digital Land Mobile Radio Communication (DMRII)*, Stockholm, Sweden, Oct. 1986.

[35] *Proc. Int. Conf. Digital Land Mobile Radio Communication (ICDMC) Venice*, Italy, June/July 1987.

[36] *Proc. Digital Cellular Radio Conf.*, Hagen, Germany, Oct. 12–14, 1988.

[37] "GSM recommendation," European Telecommunications Standardization Institute, Sophia Antipolis, France, 1988.

[38] A. Moloberti, "Definition of the radio subsystem for the GSM pan-European digital mobile communication system," in *Proc. ICDMC*, Venice, Italy, June/July 1987, pp. 37–46.

[39] A. W. D. Watson, "Comparison of the contending multiple access methods for the pan-European mobile radio systems," in *Inst. Elect. Eng. Colloquium Dig. No: 1986/95*, pp. 2/1–2/6, Oct. 7, 1986.

[40] L. Hanzo and J. Stefanov, "The pan-European digital cellular mobile radio system-known as GSM," in *Mobile Radio Communications*, R. Steele, Ed. London: Pentech, 1992, ch. 8, pp. 677–773.

[41] *Dual-mode Subscriber Equipment—Network Equipment Compatibility Specification,* Interim Standard IS-54, Telecommunications Industry Association, 1989.

[42] *Public Digital Cellular (PDC) Standard,* RCR STD-27.

[43] Mobile Station—Base Station Compatibility Standard for Dual-Mode Wideband Spread Spectrum Cellular System, EIA/TIA Interim Standard IS-95, 1993.

[44] "Advanced communications technologies and services (ACTS) workplan," European Commission, DGXIII-B-RA946043-WP, Aug. 1994.

[45] J. Schwartz da Silva, B. Arroyo-Fernandez, B. Barani, J. Pereira, and D. Ikonomou, "Mobile and personal communications: ACTS and beyond," in European Commission, DGXIII-B-RA946043-WP, Aug. 1994, pp. 379–415.

[46] K. Pehkonen, H. Holma, I. Keskitalo, E. Nikula, and T. Nestman, "A performance analysis of TDMA and CDMA based air interface solutions for UMTS high bit rate services," in *Proc. PIMRC'97*, Helsinki, Sept. 1997, pp. 22–26.

[47] T. Ojanpera, P. Ranta, S. Hamalainen, and A. Lappetelainen, "Analysis of CDMA and TDMA for 3rd generation mobile radio systems," in *Proc. VTC'97*, Phoenix, AZ, May 1997, vol. 2, pp. 840–844.

[48] K. Pajukoski and J. Savisalo, "Wideband CDMA test system," in *Proc. PIMRC'97*, Helsinki, Sept. 1997, pp. 669–673.

[49] A. Klein, R. Pirhonen, J. Sköld, and R. Suoranta, "FRAMES Multiple access mode 1—Wideband TDMA with and without spreading," in *Proc. PIMRC'97*, Helsinki, Sept. 1997, pp. 37–41.

[50] P. W. Baier, P. Jung, and A. Klein, Taking the challenge of multiple access for third-generation cellular mobile radio systems—A European view," *IEEE Commun. Mag.*, vol. 34, no. 2, pp. 82–89, Feb. 1996.

[51] B. Engstroem and C. Oesterberg, "A system for test of multiaccess methods based on OFDM," in *Proc. VTC'94*, Stockholm, Sweden, 1994, pp. 1843–1847.

[52] F. Adachi *et al.*, "Coherent DS-CDMA—Promising multiple access for wireless multimedia mobile communications," in *Proc. IEEE ISSSTA'96*, Mainz, Germany, Sept. 1996, pp. 351–358.

[53] J. Litva and T. K.-Y. Lo, Eds., *Digital Beamforming in Wireless Communications*. Norwood, MA: Artech House, 1996.

[54] T. Ojanpera, "Overview of research activities for third generation mobile communications," in *Digital Beamforming in Wireless Communications*, J. Litva and T. K.-Y. Lo, Eds. Norwood, MA: Artech House, 1996, pp. 415–446

[55] R. Kohno, "Spatial and temporal communication theory using software antennas for wireless communications," in *Digital Beamforming in Wireless Communications*, J. Litva and T. K.-Y. Lo, Eds. Norwood, MA: Artech House, 1996, pp. 293–322.

[56] P. W. Baier, J. Blanz, and R. Schmalenberger, "Fundamentals of smart antennas for mobile radio applications," in *Digital Beamforming in Wireless Communications*, J. Litva and T. K.-Y. Lo, Eds. Norwood, MA: Artech House, 1996, pp. 345–376.

[57] A. Polydoros and K. M. Chugg, "Per-survivor processing," in *Digital Beamforming in Wireless Communications*, J. Litva and T. K.-Y. Lo, Eds. Norwood, MA: Artech House, 1996, pp. 41–72.

[58] S. Verdu, "Minimum probability of error for asynchronous Gaussian multiple access channels," *IEEE Trans. Inform. Theory*, vol. 32, pp. 85–96, Jan. 1986.

[59] P. Jung and J. Blanz, "Joint detection with coherent receiver antenna diversity in CDMA mobile radio systems," *IEEE Trans. Veh. Technol.*, vol. 44, pp. 76–88, Feb. 1995.

[60] A. Klein, G. K. Kaleh, and P. W. Baier, "Zero forcing and minimum mean square error equalization for multiuser detection in code division multiple access channels," *IEEE Trans. Veh. Technol.*, vol. 45, pp. 276–287, May 1996.

[61] Z. Zvonar and D. Brady, "Suboptimal multiuser detector for frequency selective Rayleigh fading synchronous CDMA channels," *IEEE Trans. Commun.*, vol. 43, pp. 154–157, Feb.–Apr. 1995.

[62] Y. Sanada and M. Nakagawa, "A multiuser interference cancellation technique utilizing convolutional codes and multicarrier modulation for wireless indoor communications," *IEEE J. Select. Areas Commun.*, vol. 14, pp. 1500–1509, Oct. 1996.

[63] P.-A. Sung and K.-C. Chen, "A linear minimum mean square error multiuser receiver in Rayleigh fading channels," *IEEE J. Select. Areas Commun.*, vol. 14, pp. 1583–1594, Oct. 1996.

[64] L. Wei, L. K. Rasmussen, and R. Wyrwas, "Near optimum tree-search detection schemes for bit-synchronous multiuser CDMA systems over Gaussian and two-path Rayleigh-fading channels," *IEEE Trans. Commun.*, vol. 45, pp. 691–700, June 1997.

[65] D. Dahlhaus, A. Jarosch, B. H. Fleury, and R. Heddergott, "Joint demodulation in DS/CDMA systems exploiting the space and time diversity of the mobile radio channel," in *Proc. 1997 Int. Symp. Personal, Indoor and Mobile Radio Communications (PIMRC'97)*, pp. 47–52.

[66] "Special issue on HIPERLAN," *Wireless Personal Commun. J.,* vol. 3, no. 4; and vol. 4, no. 1, pp. 341–453, 1997.

[67] "Radio equipment and systems (RES); High Performance Radio Local Area Network (HIPERLAN), Type 1," functional specifications, ETSI Final Draft prETS 300 652.

[68] W. T. Webb and L. Hanzo, *Modern Quadrature Amplitude Modulation: Principles and Applications for Fixed and Wireless Channels*. New York: IEEE Press/Pentech, 1994, p. 557.

[69] J. B. Anderson, T. Aulin, and C.-E. Sundberg, *Digital Phase Modulation*. New York: Plenum, 1985.

[70] P. Sheldon, J. Cosmas, and A. Permain, "Dynamically adaptive control system for MPEG-4," in *Proc. 2nd Int. Workshop Mobile Multimedia Communications*, Bristol, UK, Apr. 11–13, 1995.

[71] Y.-Q. Zhang, F. Pereira, T. Sikora, and C. Reader, Eds., "Special issue on MPEG4," *IEEE Trans. Circuits Syst. Video Technol.,* vol. 7, no. 1, Feb. 1997.

[72] C. E. Shannon, "A mathematical theory of communication," *Bell Syst. Tech. J.*, vol. 27, pp. 379–423, June 1948; pp. 623–656, Oct. 1948.

[73] J. Hagenauer, "Quellengesteuerte kanalcodierung fuer sprach- und tonuebertragung im mobilfunk," in *Aachener Kolloquium Signaltheorie*, Mobile Kommunikationssysteme, Mar. 23–25, 1994, pp. 67–76.

[74] ——, "Source-controlled channel decoding," *IEEE Trans. Commun.*, vol. 43, no. 9, pp. 2449–2457, Sept. 1995.

[75] A. J. Viterbi, "Wireless digital communications: A view based on three lessons learned," *IEEE Commun. Mag.*, pp. 33–36, Sept. 1991.

[76] N. Jayant, "Signal compression: Technology targets and research directions," *IEEE J. Select. Areas Commun.*, vol. 10, pp. 796–818, June 1992.

[77] N. Hubing, Ed., "Special issue on speech and image coding," *IEEE J. Select. Areas Commun.*, vol. 10, June 1992.

[78] A. Gersho, "Advances in speech and audio compression," *Proc. IEEE*, vol. 82, pp. 900–918, June 1994.

[79] K. H. H. Wong and L. Hanzo, "Channel coding," in *Mobile Radio Communications*, R. Steele, Ed. London: IEEE Press/Pentech, 1992, ch. 4, pp. 347–488.

[80] *Coding of Moving Pictures and Associated Audio for Digital*

Storage Media up to About 1.5 Mbit/s, ISO/IEC 11172 MPEG 1 International Standard, pt. 1–3, 1992.

[81] *Information Technology: Generic Coding of Moving Video and Associated Audio Information*, ISO/IEC CD 13818 MPEG 2 International Standard, pt. 1–3, 1992.

[82] L. Hanzo and J. P. Woodard, "An intelligent multimode voice communications system for indoors communications," *IEEE Trans. Veh. Technol.*, vol. 44, pp. 735–749, Nov. 1995.

[83] L. Hanzo, R. Salami, R. Steele, and P. M. Fortune, "Transmission of digitally encoded speech at 1.2 KBd for PCN," *Proc. Inst. Elect. Eng.*, vol. 139, pt. I, no. 4, pp. 437–447, Aug. 1992.

[84] J. D. Markel and A. H. Gray, Jr., *Linear Prediction of Speech*. New York: Springer-Verlag, 1976.

[85] N. S. Jayant and P. Noll, *Digital Coding of Waveforms*. Englewood Cliffs, NJ: Prentice-Hall, 1984.

[86] L. R. Rabiner and R. W. Shafer, *Digital Processing of Speech Signals*. Englewood Cliffs, NJ: Prentice-Hall, 1978.

[87] D. O'Shaugnessy, *Speech Communications—Human and Machine*. Reading, MA: Addison-Wesley, 1987.

[88] S. Furui, *Digital Speech Processing, Synthesis and Recognition*. Marcel Dekker, 1989.

[89] A. M. Kondoz, *Digital Speech: Coding for Low Bit Rate Communications Systems*. New York: Wiley, 1994.

[90] B. Kleijn and K. K. Paliwal, *Speech Coding and Synthesis*. Amsterdam, The Netherlands: Elsevier, 1995.

[91] R. A. Salami, L. Hanzo, R. Steele, K. H. J. Wong, and I. Wassell, "Speech coding," in *Mobile Radio Communications*, R. Steele, Ed. London: IEEE Press/Pentech, 1992, ch. 3, pp. 186–346.

[92] J. B. Anderson and S. Mohan, *Source and Channel Coding—An Algorithmic Approach*. Norwell, MA: Kluwer, 1991.

[93] H. B. Law and R. A. Seymour, "A reference distortion system using modulated noise," Inst. Elect. Eng. Paper no. 399-2E, Nov. 1962.

[94] *Methods for the Calculation of the Articulation Index*, ANSI Standard 53.5-1965, 1969.

[95] A. S. House, C. E. Williams, M. H. L. Hecker, and K. D. Kryter, "Articulation testing methods: Consonated differentiation with closed-response set," *J. Acoust. Soc. Amer.*, pp. 158–166, Jan. 1965.

[96] A. H. Gray and J. D. Markel, "Distance measures for speech processing," *IEEE Trans. Acoust., Speech, Signal Processing*, vol. ASSP-24, pp. 380–391, Oct. 1979.

[97] N. Kitawaki, M. Honda, and K. Itoh, "Speech quality assessment methods for speech coding systems," *IEEE Commun. Mag.*, vol. 22, pp. 26–33, Oct. 1984.

[98] N. Kitawaki, H. Nagabucki, and K. Itoh, "Objective quality evaluation for low-bit-rate speech coding systems," *IEEE J. Select. Areas Commun.*, vol. 6, pp. 242–249, Feb. 1988.

[99] S. Wang, A. Sekey, and A. Gersho, "An objective measure for predicting subjective quality of speech coders," *IEEE J. Select. Areas Commun.*, vol. 10, pp. 819–829, June 1992.

[100] U. Halka and U. Heute, "A new approach to objective quality-measures based on attribute matching," *Speech Commun.*, Band 11, pp. 15–30, 1992.

[101] K. Y. Lee, A. M. Kondoz, and B. G. Evans, "Speaker adaptive vector quantization of LPC parameters of speech," *Electron. Lett.*, vol. 24, no. 22, pp. 1392–1393, Oct. 27, 1988.

[102] W. T. K. Wong and I. Boyd "Optimal quantization performance of LPC parameters for speech coding," in *Proc. EUROSPEECH'89*, pp. 344–347.

[103] R. Laroia, N. Phamdo, and N. Farvardin, "Robust and efficient quantization of speech LSP parameters using structured vector quantisers," in *Proc. ICASSP'91*, Toronto, Ont., Canada, May 1992, pp. 641–644.

[104] K. K. Paliwal and B. S. Atal, "Efficient vector quantization of LPC parameters at 24 bits/frame," *IEEE Trans. Speech Audio Processing*, vol. 1, pp. 3–14, Jan. 1993.

[105] P. Kroon and E. F. Deprettere, "Regular pulse excitation—A novel approach to effective multipulse coding of speech," *IEEE Trans. Acoust., Speech, Signal Processing*, vol. ASSP-31, pp. 1054–1063, 1986.

[106] P. Vary, K. Hellwig, R. Hofmann, R. Sluyter, C. Galland, and M. Rosso, "Speech codec for the European mobile radio system," in *Proc. ICASSP*, Apr. 1988, pp. 227–230.

[107] I. A. Gerson and M. A. Jasuik, "Vector sum excited linear prediction (VSELP) speech coding at 8 kbps," *IEEE J. Select. Areas Commun.*, vol. 8, pp. 461–464, 1990.

[108] ——, "Vector sum excited linear prediction (VSELP)," in *Advances in Speech Coding*, B. S. Atal, V. Cuperman, and A. Gersho, Eds. Norwell, MA: Kluwer, 1991, pp. 69–80.

[109] I. A. Gerson, M. A. Jasiuk, J.-M. Muller, J. M. Nowack, and E. H. Winter, "Speech and channel coding for the half-rate GSM channel," in *Proc. ITG-Fachbericht 130*, VDE-Verlag, Berlin, Nov. 1994, pp. 225–233.

[110] I. A. Gerson and M. A. Jasiuk, "Vector sum excited linear prediction (VSELP) speech coding at 8 kbps," in *Proc. IEEE ICASSP'90*, pp. 461–464.

[111] ——, "Techniques for improving the performance of CELP-type speech codecs," *IEEE J. Select. Areas Commun.*, vol. 10, pp. 858–865, June 1992.

[112] J. Campbell, V. Welch, and T. Tremain, "An expandable error-protected 4800 bps CELP coder U.S. federal standard 4800 bps voice coder," in *Proc. ICASSP*, 1989, pp. 735–738.

[113] T. Ohya, H. Suda, and T. Miki, "5.6 kbits/s PSI-CELP of the half-rate PDC speech coding standard," in *Proc. IEEE Conf. Vehicular Technology*, June 1994, pp. 1680–1684.

[114] W. B. Kleijn, "Encoding speech using prototype waveforms," *IEEE Trans. Acoust., Speech, Signal Processing*, vol. 38, pp. 386–399, Oct. 1993.

[115] D. W. Griffin and J. S. Lim, "Multiband excitation vocoder," *IEEE Trans. Acoust., Speech, Signal Processing*, vol. 33, pp. 1223–1235, Aug. 1988.

[116] D. J. Hiotakakos and C. S. Xydeas, "Low bit rate coding using an interpolated zinc excitation model," in *Proc. IEEE Singapore Int. Conf. Communications Systems*, Nov. 1994, pp. 865–869.

[117] J. H. Chen, R. C. Cox, Y. C. Lin, N. Jayant, and M. J. Melchner, "A low-delay CELP codec for the CCITT 16 kb/s speech coding standard," *IEEE J. Select. Areas Commun.*, vol. 10, pp. 830–849, June 1992.

[118] A. Kataoka, J.-P. Adoul, P. Combescure, and P. Kroon, "ITU-T 8-kbits/s standard speech codec for personal communication services," in *Proc. Int. Conf. Universal Personal Communications*, Tokyo, Japan, Nov. 1995, pp. 818–822.

[119] A. McCree, K. Fruong, E. B. George, T. P. Barnwell, and V. Viswanathan, "A 2.4 kbit/s MELP candidate for the new US federal standard," in *Proc. ICASSP'96*, Atlanta, GA, 1996, pp. 200–203.

[120] R. P. Ramachandran, M. M. Sondhi, N. Seshadri, and B. S. Atal, "A two codebook format for robust quantization of line spectral frequencies," *IEEE Trans. Speech Audio Processing*, vol. 3, pp. 157–168, May 1995.

[121] R. A. Salami, C. Laflamme, and J. P. Adoul, "ACELP speech coding at 8kbit/s with a 10 ms frame: A candidate for CCITT standardization," in *Proc. IEEE Workshop Speech Coding for Telecommunications*, Sainte-Adele, Quebec, Canada, Oct. 13–15, 1993, pp. 23–24.

[122] R. A. Salami, C. Laflamme, J.-P. Adoul, and D. Massaloux, "A toll quality 8 Kb/s speech codec for the personal communications system (PCS)," *IEEE Trans. Veh. Technol.*, vol. 43, pp. 808–816, Aug. 1994.

[123] "Coding of speech at 8 kbit/s using conjugate-structure algebraic code-excited linear prediction (CS-ACELP)," ITU draft recommendation G.729, Feb. 1996.

[124] J. P. Campbell, Jr., T. E. Tremain, and V. C. Welch, "The DoD 4.8 kbps standard (federal standard 1016)," in *Advances in Speech Coding*. Norwell, MA: Kluwer, 1990, pp. 121–133.

[125] J.-P. Adoul and C. Lamblin, "A comparison of some algebraic structures for CELP coding of speech," in *Proc. ICASSP'87*, pp. 1953–1956.

[126] J.-P. Adoul, P. Magillian, M. Deepnat, S. Moriset, "Fast CELP coding based on algebraic codes," in *Proc. ICASSP'87*, pp. 1957–1960.

[127] C. Lamblin *et al.*, "Fast CELP coding based on the Barnes–Wall lattice in 16 dimension," in *Proc. ICASSP'89*, Glasgow, UK, pp. 61–64.

[128] H. C. Laflamme, J.-P. Adoul, H. Y. Su, and S. Morissette, "On reducing the complexity of codebook search in CELP through the use of algebraic codes," in *Proc. ICASSP 1990*, Albuquerque, NM, 1990, pp. 177–180.

[129] R. A. Salami, "Binary pulse excitation: A novel approach to low complexity CELP coding," in *Advances in Speech Coding*, B. S. Atal, V. Cupern, and A. Gersho, Eds. Norwell, MA: Kluwer, 1991.

[130] I. A. Gerson and M. A. Jasiuk, "Vector sum excitation lin-

ear prediction (VSELP) speech coding at 8 kbps," in *Proc. ICASSP'90*, Albuquerque, NM, Apr. 3–6, 1990, pp. 461–464.

[131] X. Maitre, "7 kHz audio coding within 64 kbit/s," *IEEE J. Select. Areas Commun.*, vol. 6, pp. 283–298, Feb. 1988.

[132] S. R. Quackenbush, "A 7 kHz bandwidth, 32 kbps speech coder for ISDN," in *Proc. ICASSP'91*, pp. 1–4.

[133] J. D. Johnston, "Transform coding of audio signals using perceptual noise criteria," *IEEE J. Select. Areas Commun.*, vol. 6, no. 2, pp. 314–323, 1988.

[134] E. Ordentlich and Y. Shoham, "Low-delay code-excited linear-predictive coding of wideband speech at 32 kbps," in *Proc. ICASSP'91*, pp. 9–12.

[135] A. W. Black, A. M. Kondoz, and B. G. Evans, "High quality low delay wideband speech coding at 16 kbit/sec," in *Proc. 2nd Int. Workshop Mobile Multimedia Communications*, Bristol University, UK, Apr. 11–14, 1995.

[136] C. Laflamme *et al.*, "16 kbps wideband speech coding technique based on Algebraic CELP," in *Proc. ICASSP'91*, pp. 13–16.

[137] R. Salami, C. Laflamme, and J.-P. Adoul, "Real-time implementation of a 9.6 kbit/s ACELP wideband speech coder," in *Proc. GLOBECOM'92*.

[138] V. E. Sanchez-Calle, C. Laflamme, R. Salami, and J.-P. Adoul, "Low-delay algebraic CELP coding of wideband speech," in *Signal Processing VI: Theories and Applications*, J. Vandewalle, R. Boite, M. Moonen, and A. Oosterlink, Eds. Amsterdam, The Netherlands: Elsevier, 1992, pp. 495–498.

[139] *Proc. 2nd Int. Workshop Mobile Multimedia Communications*, MoMuC-2, Bristol, UK, Apr. 11–14, 1995.

[140] S. Sheng, A. Chandrakasan, and R. W. Brodersen, "A portable multimedia terminal," *IEEE Commun. Mag.*, vol. 30, pp. 64–75, Dec. 1992.

[141] "Special issue on very low bit rate video coding," *IEEE Trans. Circuits Syst. Video Technol.*, vol. 4, June 1994.

[142] B. Girod *et al.*, "Special issue on image sequence compression," *IEEE Trans. Image Processing*, vol. 3, Sept. 1994.

[143] A. Netravali and B. Haskell, *Digital Pictures: Representation and Compression*. New York: Plenum, 1988.

[144] J. W. Woods, Ed., *Subband Image Coding*. Norwell, MA: Kluwer, 1991.

[145] R. Stedman, H. Gharavi, L. Hanzo, and R. Steele, "Transmission of subband-coded images via mobile channels," *IEEE Trans. Circuits Syst. Video Technol.*, vol. 3, pp. 15–27, Feb. 1993.

[146] J. Katto, J. Ohki, S. Nogaki, and M. Ohta, "A wavelet codec with overlapped motion compensation for very low bit-rate environment," *IEEE Trans. Circuits Syst. Video Technol.*, vol. 4, pp. 328–338, June 1994.

[147] P. Strobach, "Tree-structured scene adaptive coder," *IEEE Trans. Commun.*, vol. 38, pp. 477–486, 1990.

[148] J. Vaisey and A. Gersho, "Image compression with variable block size segmentation," *IEEE Trans. Signal Processing*, vol. 40, pp. 2040–2060, Aug. 1992.

[149] A. Gersho and R. M. Gray, *Vector Quantization and Signal Compression*. Norwell, MA: Kluwer, 1992.

[150] L. Torres and J. Huguet, "An improvement on codebook search for vector quantization," *IEEE Trans. Commun.*, vol. 42, pp. 208–210, Feb. 1994.

[151] B. Ramamurthi and A. Gersho, "Classified vector quantization of images," *IEEE Trans. Commun.*, vol. COM-31, no. 11, pp. 1105–1115, Nov. 1986.

[152] L. Hanzo, R. Stedman, and J. C. S. Cheung, "A portable multimedia communicator scheme," in *Multimedia Technologies and Future Applications*, R. I. Damper, W. Hall, and J. W. Richards, Eds. London: Pentech, 1993, pp. 31–54.

[153] S. L. F.-M. Wang, "Hybrid video coding for low bit-rate applications," in *Proc. IEEE ICASSP*, Apr. 19–22, 1994, pp. 481–484.

[154] J. F. Arnold, X. Zhang, and M. C. Cavenor, "Adaptive quadtree coding of motion-compensated image sequences for use on the broadband ISDN," *IEEE Trans. Circuits Systems Video Technol.*, vol. 3, pp. 222–229, June 1993.

[155] E. Shustermann and M. Feder, "Image compression via improved quadtree decomposition algorithms," *IEEE Trans. Image Processing*, vol. 3, pp. 207–215, Mar. 1994.

[156] *Proc. Int. Workshop Coding Techniques for Very Low Bit-rate Video*, Shinagawa, Tokyo, Japan, Nov. 8–10, 1995.

[157] K. H. Tzou and H. G. Mussmann, and K. Aizawa, Eds., "Special issue on very low bit rate video coding," *IEEE Trans. Circuits Syst. Video Technol.*, vol. 4, pp. 213–357, June 1994.

[158] N. Hubing, Ed., "Special issue on speech and image coding," *IEEE J. Select. Areas Commun.*, vol. 10, pp. 793–976, June 1992.

[159] B. Girod *et al.*, Eds., "Special issue on image sequence compression," *IEEE Trans. Image Processing*, vol. 3, pp. 465–716, Sept. 1994.

[160] M. F Chowdhury, A. I. Clark, A. C. Downton, E. Morimatsu, and D. E. Pearson, "A switched model-based coder for video signals," *IEEE Trans. Circuits Syst. Video Technol.*, vol. 4, pp. 228–235, June 1994.

[161] G. Bozdagi, A. M. Tekalp, and L. Onural, "3-D motion estimation and wireframe adaptation including photometric effects for model-based coding of facial image sequences," *IEEE Trans. Circuits Syst. Video Technol.*, vol. 4, pp. 246–256, June 1994.

[162] C. S. Choi, K. Aizawa, H. Harashima, and T. Takeb, "Analysis and synthesis of facial image sequences in model-based image coding," Special Issue of the *IEEE Trans. Circuits and Systems for Video Tech.*, vol. 4, no. 3, pp. 257–275, June 1994.

[163] H. Gharavi, "Subband coding of video signal," in *Subband Image Coding*, J. W. Woods, Ed. Kluwer, 1991, ch. 6, pp. 229–271.

[164] K. N. Ngan and W. L. Chooi, "Very low bit rate video coding using 3D subband approach," *IEEE Trans. Circuits Syst. Video Technol.*, vol. 4, pp. 309–316, June 1994.

[165] L. Hanzo and J. Streit, "A fractal video communicator," in *Proc. IEEE VTC'94*, Stockholm, Sweden, June 7–11, pp. 1030–1034.

[166] M. Khansari, A. Jalali, E. Dubois, and P. Mermelstein, "Robust low bit-rate video transmission over wireless access systems," in *Proc. Int. Communications Conf. (ICC)*, 1994, pp. 571–575.

[167] N. Färber, E. Steinbach, and B. Girod, "Robust H.263 video transmission over wireless channels," in *Proc. Int. Picture Coding Symp. (PCS)*, Melbourne, Australia, Mar. 1996, pp. 575–578.

[168] E. Steinbach, A. Hanjalic, and B. Girod, "3D motion and scene structure estimation with motion dependent distortion of measurement windows," in *Proc. ICIP-96*, Lausanne, Switzerland, Sept. 16–19, 1996, vol. 1, pp. 61–68.

[169] M. Horn and B. Girod, Performance analysis of multiscale motion compensation techniques in pyramid coders, in *Proc. ICIP-96*, Lausanne, Switzerland, Sept. 16–19, 1996, vol. 3, pp. 255–258.

[170] E. Steinbach, N. Faerber, and B. Girod, "Standard compatible extension of H.263 for robust video transmission in mobile environments," *IEEE Trans. Circuits Syst. Video Technol.*, to be published. (See also http://www-nt.e-technik.uni-erlangen.de/girod/publications.html.)

[171] B. Girod, E. Steinbach, and N. Faerber, "Performance of the H.263 video compression standard," *J. VLSI Signal Process.*, to be published. (See also http://www-nt.e-technik.uni-erlangen.de/girod/publications.html.)

[172] B. Girod, N. Faerber, and E. Steinbach, "Standards based video communication at very low bit-rates," in *Proc. VIII Eur. Signal Processing Conf. (EUSIPCO-96)*, Trieste, Italy, Sept. 10–13, 1996.

[173] N. Faerber, E. Steinbach, and B. Girod, "Robust H.263 compatible transmission for mobile video server access," in *Proc. 1st Int. Workshop Wireless Image/Video Communications*, Loughborough University, UK, Sept. 4–5, 1996, pp. 8–13.

[174] F. Eryurtlu, A. H. Sadka, and A. M. Kondoz, "Error robustness improvement of video codecs with two-way decodable codes," *Electron. Lett.*, vol. 33, no. 1, pp. 41–43, Jan. 2, 1997.

[175] A. H. Sadka, F. Eryurtlu, and A. M. Kondoz, "Improved performance H.263 under erroneous transmission conditions," *Electron. Lett.*, vol. 33, no. 2, pp. 122–124, Jan. 16, 1997.

[176] P. Cherriman and L. Hanzo, "Programmable H.263-based wireless video transceivers for interference-limited environments," *IEEE Trans. Circuits Syst. Video Technol.*, to be published.

[177] P. Cherriman and L. Hanzo, "H.261 and H.263 wireless videophone performance in interference-limited scenarios," in *Proc. PIMRC'96*, Taipei, Taiwan, pp. 158–162, Oct. 15–18, 1996.

[178] P. Cherriman and L. Hanzo, submitted for publication. (See also http://www-mobile.ecs.soton.ac.uk.)

[179] T. Keller, P. Cherriman, and L. Hanzo, "Orthogonal frequency division multiplex transmission of H.263 encoded video over wireless ATM networks," in *Proc. ACTS Summit'97*, Aalborg, Denmark, Oct. 1997, pp. 276–281.

[180] R. M. Pelz, "An unequal error protected $p \times 8$ kbit/s video transmission for DECT," in *Proc. IEEE Vehicular Technology Conf.*, 1994, pp. 1020–1024.

[181] T. Chen, "A real-time software based end-to-end wireless visual communications simulation platform," in *Proc. SPIE Conf. Visual Communications and Image Processing*, 1995, pp. 1068–1074.

[182] K. Illgner and D. Lappe, "Mobile multimedia communications in a universal telecommunications network," in *Proc. SPIE Conf. Visual Communications and Image Processing*, 1995, pp. 1034–1043.

[183] Y. Zhang, "Very low bit rate video coding standards," in *Proc. SPIE Conf. Visual Communications and Image Processing*, 1995, pp. 1016–1023.

[184] H. Ibaraki *et al.*, "Mobile video communication techniques and services," in *Proc. SPIE Conf. Visual Communications and Image Processing*, 1995, pp. 1024–1033.

[185] K. Watanabe *et al.*, "A study on transmission of low bit-rate coded video over radio links," in *Proc. SPIE Conf. Visual Communications and Image Processing*, 1995, pp. 1025–1029.

[186] J. Streit, "Digital image compression," Ph.D. dissertation, Dept. of Electronics, Univ. of Southampton, 1996.

[187] J. Streit and L. Hanzo, "Vector-quantized low-rate cordless videophone systems," *IEEE Trans. Veh. Technol.*, vol. 42, pp. 340–357, May 1997.

[188] L. Hanzo and J. Streit, "Adaptive low-rate wireless videophone systems," *IEEE Trans. Circuits Syst. Video Technol.*, vol. 5, pp. 305–319, Aug. 1995.

[189] J. Streit and L. Hanzo, "Quadtree-based parametric wireless videophone systems," *IEEE Trans. Circuits Syst. Video Technol.*, vol. 6, pp. 225–237, Apr. 1996.

[190] ——, "Comparative study of programmable-rate videophone codecs for existing and future multimode wireless systems," *Eur. Trans. Telecommun.*, vol. 8, no. 6, pp. 271–284, 1997.

[191] A. K. Jain, *Fundamentals of Digital Image Processing*. Englewood Cliffs, NJ: Prentice-Hall, 1989.

[192] P. Cherriman, "Packet video communications," Ph.D. minithesis, Dept. of Electr., Univ. of Southampton, UK, 1996.

[193] "Video Coding for Low Bitrate Communication," International Telecommunications Union, Geneva, Switzerland, ITU Recommendation H.263, 1996.

[194] M. W. Whybray and W. Ellis, "H.263—Video coding recommendation for PSTN videophone and multimedia," in *Inst. Elect. Eng. Colloquium (Dig.)*, England, June 1995, pp. 6/1–6/9.

[195] M. Khansari, A. Jalali, E. Dubois, and P. Mermelstein, "Low bit-rate video transmission over fading channels for wireless microcellular systems," *IEEE Trans. Circuits Syst. Video Technol.*, vol. 6, pp. 1–11, Feb. 1996.

[196] J. C. Arnbak, J. H. Bons, and J. W. Vieveen, "Graphical correspondence in electronic-mail networks using personal computers," *IEEE J. Select. Areas Commun.*, vol. SAC-7, pp. 257–267, Feb. 1989.

[197] M. Klerk, R. Prasad, J. H. Bons, and N. B. J. Weyland, "Introducing high-resolution line graphics in UK teletext using differential chain coding," *Proc. Inst. Elect. Eng.*, vol. 137, pt. I, pp. 325–334, Dec. 1990.

[198] K. Liu and R. Prasad, "Performance analysis of differential chain coding," *Eur. Trans. Telecommun. Related Technol.*, vol. 3, pp. 323–330, July–Aug. 1992.

[199] D. L. Neuhoff and K. G. Castor, "A rate and distortion analysis of chain codes for line drawings," *IEEE Trans. Inform. Theory*, vol. IT-31, pp. 53–68, Jan. 1985.

[200] A. B. Johannessen, R. Prasad, N. B. J. Weyland, and J. H. Bons, "Coding efficiency of multiring differential chain coding," *Proc. Inst. Elect. Eng.*, vol. 139, pt. I, Apr. 1992, pp. 224–232.

[201] R. Prasad, J. W. Vivien, J. H. Bons, and J. C. Arnbak, "Relative vector probabilities in differential chain coded line drawings," in *Proc. IEEE Pacific Rim Conf. Communications, Computers and Signal Processing*, Victoria, Canada, June 1989, pp. 138–142.

[202] L. Yang, H. I. Cakil, and R. Prasad, "On-line handwriting processing in indoor and outdoor radio environment for multimedia," in *Proc. IEEE VTC'94*, Stockholm, Sweden, pp. 1015–1019.

[203] R. Prasad, P. A. D. Spaargaren, and J. H. Bons, "Teletext reception in a mobile channel for a broadcast tele-information system," *IEEE Trans. Veh. Technol.*, vol. 42, pp. 535–545, Nov. 1993.

[204] L.-P. W. Niemel and R. Prasad, "A novel description of handwritten characters for use with generalized Fourier descriptors," *Eur. Trans. Telecommun.*, vol. 3, no. 5, pp. 455–464, Sept.–Oct. 1992.

[205] ——, "An improved character description method based on generalized Fourier descriptors," *Eur. Trans. Telecommun.*, vol. 5, no. 3, pp. 371–376, May–June 1994.

[206] H. Yuen and L. Hanzo, "A novel coding scheme for the transmission of on-line handwriting," in *Proc. Globecom'95*, Singapore, Nov. 13–17, 1995, pp. 2284–2288.

[207] L. Hanzo and H. Yuen, "Wireless multilevel graphical correspondence," *Eur. Trans. Commun.*, vol. 8, no. 3, pp. 271–283, May–June 1997.

[208] C. C. Tappert, C. Y. Suen, and T. Wakahara, "The state of the art in on-line handwriting recognition," *IEEE Trans. Pattern Anal. Machine Intell.*, vol. 12, pp. 787–808, 1990.

[209] R. Plamondon and G. Lorette, "Automatic signature verification and writer identification—The state of the art," *Pattern Recognit.*, vol. 22, no. 2, pp. 107–131, 1989.

[210] S. R. Veltman and R. Prasad, "Hidden Markov models applied to on-line handwritten isolated character recognition," *IEEE Trans. Image Processing*, vol. 3, no. 3, pp. 314–318, 1994.

[211] L. Yang and R. Prasad, "On-line recognition of handwritten characters using differential angles and structural descriptors," *Pattern Recognit. Lett.*, vol. 14, no. 12, pp. 1019–1024, 1993.

[212] M.-Y. Chen, "Off-line handwritten word recognition using a hidden Markov model type stochastic network," *IEEE Trans. Pattern Anal. Machine Intell.*, vol. 16, no. 5, pp. 481–496, 1994.

[213] L. Yang, B. K. Widjaja, and R. Prasad, "Application of hidden Markov models for signature verification," *Pattern Recognit.*, vol. 28, no. 2, pp. 161–170, 1995.

[214] L. Hanzo, and R. Steele, "The Pan-European mobile radio system, Part 1 and 2," *Eur. Trans. Telecommun.*, vol. 5, no. 2, pp. 245–276, Mar.–Apr. 1994.

[215] P. Vary and R. J. Sluyter, "MATS-D speech codec: Regular-pulse excitation LPC," in *Proc. Nordic Conf. Mobile Radio Communications*, 1986, pp. 257–261.

[216] J. D. Parsons, *The Mobile Radio Propagation Channel*. London: Pentech, 1992.

[217] D. Greenwood and L. Hanzo, "Characterization of mobile radio channels," in *Mobile Radio Communications*, R. Steele, Ed. London: Pentech, 1992, ch. 2, pp. 92–185.

[218] D. J. Goodman and S. X. Wei, "Efficiency of packet reservation multiple access," *IEEE Trans. Veh. Technol.*, vol. 40, pp. 170–176, Feb. 1991.

[219] X. Qiu and V. K. Li, "Dynamic reservation multiple access (DRAMA): A new multiple access scheme for personal communication systems (PCS)," *Wireless Networks*, vol. 2, pp. 117–128, 1996.

[220] D. J. Goodman and S. X. Wei, "Efficiency of packet reservation multiple access," *IEEE Trans. on Veh. Technol.*, vol. 40, pp. 170–176, Feb. 1991.

[221] S. Nanda, D. J. Goodman, and U. Timor, "Performance of PRMA: A packet voice protocol for cellular systems," *IEEE Trans. Veh. Technol.*, vol. 40, pp. 584–598, Aug. 1991.

[222] J. DeVile, "A reservation multiple access scheme for an adaptive TDMA air-interface," in *Proc. Winlab Workshop*, Rutgers—The State University, New Brunswick, NJ, Sept. 1993.

[223] J. Dunlop, D. Robertson, P. Cosimi, and J. D. Vile, "Development and optimization of a statistical multiplexing mechanism for ATDMA," in *Proc. IEEE 44th Veh. Technol. Conf.*, Stockholm, Sweden, June 1994, pp. 1040–1044.

[224] N. Amitay and S. Nanda, "Resource auction multiple access (RAMA) for statistical multiplexing of speech in wireless PCS," *IEEE Trans. Veh. Technol.*, vol. 43, pp. 584–595, Aug. 1994.

[225] F. J. Panken, "Multiple-access protocols over the years: A taxonomy and survey," in *Proc. 1996 IEEE Int. Conf. Communication Systems (ICCS)*, Nov. 1996, pp. 2.1.1–2.1.5.

[226] J. Brecht, L. Hanzo, and M. D. Buono, "Multi-frame packet reservation multiple access for variable-rate users," in *Proc. PIMRC'97*, Helsinki, Finland, Sept. 1–4, 1997, pp. 430–438.

[227] J. Brecht, M. D. Buono, and L. Hanzo, "Multi-frame packet reservation multiple access using oscillation-scaled histogram-based Markov modeling of video codecs," *Image Commun.*, to be published. (See also http://www-mobile.ecs.soton.ac.uk/.)

[228] J. Brecht and L. Hanzo, "Statistical packet assignment multiple access for wireless asynchronous transfer mode systems," in

Proc. ACTS Summit'97, Aalborg, Denmark, Oct. 1997, pp. 734–738.

[229] J. Williams, L. Hanzo, R. Steele, and J. C. S. Cheung, "A comparative study of microcellular speech transmission schemes," *IEEE Trans. Veh. Technol.*, vol. 43, pp. 909–924, Nov. 1994.

[230] J. C. S. Cheung, L. Hanzo, W. T. Webb, and R. Steele, "Effects of packet reservation multiple access on objective speech quality," *Electron. Lett.*, vol. 29, no. 2, pp. 152–153, Jan. 21, 1993.

[231] L. Hanzo, J. C. S. Cheung, R. Steele, and W. T. Webb, "Performance of PRMA schemes via fading channels," in *Proc. IEEE VTC'93*, Secaucus, NJ, May 1993, pp. 913–916.

[232] M. Eastwood and L. Hanzo, "Packet reservation multiple access for wireless multimedia communications," *Electron. Lett.*, vol. 29, no. 13, pp. 1178–1179, June 24, 1993.

[233] L. Hanzo, J. C. S. Cheung, and R. Steele, "PRMA efficiency in adaptive transceivers," *Electron. Lett.*, vol. 29, no. 8, pp. 697–698, Apr. 15, 1993.

[234] C. N. Campopiano and B. G. Glazer, "A coherent digital amplitude and phase modulation scheme," *IRE Trans. Commun. Syst.*, vol. CS-10, pp. 90–95, 1962.

[235] G. D. Forney *et al.*, "Efficient modulation for band-limited channels," *IEEE J. Select. Areas Commun.*, vol. SAC-2, pp. 632–647, Sept. 1984.

[236] K. Feher, "Modems for emerging digital cellular mobile systems," *IEEE Trans. Veh. Technol.*, vol. 40, no. 2, pp. 355–365, May 1991.

[237] M. Iida and K. Sakniwa, "Frequency selective compensation technology of digital 16-QAM for microcellular mobile radio communication systems," in *Proc. VTC'92*, Denver, CO, pp. 662–665.

[238] R. J. Castle and J. P. McGeehan, "A multilevel differential modem for narrowband fading channels," in *Proc. VTC'92*, Denver, CO, pp. 104–109.

[239] D. J. Purle, A. R. Nix, M. A. Beach, and J. P. McGeehan, "A preliminary performance evaluation of a linear frequency hopped modem, in *Proc. VTC'92*, Denver, CO, pp. 120–124.

[240] Y. Kamio and S. Sampei, "Performance of reduced complexity DFE using bidirectional equalizing in land mobile communications," in *Proc. VTC'92*, Denver, CO, pp. 372–376.

[241] T. Nagayasu, S. Sampei, and Y. Kamio, "Performance of 16-QAM with decision feedback equalizer using interpolation for land mobile communications," in *Proc. VTC'92*, Denver, CO, pp. 384–387.

[242] E. Malkamaki, "Binary and multilevel offset QAM, spectrum efficient modulation schemes for personal communications," in *Proc. VTC'92*, Denver, CO, pp. 325–378.

[243] Z. Wan and K. Feher, "Improved efficiency CDMA by constant envelope SQAM," in *Proc. VTC'92*, Denver, CO, pp. 51–55.

[244] H. Sasaoka, "Block coded 16-QAM/TDMA cellular radio system using cyclical slow frequency hopping," in *Proc. VTC'92*, Denver, CO, pp. 405–408.

[245] W. T. Webb, L. Hanzo, and R. Steele, "Bandwidth-efficient QAM schemes for Rayleigh-fading channels," *Proc. Inst. Elect. Eng.*, vol. 138, no. 3, pp. 169–175, June 1991.

[246] L. Hanzo, R. Steele, and P. M. Fortune, "A subband coding, BCH coding and 16-QAM system for mobile radio speech communications," *IEEE Veh. Technol.*, vol. 39, pp. 327–339, Nov. 1990.

[247] P. M. Fortune, L. Hanzo, and R. Steele, "On the computation of 16-QAM and 64-QAM performance in Rayleigh-fading channels," *IEICE Trans. Commun.*, vol. E75-B, no. 6, pp. 466–475, June 1992.

[248] A. S. Wright and W. G. Durtler, "Experimental performance of an adaptive digital linearized power amplifier," *IEEE Trans. Veh. Technol.*, vol. 41, pp. 395–400, Nov. 1992.

[249] M. Faulkner and T. Mattson, "Spectral sensitivity of power amplifiers to quadrature modulator misalignment," *IEEE Trans. Veh. Technol.*, vol. 41, pp. 516–525, Nov. 1992.

[250] P. B. Kennington *et al.*, "Broadband linear amplifier design for a PCN base-station," in *Proc. 41st IEEE VTC*, May 1991, pp. 155–160.

[251] R. J. Wilkinson *et al.*, "Linear transmitter design for MSAT terminals," in *Proc. 2nd Int. Mobile Satellite Conf.*, June 1990.

[252] S. P. Stapleton and F. C. Costescu, "An adaptive predistorter for a power amplifier based on adjacent channel emissions," *IEEE Trans. Veh. Technol.*, vol. 41, pp. 49–57, Feb. 1992.

[253] ——, "An adaptive predistorter for a power amplifier based on adjacent channel emissions," *IEEE Trans. Veh. Technol.*, vol. 41, pp. 49–57, Feb. 1992.

[254] S. P. Stapleton, G. S. Kandola, and J. K. Cavers, "Simulation and analysis of an adaptive predistorter utilizing a complex spectral convolution," *IEEE Trans. Veh. Technol.*, vol. 41, pp. 387–394, Nov. 1992.

[255] J. K. Cavers, "An analysis of pilot symbol assisted modulation for Rayleigh fading channels," *IEEE Trans. Veh. Technol.*, vol. 40, pp. 686–693, Nov. 1991.

[256] A. Bateman and J. P. McGeehan, "Feedforward transparent tone in band for rapid fading protection in multipath fading," in *Proc. Inst. Elect. Eng. Int. Conf. Communications*, 1986, vol. 68, pp. 9–13.

[257] A. Bateman, "Feedforward transparent tone in band: Its implementation and applications," *IEEE Trans. Veh. Technol.*, vol. 39, pp. 235–243, Aug. 1990.

[258] J. K. Cavers, "The performance of phase locked transparent tone in band with symmetric phase detection," *IEEE Trans. Commun.*, vol. 39, pp. 1389–1399, Sept. 1991.

[259] R. Steele and W. T. Webb, "Variable rate QAM for data transmission over Rayleigh fading channels," in *Proc. IEEE Wireless'91*, Calgary, Alberta, Canada, 1991, pp. 1–14.

[260] W. Webb and R. Steele, "Variable rate QAM for mobile radio," *IEEE Trans. Commun.*, vol. 43, pp. 2223–2230, 1995.

[261] Y. Kamio, S. Sampei, H. Sasaoka, and N. Morinaga, "Performance of modulation-level-control adaptive-modulation under limited transmission delay time for land mobile communications," in *Proc. IEEE 45th Vehicular Technology Conf.*, 1995, pp. 221–225.

[262] S. Sampei, S. Komaki, and N. Morinaga, "Adaptive modulation/TDMA scheme for large capacity personal multi-media communication systems," *IEICE Trans. Commun.*, vol. 77, no. 9, pp. 1096–1103, 1994.

[263] M. Morimoto, H. Harada, M. Okada, and S. Komaki, "A study on power assignment of hierarchical modulation schemes for digital broadcasting," *IEICE Trans. Commun.*, vol. 77, no. 12, pp. 1495–1500, 1994.

[264] S. Otsuki, S. Sampei, and N. Morinaga, "Square-QAM adaptive modulation TDMA/TDD systems using modulation level estimation with Walsh function," *Electron. Lett.*, pp. 169–171, Nov. 1995.

[265] S.-G. Chua and A. Goldsmith, "Variable-rate variable-power mQAM for fading channels," in *Proc. IEEE 46th Vehicular Technology Conf.*, 1996, pp. 815–819.

[266] D. A. Pearce, A. G. Burr, and T. C. Tozer, "Comparison of counter-measures against slow Rayleigh fading for TDMA systems," in *IEEE Colloquium Advanced TDMA Techniques and Applications*, 1996, pp. 9/1–9/6.

[267] J. M. Torrance and L. Hanzo, "Upper bound performance of adaptive modulation in a slow Rayleigh fading channel," *Electron. Lett.*, pp. 169–171, Apr. 1996.

[268] ——, "Adaptive modulation in a slow Rayleigh fading channel," in *Proc. IEEE 7th Personal, Indoor and Mobile Radio Communications (PIMRC) Conf.*, 1996, pp. 497–501.

[269] ——, "Optimization of switching levels for adaptive modulation in a slow Rayleigh fading channel," *Electron. Lett.*, pp. 1167–1169, June 1996.

[270] ——, "Demodulation level selection in adaptive modulation," *Electron. Lett.*, vol. 32, no. 19, pp. 1751–1752, Sept. 12, 1996.

[271] ——, "Latency considerations for adaptive modulation in slow Rayleigh fading," in *Proc. IEEE VTC'97*, Phoenix, AZ, 1997, pp. 1204–1209.

[272] ——, *Statistical Multiplexing for Mitigating Latency in Adaptive Modems, PIMRC'97*, Helsinki, Finland, Sept. 1–4, 1997, pp. 938–942.

[273] M.-S. Alouini and A. Goldsmith, "Area spectral efficiency of cellular mobile radio systems," in *Proc. IEEE VTC'97*, Phoenix, AZ, pp. 652–656.

[274] ——, "Capacity of nakagami multipath fading channels," in *Proc. IEEE VTC'97*, Phoenix, AZ, pp. 652–656.

[275] K. R. Narayanan and L. J. Cimini Jr., "Equalizer adaptation algorithms for high speed wireless communications," in *Proc. IEEE VTC'96*, pp. 681–685.

[276] J. Wu and A. H. Aghvami, "A new adaptive equalizer with channel estimator for mobile radio communications," *IEEE Trans. Veh. Technol.*, vol. 45, pp. 467–474, Aug. 1996.

[277] Y. Gu and T. Le-Ngoc, "Adaptive combined DFE/MLSE techniques for ISI channels," *IEEE Trans. Commun.*, vol. 44, pp. 847–857, July 1996.

[278] A. P. Clark and R. Harun, "Assessment of Kalman-filter channel estimators for an HF radio link," *Proc. Inst. Elect. Eng.*, vol. 133, pp. 513–521, Oct. 1986.

[279] R. W. Chang, "Synthesis of band-limited orthogonal signals for multichannel data transmission," *Bell Syst. Tech. J.*, vol. 46, pp. 1775–1796, Dec. 1966.

[280] M. S. Zimmermann and A. L. Kirsch, "The AN/GSC-10/KATHRYN/ variable rate data modem for HF radio," *IEEE Trans. Commun. Technol.*, vol. COM-15, no. 2, Apr. 1967.

[281] E. N. Powers and M. S. Zimmermann, "A digital implementation of a multichannel data modem," in *Proc. IEEE Int. Conf. Commun.*, Philadelphia, PA, 1968.

[282] B. R. Saltzberg, "Performance of an efficient parallel data transmission system," *IEEE Trans. Commun. Technol.*, vol. COM-15, Dec. 1967.

[283] R. W. Chang and R. A. Gibby, "A theoretical study of performance of an orthogonal multiplexing data transmission scheme," *IEEE Trans. Commun. Technol.*, vol. COM-16, no. 4, Aug. 1968.

[284] S. B. Weinstein and P. M. Ebert, "Data transmission by frequency division multiplexing using the discrete Fourier transform," *IEEE Trans. Commun. Technol.*, vol. COM-19, no. 5, Oct. 1971.

[285] A. Peled and A. Ruiz, "Frequency domain data transmission using reduced computational complexity algorithms," in *Proc. ICASSP*, 1980, pp. 964–967.

[286] B. Hirosaki, "An orthogonally multiplexed QAM system using the discrete Fourier transform," *IEEE Trans. Commun.*, vol. COM-29, no. 7, July 1981.

[287] H. J. Kolb, "Untersuchungen über ein digitales mehrfrequenzverfahren zur Datenübertragung," *Ausgewählte Arbeiten über Nachrichtensysteme*, Universität Erlangen-Nürnberg, no. 50, 1981.

[288] H. W. Schüssler, "Ein digitales mehrfrequenzverfahren zur Datenüber-tragung," *Professoren-Konferenz, Stand und Entwicklungsaussichten der Daten und Telekommunikation*, Darmstadt, Germany, pp. 179–196, 1983.

[289] J. Cimini, "Analysis and simulation of a digital mobile channel using orthogonal frequency division multiplexing," *IEEE Trans. Commun.*, vol. COM-33, pp. 665–675, July 1985.

[290] K. Preuss, "Ein Parallelverfahren zur schnellen Datenübertragung Im Ortsnetz," *Ausgewählte Arbeiten über Nachrichtensysteme*, Universität Erlangen-Nürnberg, no. 56.

[291] R. Rückriem, "Realisierung und messtechnische untersuchung an einem digitalen parallelverfahren zur Datenübertragung im fernsprechkanal," *Ausgewählte Arbeiten über Nachrichtensysteme*, Universität Erlangen-Nürnberg, no. 59.

[292] F. Mueller-Roemer, "Directions in audio broadcasting," *J. Audio Eng. Soc.*, vol. 41, no. 3, pp. 158–173, Mar. 1993.

[293] G. Plenge, "DAB—A new radio broadcasting system-state of development and ways for its introduction," *Rundfunktech. Mitt.*, vol. 35, no. 2, p. 45ff, 1991.

[294] M. Alard and R. Lassalle, "Principles of modulation and channel coding for digital broadcasting for mobile receivers," *EBU Rev., Tech. no. 224*, pp. 47–69, Aug. 1987.

[295] *Proc. 1st Int. Symp. (DAB)*, Montreux, Switzerland, June 1992.

[296] I. Kalet, "The multitone channel," *IEEE Trans. Commun.*, vol. 37, pp. 119–124, Feb. 1989.

[297] J. P Woodard, T. Keller, and L. Hanzo, "Turbo-coded orthogonal frequency division multiplex transmission of 8 kbps encoded speech," in *Proc. ACTS'97*, Aalborg, Denmark, Oct. 1997, pp. 894–899.

[298] T. Keller, J. P. Woodard, and L. Hanzo, "Turbo-coded parallel modem techniques for personal communications," in *Proc. IEEE VTC'97*, Phoenix, AZ, 1997, pp. 2158–2162.

[299] T. Keller and L. Hanzo, Orthogonal frequency division multiplex synchronization techniques for wireless local area networks," in *Proc. Personal, Indoor and Mobile Radio Communications, PIMRC'96*, Taipei, Taiwan, Oct. 15–18, 1996, pp. 963–967.

[300] F. Daffara and O. Adami, "A new frequency detector for orthogonal multicarrier transmission techniques," in *Proc. IEEE 45th Vehicular Technology Conf.*, Chicago, IL, July 15–28, 1995, pp. 804–809.

[301] M. Sandell, J.-J. van de Beek, P. O. Börjesson, "Timing and frequency synchronization in OFDM systems using the cyclic prefix," in *Proc. Int. Symp. Synchronization*, Essen, Germany, Dec. 14–15, 1995, pp. 16–19.

[302] R. V. Cox, J. Hagenauer, N. Seshadri, and C. E. W. Sundberg, "Subband speech coding and matched convolutional channel coding for mobile radio channels," *IEEE Trans. Signal Processing*, vol. 39, pp. 1717–1731, Aug. 1991.

[303] J. Hagenauer, "Rate-compatible punctured convolutional codes (RCPC) and their applications," *IEEE Trans. Commun.*, vol. 36, pp. 389–400, Apr. 1988.

[304] R. A. Salami, K. H. H. Wong, R. Steele, and D. Appleby, "Performance of error-protected binary pulse excitation coders at 11.4 Kb/s over mobile radio channels," in *Proc. ICASSP'90*, pp. 473–476.

[305] G. Ungerboeck, "Trellis-coded modulation with redundant signal sets, Part I and II," *IEEE Commun. Mag.*, vol. 25, pp. 5–21, Feb. 1987.

[306] E. Biglieri and M. Luise, "Coded modulation and bandwidth-efficient transmission," in *Proc. 5th Tirrenia Int. Workshop*, Amsterdam, The Netherlands, Sept. 8–12, 1991.

[307] "Special issue on coded modulation," *IEEE Commun. Mag.*, vol. 29, no. 12, Dec. 1991.

[308] J. Hagenauer, "Iterative decoding of binary block and convolutional codes," *IEEE Trans. Inform. Theory*, vol. 62, pp. 429–445, 1996.

[309] L. F. Wei, "Coded modulation with unequal error protection," *IEEE Trans. Commun.*, vol. 41, pp. 1439–1450, Oct. 1993.

[310] C. Berrou, A. Glavieux, and P. Thitimajshima, "Near Shannon limit error-correcting coding and decoding: Turbo-codes," in *Proc. ICC*, 1993, pp. 1064–1070.

[311] A. J. Viterbi, "Error bounds for convolutional codes and an asymptotically optimum decoding algorithm," *IEEE Trans. Inform. Theory*, vol. 13, pp. 260–269, 1967.

[312] J. Hagenauer and P. Hoeher, "A Viterbi algorithm with soft-decision outputs and its applications," in *Proc. IEEE GLOBECOM'89*, Dallas, TX, 1989, pp. 1680–1686.

[313] J. Hagenauer, E. Offer, and L. Papke, "Iterative decoding of binary block and convolutional codes," *IEEE Trans. Inform. Theory*, vol. 42, no. 2, pp. 429–445, 1996.

[314] J. Hagenauer, P. Robertson, and L. Papke, "Iterative ("TURBO") decoding of systematic convolutional codes with the MAP and SOVA algorithms," in *ITG Fachtagung, Codierung für Quelle, Kanal und Übertrager*, Muenchen, Germany, 1994, pp. 21–29.

[315] P. Robertson, E. Villebrun, and P. Hoeher, "A comparison of optimal and sub-optimal MAP decoding algorithms operating in the log domain," in *Proc. IEEE Int. Conf. Communications*, 1995, pp. 1009–1013.

[316] P. Jung, "Comparison of turbo-code decoders applied to short frame transmission systems," *IEEE J. Select. Areas Commun.*, vol. 14, no. 3, pp. 530–537, 1996.

[317] P. Jung and M. Naßhan, "Performance evaluation of turbo codes for short frame transmission systems," *Electron. Lett.*, vol. 30, no. 2, pp. 111–112, 1994.

[318] ———, "Dependence of the error performance of turbo-codes on the interleaver structure in short frame transmission systems," *Electron. Lett.*, vol. 30, no. 4, pp. 287–288, 1994.

[319] A. S. Barbulescu and S. S. Pietrobon, "Interleaver design for turbo codes," *Electron. Lett.*, vol. 30, no. 25, pp. 2107–2108, 1994.

[320] O. Joerssen and H. Mayr, "Terminating the trellis of turbo-codes," *Electron. Lett.*, vol. 30, no. 16, pp. 1285–1286, 1994.

[321] P. Robertson and T. Wörz, "Coded modulation scheme employing turbo codes," *Electron. Lett.*, vol. 31, no. 18, pp. 1546–1547, 1995.

[322] ———, "A novel bandwidth efficient coding scheme employing turbo codes," in *Proc. ICC'96*, to be published.

[323] S. Benedetto, D. Divsalar, B. Montorsi, and F. Pollara, "Bandwidth efficient parallel concatenated coding schemes," *Electron. Lett.*, vol. 31, no. 24, pp. 2067–2069, 1995.

[324] M. Breiling and L. Hanzo, "Non-iterative optimum super-trellis decoding of turbo codes," *Electron. Lett.*, vol. 33, no. 10, pp. 848–849, May 8, 1997.

[325] ———, submitted for publication.

[326] ———, "Optimum noniterative turbo-decoding," in *Proc.*

PIMRC'97, Helsinki, Finland, Sept. 1–4, 1997, pp. 714–718.

[327] D. Didascalou, "The potential of Turbo codes in trellis coding schemes," Diploma Project Rep., Univ. of Southampton, UK, 1996.

[328] M. Breiling, "Turbo coding simulation studies," Diploma Project Rep., Univ. Southampton, UK, 1997.

[329] J. Brecht, "Medium access control for multirate, multimedia wireless systems," Diploma Project Rep., Univ. Southampton, UK, 1997.

[330] GSM Recommendation 05.05, Annex 3, pp. 13–16, Nov. 1988.

[331] R. Edwards and J. Durkin, "Computer prediction of service area for VHF mobile radio networks," *Proc. IRE*, vol. 116, no. 9, pp. 1493–1500, 1969.

[332] J. Cheng and R. Steele, "Modified Viterbi equaliser for mobile radio channels having large multi-path delay," *Electron. Lett.*, vol. 25, no. 19, pp. 1309–1311, 1989.

[333] N. S. Hoult, C. A. Dace, and A. P. Cheer, "Implementation of an equaliser for the GSM system," in *Proc. 5th Int. Conf. Radio Receivers Associated Systems*, Cambridge, UK, July 24–26, 1990.

[334] R. D'Avella, L. Moreno, and M. Sant'Agostino, "An adaptive MLSE receiver for TDMA digital mobile radio," *IEEE J. Select. Areas Commun.*, vol. 7, pp. 122–129, Jan. 1989.

[335] J. C. S. Cheung, "Adaptive equalisers for wideband time division multiple access mobile radio," Ph.D. dissertation, Dept. of Electronics and Computer Science, Univ. of Southampton, UK.

[336] M. R. L. Hodges, S. A. Jensen, and P. R. Tattersall, "Laboratory testing of digital cellular radio systems," *BTRL J.*, vol. 8, no. 1, pp. 57–66, Jan. 1990.

[337] M. Hata, "Empirical formula for propagation loss in land mobile radio," *IEEE Trans. Veh. Technol.*, vol. 29, pp. 317–325, Aug. 1980.

[338] Y. Okumura, E. Ohmori, T. Kawano, and K. Fukuda, "Field strength and its variability in VHF and UHF land mobile service," *Rev. Elect. Commun. Lab.*, vol. 16, pp. 825–873, Sept.–Oct. 1968.

[339] J. Williams, L. Hanzo, and R. Steele, "Channel-adaptive voice communications," in *Proc. Inst. Elect. Eng. RRAS'95 Conf.*, Bath, UK, Sept. 26–28, 1995, no. 415, pp. 144–147.

[340] L. Hanzo, J. C. S. Cheung, R. Steele, and W. T. Webb, "A packet reservation multiple access assisted cordless telecom-munications scheme," *IEEE Trans. Veh. Technol.*, vol. 43, pp. 234–245, May 1994.

[341] W. C. Wong, "Dynamic allocation of packet reservation multiple access carriers," *IEEE Trans. Veh. Technol.*, vol. 42, pp. 385–392, Nov. 1993.

[342] W. C. Y. Lee, "Spectrum efficiency in cellular," *IEEE Trans. Veh. Technol.*, vol. 38, pp. 69–75, May 1989.

[343] T. Keller, "Orthogonal frequency division multiplex techniques for wireless local area networks," Internal Rep., Dept. of Electronics and Computer Science, Univ. of Southampton, UK, 1996.

[344] P. Cherriman, T. Keller, and L. Hanzo. (1997). Orthogonal frequency division multiplex transmission of H.263 encoded video over highly frequency-selective wireless networks. [Online]. Available WWW: http://www-mobile.ecs.soton.ac.uk/peter/robust-h263/robust.html.

[345] S. Pietrobon, "Implementation and performance of a Turbo/Map decoder," submitted for publication.

Lajos Hanzo (Senior Member, IEEE) graduated in electronics in 1976 and received the Ph.D degree in 1983.

During his 20-year career in telecommunications, he has held various research and academic posts in Hungary, Germany, and the United Kingdom. Since 1986, he has been with the Department of Electronics and Computer Science, University of Southampton, UK, and has been a Consultant to Multiple Access Communications Ltd., UK. He has coauthored two books on mobile radio communications, published more than 180 research papers, organized and chaired conference sessions, and presented overview lectures, and was awarded a number of distinctions. Currently, he is managing a research team working on a range of research projects in the field of wireless multimedia communications under the auspices of the Engineering and Physical Sciences Research Council, UK, the European Advanced Communications Technologies and Services Program, and the Mobile Virtual Centre of Excellence. He holds the Chair of Telecommunications.